WEGA PARAMETER CALCULATIONS

IN EQUILIBRIUM

Horst D. Pacher

IPP 2/226 Januar 1975

MAX-PLANCK-INSTITUT FÜR PLASMAPHYSIK

GARCHING BEI MÜNCHEN

MAX-PLANCK-INSTITUT FÜR PLASMAPHYSIK

GARCHING BEI MÜNCHEN

WEGA PARAMETER CALCULATIONS IN EQUILIBRIUM

Horst D. Pacher

IPP 2/226 Januar 1975

Die nachstehende Arbeit wurde im Rahmen des Vertrages zwischen dem Max-Planck-Institut für Plasmaphysik und der Europäischen Atomgemeinschaft über die Zusammenarbeit auf dem Gebiete der Plasmaphysik durchgeführt.

WEGA PARAMETER CALCULATIONS IN EQUILIBRIUM

IPP 2/226 Horst D. Pacher

Abstract

Calculations of power balance in equilibrium have been carried out for WEGA, taking into account profile factors and impurities. For reasonable parameters, T_e lies between 1 and 2 keV, T_i between 250 and 500 eV. The ohmic heating power lies between 50 and 100 kW. An additional input power into the plasma of 200 kW results in an increase of electron and ion temperatures by a factor 2. T_e and T_i have been calculated for various n, a, I, iota, Z_{eff}, c^2, B, and heating powers.

WEGA INTERNAL REPORT

WEGA PARAMETER CALCULATIONS IN EQUILIBRIUM

IPP 2/226 Horst D. Pacher

I) Introduction

WEGA (Wendelstein Experiment in Grenoble for the Application of RF heating) is an ohmically heated stellarator of the Wendelstein type which is being built and will be operated in collaboration between the three institutes C.E.N. Grenoble (Grenoble, France), Max-Planck-Institut für Plasmaphysik (Garching, Germany), and Ecole Royale Militaire (Bruxelles, Belgium), under the auspices of EURATOM. The experiment is situated in Grenoble, France. It is the purpose of this report to investigate the parameter range which may be expected to be attained in WEGA.

Here, the power balance equations are solved for the electronand ion temperatures under certain simplifying assumptions. In particular, it is assumed that equilibrium has been attained, and therefore no time derivatives of any quantities appear. One species of impurities is taken into account, and profile effects are included approximately, as described in more detail below.

The input power to the electrons consists of Ohmic Heating W_{OH} and an additional input power W_e^h (e.g. from RF Heating or Neutral Injection). The input power to the ions consists of the electron-ion collisional exchange W_{ei} and an additional input power W_i^h (e.g. RF or neutral injection). The electron loss processes are pseudoclassical electron heat conduction W_e^{PC} and, in addition, the energy lost by convection (particle loss). It is assumed that the particle loss is neoclassical (plateau regime), as found in the ohmically heated stellarator Wendelstein II b (W II b), for example. Therefore, the power lost due to convection

is given by W_e^p = Total Particle energy / confinement time (particle). The ion loss is assumed to be the minimum of plateau regime ion heat conduction W_i^p and banana regime ion heat conduction W_i^b. Although the calculations have been performed for both plateau and banana regime ion heat conduction, the results given in this report all refer to a calculation with a continued plateau, since this gives a more conservative estimate. Since to date no Tokamak results showing banana regime heat conduction have been obtained, and, furthermore, it can be expected that the heat conduction in a stellarator is larger than in a Tokamak (superbananas) this seems to be a realistic approach.

II) Equations

Following the arguments given in the introduction, the following equations have been used to calculate the electron and ion temperatures:

Electron power balance

$$W_{OH} + W_e^h = W_e^{PC} + W_e^p + W_{ei} \qquad \ldots\ (1)$$

Ion power balance

$$W_{ei} + W_i^h = W_i^p \qquad \ldots\ (2)$$

To show the temperature dependences explicitly, (1) and (2) may be rewritten:

$$A_{OH} Te^{-3/2} + W_e^h = A_e^{PC} Te^{1/2} + A_e^P T_e^{5/2} + A_{ei} \frac{Te - Ti}{T_e^{3/2}}$$

$$A_{ei} \frac{Te - Ti}{Te^{3/2}} + W_i^h = A_i^P T_i^{5/2}$$

The equations for the various terms of (1) and (2) are given in Table I. Each of these expressions consistsof the power loss per unit volume w, calculated for a pure electron-hydrogen plasma and expressed in terms of the peak electron density and peak electron and ion temperatures, multiplied by the volume, an impurity factor including the effect of one impurity species as well as the effect of using a gas other than hydrogen as the main ion species, and a profile factor P including the effect of the radial variation of density, temperature, current density, and

TABLE I: TERMS OF THE POWER BALANCE EQUATIONS

TERM	TOTAL POWER (kW)	IMPURITY FACTOR ($T_o = T_i$)	PROFILE FACTOR (PARABOLIC)
Ohmic Heating	$W_{OH} = 4.17 \cdot 10^{-10} \frac{B^2 \kappa_I^2}{R^2} \frac{\ln\Lambda}{T_e^{3/2}} \varepsilon_2 \varepsilon_3 \cdot Vol \cdot \zeta_{OH} \cdot P_{OH}$	$\zeta_{OH} = Z_{eff}$	$P_{OH} = 2.5$
Pseudoclassical Electron Heat Conduction	$W_e^{Pc} = 1.52 \cdot 10^{-25} C_{Pc}^2 \frac{n_e^2 \ln\Lambda R^2}{B^2 \kappa^2 a^4} T_e^{1/2} \cdot Vol \cdot \zeta_e^{Pc} \cdot P_e^{Pc}$	$\zeta_e^{Pc} = Z_{eff}$	$P_e^{Pc} = 4 \int_0^1 \frac{(1-u^2)^{1/2}}{\tilde{\kappa}^2} u^2 du^2$
Plateau Regime Electron Connection	$W_e^P = 4.55 \cdot 10^{-6} \frac{n_e T_e^{5/2}}{B^2 \kappa^2 Ra^2} \cdot Vol \cdot \zeta_e^P \cdot P_e^P$	$\zeta_e^P = 1$	$P_e^P = 4 \int_0^1 \frac{(1-u^2)^{3/2}}{\tilde{\kappa}} u^2 du^2$
Electron – Ion Heat Transfer	$W_{ei} = 2.41 \cdot 10^{-32} n_e^2 \ln\Lambda \frac{T_e - T_i}{T_e^{3/2}} \cdot Vol \cdot \zeta_{ei} \cdot P_{ei}$	$\zeta_{ei} = \frac{Z_o - Z_{eff}}{Z_o - Z_i} \frac{Z_i}{A_i} + \frac{Z_i - Z_{eff}}{Z_i - Z_o} \frac{Z_o}{A_o}$	$P_{ei} = 0.4$
Plateau Regime Ion Heat Conduction	$W_i^P = 1.47 \cdot 10^{-4} \frac{n_e T_i^{5/2}}{B^2 \kappa Ra^2} \cdot Vol \cdot \zeta_i^P \cdot P_i^P$	$\zeta_i^P = \frac{Z_o - Z_{eff}}{Z_o - Z_i} \frac{A_i^{1/2}}{Z_i} + \frac{Z_{eff} - Z_i}{Z_o - Z_i} \frac{A_o^{1/2}}{Z_o}$	$P_i^P = 4 \int_0^1 \frac{(1-u^2)^{5/2}}{\tilde{\kappa}} u^2 du^2$
Banana Regime Ion Heat Conduction	$W_i^b = 3.45 \cdot 10^{-24} \frac{n_e^2 T_i^{1/2} \ln\Lambda}{B^2 \kappa^2 R^2} \left(\frac{R}{a}\right)^{7/2} \cdot Vol \cdot \zeta_i^b \cdot P_i^b$	$\zeta_i^b = \frac{(Z_o - Z_{eff})^2}{(Z_o - Z_i)^2} \cdot \frac{Z_i^2}{A_i^{1/2}} + \frac{(Z_{eff} - Z_i)^2}{(Z_o - Z_i)^2} \frac{Z_o^2}{A_i^{1/2}}$	$P_i^b = 1.886$

UNITS: W [kW], R, a [cm], B [G], $Vol = 2\pi^2 Ra^2$ [cm^3], T_e, T_i [keV], n [cm^{-3}], I [A]

FURTHER EXPRESSIONS: $\kappa_I = \frac{RI}{5a^2 B}$, $\tilde{\kappa} = \frac{\kappa_I \left(\frac{1 - (1-u^2)^{5/2}}{u^2} \right) + \kappa_o}{\kappa_I + \kappa_o}$, $u = \frac{r}{a}$,

$V = \frac{W_{OH}}{I} \cdot 10^3$ [V], $\ln\Lambda = \ln 4.74 \cdot 10^{14} \frac{T_e^{3/2}}{n^{1/2}} \sim 19$

$E = 1.58 \cdot 10^{-15} n (T_e + T_i) Ra^2$ [joule]

$\beta_\Theta = 1.34 \cdot 10^{-8} \frac{n (T_e + T_i) R^2}{\kappa^2 a^2 B^2}$

$\tau_E'' = \frac{E}{W_{OH} - W_e^{\ln} + W_i^{\ln}}$ [msec]

rotational transform. The power densities w are calculated in Appendix I. The impurity factors ζ are calculated in Appendix II in terms of the ionization level Z and the mass A of main and impurity species as well as the relative concentration of the impurity, expressed in terms of the "effective charge" Z_{eff}. It is assumed that the relative concentration, i.e. Z_{eff}, Z, and A are independent of radius. Furthermore, it is shown in Appendix II that, for all cases of interest, the ion and impurity ion temperatures may be assumed equal.

The profile factors are calculated in Appendix III for a general profile, and are given in Table I and in all the results presented here for a parabolic distribution of n, T_e, and T_i (as obtained in, for example, W II b).

Some radiation losses have been calculated in Appendix IV. It is shown there that, for the expected WEGA parameters, the losses from bremsstrahlung are in the neighbourhood of 125 watts, and the losses from electron synchrotron radiation are 460 watts, both of which are therefore negligible when compared with the ohmic heating power of 50 kW. Line radiation has not been calculated. However, if the main impurity is oxygen, it may be expected to be fully ionized at the expected electron temperature of over 1 keV over the body of the plasma. Therefore, in this case, line radiation losses may be expected to be small and coming only from the edge of the plasma.

A much more difficult question is the question of recycling, ionization, and charge exchange. This question has not been treated here in detail, since for a reasonable solution one should solve the radial equations (e.g. by the DÜchs code), under assumptions concerning the exact recycling process, impurity transport, etc. Instead, we make here the ad hoc assumption that the density and temperature profiles are given (here assumed as parabolic). In fact, this assumption means that the profile establishes itself in such a way that energy is transported from the interior of the plasma, $r \leq a$, by heat conduction and convection to the outside region, $r > a$, where it is dumped into ionization and charge exchange. Experimentally from the experience in similarly sized Tokamaks and in W II b,

a profile of roughly this type establishes itself, so that we may expect that the standard case calculated for WEGA corresponds reasonably well to reality. Whether this situation still obtains in the more exotic cases calculated, for instance with addition heating, is an open question. All that can be said is that the losses should certainly increase with increasing temperature, but not whether they increase in precisely the way assumed here. More detailed calculations including the recycling and the radial dependence are necessary.

From the above, it is clear that one of the most important unknown parameters is the density, which turns out in the calculations to be a rather critical parameter. However, it has been found that in ohmically heated plasmas the accessible density range (1.10^{13} in W II b to 6.10^{13} in TFR) is rather small, with poor confinement occurring at low densities because of runaways and difficulties in the startup phase, and disruptions occurring at high densities. Experimentally, it is found that, in "good" conditions, T_e/T_i is of the order of 2 to 3 and the poloidal beta is of the order of one-half. From these experimental results of other devices we may conclude that the standard case chosen for WEGA, i.e. $n = 3.10^{13}$ at the centre ($T_e/T_i = 3.3$, poloidal beta = 0.44) should occur in practice. In order to take into account possible variations from this standard case, the density is usually varied along with the other parameters in these calculations.

In conclusion to these general comments on the calculations, it should be pointed out once again that these are <u>equilibrium</u> calculations. Whether and at what time this equilibrium is reached depends on the exact conditions of the startup phase, the recycling, as well as on the exact vertical field and ohmic heating program.

III) Results of Calculation For Wendelstein II b

The input parameters and results of the calculation for W II b are given in Table II. The various parameters correspond to those given for the discharge in Ref.1. The calculated peak electron temperature corresponds well to the measured value (165 vs 160 eV). The calculated peak ion temperature is 56 eV, which is to be compared with 35 eV measured near the edge by an ion energy analyzer, and about 50 eV peak temperature measured spectroscopically. The calculated ohmic heating power corresponds almost exactly to the measured value, showing that in the W II b experiment no anomalous resistivity is observed. For the W II b case the main impurity was taken to be oxygen with $Z_{eff} = 2.2$, as measured, and with a Z of 5, as expected at this density and electron temperature.

The very good agreement of the calculated values for T_e, T_i, and ohmic heating power with the experimentally observed values serves to give some confidence in the applicability of the calculation to WEGA.

IV) Results of Calculation for WEGA Standard Case

The input parameters of the WEGA standard case as well as the results are given in Table III.

The main field B of 14.4 kG corresponds to the maximum field attainable in phase I of WEGA operation. In a later phase, this field will be increased to 25 kG. The reasons for choosing a peak density of 3.10^{13} cm^{-3} for the standard case, as well as parabolic profiles for the density and temperature have been given in Section II. The pseudoclassical factor c^2_{pc} has been taken as 3 for the standard case, which is justified by comparing tokamak results (c^2_{pc} = 5 to 10) with ohmically heated stellarator results (best result for W II b: c^2_{pc} = 3) which shows that the pseudoclassical heat conduction is improved by stellarator effects over the value obtainable in tokamaks. In agreements with the W II b results, and also to remain conservative, the anomalous resistivity factor $\varepsilon_2 \varepsilon_3$ has been taken to be 1, i.e. Spitzer resistivity. The minor radius of 13cm (compared with a vacuum vessel inner radius

TABLE II

W II b CALCULATIONS - INPUT PARAMETERS AND RESULTS

Input Parameters as given in Ref. 1

Main Field:	$B = 7.7$ kG
Peak Density:	$n = 1.10^{13}$ cm^{-3}
Pseudoclass. Factor:	$c^2_{pc} = 5$
Anomalous Resistivity:	$\varepsilon_2 \varepsilon_3 = 1$
Major Radius:	$R = 50$ cm
Minor Radius:	$a = 4$cm
Plasma Current:	$I = 30.8$ kA
$\varkappa$ (current):	$\varkappa_I = 0.25$
$\varkappa$ (helical):	$\varkappa_o = 0.10$
$\varkappa$ (total):	$\varkappa = 0.35$
$\ln \Lambda$:	$\ln \Lambda = 15.0$
Effective charge:	$Z_{eff} = 2.2$
Impurity charge:	$Z = 5$
Impurity A :	$A_o = 16$
Additional Heating Electrons:	$W_e^h = 0$
Additional Heating Ions:	$W_i^h = 0$

Results

Peak Electron Temperature:	$T_e = 0.166$ keV
Peak Ion Temperature:	$T_i = 0.056$ keV
Ohmic Heating Power:	$W_{OH} = 11.92$ kW
Pseudoclass. Elect. Heat Cond.:	$W_e^{PC} = 11.48$ kW
Plateau Electron Convection:	$W_e^P = 0.15$ kW
Electron-Ion Heat Transfer:	$W_{ei} = 0.29$ kW
Plateau Ion Heat Cond.:	$W_i^P = 0.29$ kW
Poloidal Beta:	$\beta_\theta = 0.64$
Energy Content of Plasma:	$E = 2.8$ Joule
Energy Replacement Time:	$\tau'_E = 0.24$ msec

Coefficients Used

Profile Factors	Impurity Factors	Power Coefficients
$P_{OH} = 2.5$	$\zeta_{OH} = 2.20$	$A_{OH} = 0.806$
$Pe^{PC} = 0.53$	$\zeta_e^{PC} = 2.20$	$A_e^{PC} = 28.18$
$Pe^P = 0.30$	$\zeta_e^P = 1.00$	$A_e^P = 12.99$
$Pei = 0.40$	$\zeta_{ei} = 0.79$	$Aei = 0.18$
$Pi^P = 0.30$	$\zeta_i^P = 0.94$	$A_i^P = 390.17$

TABLE III

WEGA STANDARD CASE - INPUTS AND RESULTS

Input Parameters

Main Field:	$B = 14.4\ kG$
Peak Density:	$n = 3.10^{13} cm^{-3}$
Pseudoclass. Factor:	$c_{pc}^2 = 3$
Anomalous Resistivity:	$\varepsilon_2 \varepsilon_3 = 1$
Major Radius:	$R = 72\ cm$
Minor Radius:	$a = 13\ cm$
Plasma Current:	$I = 60\ kA$
κ (current):	$\kappa_I = 0.355$
κ (helical):	$\kappa_o = 0.12$
κ (total):	$\kappa = 0.475$
$\ln \Lambda$:	$\ln \Lambda = 19$
Effective Charge:	$Z_{eff} = 3$
Impurity Charge:	$Z = 8$
Impurity A :	$A_o = 16$
Additional Heating Electrons:	$W_e^h = 0$
Additional Heating Ions:	$W_i^h = 0$

Results

Peak Electron Temperature :	$T_e = 1.27\ keV$
Peak Ion Temperature :	$T_i = 0.387\ keV$
Ohmic Heating Power:	$W_{OH} = 50.24\ kW$
Pseudoclass. Electron Heat Cond.:	$W_e^{PC} = 14.27\ kW$
Plateau Electron Convection :	$W_e^P = 15.00\ kW$
Electron-Ion Heat Transfer:	$W_{ei} = 20.97\ kW$
Plateau Ion Heat Cond.:	$W_i^P = 20.97\ kW$
Poloidal Beta:	$\beta_\theta = 0.44$
Energy Content of Plasma:	$E = 0.956\ kJoule$
Energy Replacement Time:	$\tau_E' = 19\ msec$

Coefficients Used

Profile Factors	Impurity Factors	Power Coefficients
$P_{OH} = 2.5$	$\zeta_{OH} = 3.00$	$A_{OH} = 72.01$
$P_e^{PC} = 0.58$	$\zeta_e^{PC} = 3.00$	$A_e^{PC} = 12.66$
$P_e^P = 0.30$	$\zeta_e^P = 1.00$	$A_e^P = 8.23$
$P_{ei} = 0.40$	$\zeta_{ei} = 0.86$	$A_{ei} = 33.98$
$P_i^P = 0.30$	$\zeta_i^P = 0.86$	$A_i^P = 225.29$

of 19cm) is realistic when taking into account the ellipticity of the magnetic surfaces and the necessity of placing RF structures inside the vacuum vessel. The maximum value of the minor plasma radius (circularized) in the absence of RF structures will certainly be no larger than 16 cm. The value of the rotational transform at the edge is taken to be 0.475 ("safety factor" above q = 2) since W II b operation has shown that optimal operation is not possible for $q < 2$. This rotational transform is composed of $\iota_I = 0.355$, the rotational transform due to the ohmic heating current, and $\iota_0 = 0.12$, the rotational transform due to the helical windings. For this case, ohmic heating is substantial, and, at the same time, a substantial portion of the rotational transform is provided by the stellarator windings. This value of iota, radius, and B gives an ohmic heating current of 60 kA. The maximum attainable ohmic heating current in WEGA is 80 to 100 kA. Z_{eff} has been taken as 3 by comparison with ST and W II b, and we have assumed that the main impurity contributing is oxygen. At these densities and temperatures, the oxygen should be fully ionized.

The results are also given in Table III. The electron temperature for this standard case is 1.27 keV, the ion temperature is 387 eV, very reasonable values when compared with ST. The ohmic heating power turns out to be 50 kW. This divides almost equally into ion losses, pseudoclassical electron heat conduction and plateau regime electron convection (particle loss). This contrasts with the conditions of W II b, in which pseudoclassical electron heat conduction is by far the dominant loss mechanism, mainly because of the poor aspect ratio there. For the WEGA standard case, $\beta_\Theta = 0.44$, the energy content of the plasma is 0.96 kilojoule, and the energy replacement time $\tau'_E = 19$ milliseconds. The gap voltage is 0.84 volts.

V) Variations of Parameters Without Heating

Starting from the WEGA standard case described in the previous section, various parameters are varied. A summary of the cases studied is given in Table IV.

TABLE IV: PARAMETER VARIATIONS STUDIED

Quantity	Symbol	Units	Case No.	1, 2	3	4	5	6	7	8	9	10
			Fig. No.	1-10	11-13	14-16	17-19	21-23 27-32	21-23 31-32	21-23 31-32	21-23 31-34	24-26
Main Field	B	kG		14.4	14.4	14.4	14.4	14.4	10	20	25	14.4
Peak Density	n	10^{13} cm^{-3}		0.7-5	3	1-3	1-3	1-3	1-3	1-3	1-3	1-3
Pseudocl. Factor	Cpc^2	-		3	3	3	10	3	3	3	3	3
Minor Radius	a	cm		10-16	13	13	10-16	13	13	13	13	13
Plasma Current	I	kA		35.5-90.9	40-120	16.9-84.5	35.5-90.9	60	41.7	83.3	104.0	60
(current)	κ_I	-		0.355	0.23-0.7	0.1-0.5	0.355	0.355	0.355	0.355	0.355	0.355
(helical)	κ_o	-		0.12	0-0.3	0-0.4	0.12	0.12	0.12	0.12	0.12	0.12
(total)	κ	-		0.475	0.23-1.0	0.5	0.475	0.475	0.475	0.475	0.475	0.475
Eff. Charge	Z_{eff}	-		3	3	3	5	3	3	3	3	1-7
Add. Heating Elect.	W_e^h	kW		0	0	0	0	0-100	0-100	0-100	0-100	0
Add. Heating Ions	W_i^h	kW		0	0	0	0	0-100	0-100	0-100	0-100	0

Underlined quantities represent variations from standard case (Table III)

The following quantities are identical for all cases:

Anom. Resistivity $\varepsilon_2 \varepsilon_3 = 1$

Major Radius $R = 72$ cm

$\ln \Lambda$ $\ln \Lambda = 19$

Impurity Charge $Z = 8$

Impurity A $A_o = 16$

a) Variation of n and a at constant iota (case 1 and 2)

n and a are varied over a range of 7.10^{12} to 5.10^{13} cm^{-3} and 10 to 12cm, respectively, keeping the total rotational transform due to the current and to the helical windings constant. Of course, the current must be varied as a result. Since iota = 0.5 is likely to be the maximum possible operating condition, the results here give the maximum temperatures as a function of the radius and the assumed density.

The results are plotted in Fig.1 to 10. It is seen that the temperatures are both a very strong function of the density, and a weaker function of radius, both temperatures increasing with plasma radius, the electron temperature decreasing with density and the ion temperature increasing with density. Fig.3 shows the range spanned by the ion and electron temperatures. The ohmic heating power, equal to the total loss, is only weakly dependent on radius, but the distribution of the losses changes. The ohmic heating power is strongly dependent on density. The energy replacement time is not strongly dependent on density, but varies strongly with radius, remaining, however, between 15 and 30 msec. The energy content of the plasma varies strongly with both parameters, going from 200 to 2000 joule over the range studied.

b) Variation of helical iota and current (case 3, Fig.11-13)

In this calculation, the restriction on the total rotational transform is disregarded in order to see the effect of the variation of ohmic heating current and helical iota directly. As a result, the temperatures obtained at the higher current values must be taken with a grain of salt (see, for example, plot of iota with current in Fig.12). In any case, although the electron temperature increases strongly with increasing current, the ion temperature is only weakly dependent on the current (Fig.11). Both temperatures are only very weakly dependent on the helical rotational transform. Therefore, the main advantage

of stellarator operation in this regime must be seen not in improving the plasma parameters significantly, but in attaining these parameters initially (improved startup phase, initial equilibrium, less difficulties with runaways), in perhaps reducing impurity levels (e.g. by placing the separatrix inside the vacuum vessel; note also that W II b has a very low Z_{eff} of 2.2), and in the possibility of maintaining equilibrium even without ohmic heating in the presence of other heating methods, also perhaps in avoiding disruptive instabilities. It is notable that the energy replacement time levels off at high currents, and that the ohmic heating power is only weakly dependent on the current.

c) Variation of helical and current iota at constant total iota (case 4, Fig.14-16)

Here we study a more realistic variation than the previous one, i.e., we keep the total rotational transform constant (at 0.5) and vary the ratio of the two components making up this transform. The right-hand side of Fig.14 therefore represents pure tokamak operation, the left-hand side pure stellarator operation. It is notable that, although the electron temperature increases with more tokamak-like operation (more current), the ion temperature remains almost exactly constant in the region of interest at constant density (iota o = 0. to 0.2, iota I = 0.5 to 0.3, resp.). The total ohmic heating power increases with more tokamak-like operation, mainly due to the greater relative importance of the electron convection losses.

d) Variation of n and a for $Z_{eff} = 5$, $c^2 = 10$ (case 5, Fig.17-20)

In order to describe a more pessimistic case, the calculations of a) (case 1 and 2) are repeated for a higher impurity level ($Z_{eff} = 5$ rather than 3) and a higher pseudoclassical electron heat conduction ($c^2 = 10$ rather than 3). The higher losses are to some extent compensated by the higher ohmic heating input due to the impurities, and the result is generally similar to the previous case, with, in particular, very similar electron and ion temperatures. (Compare,

e.g., Fig.3 and 19). The ohmic heating power level for 3.10^{13}, for example has been increased from about 50 kW to 100 kW, with now the pseudoclassical heat conduction taking the largest part of the loss. The exact ohmic heating power needed is now much more strongly dependent on the density than before (Fig.20). The weak dependence on radius is maintained.

e) Variation of B and n at constant iota (case 6, 7, 8, 9, Fig.21-23)

Here, we vary the main magnetic field and the density, keeping the total iota and its components constant, and therefore varying the ohmic heating current accordingly. Phase I operation of WEGA goes from 10 to 14.4 kG, and phase II operation will be extended to 25 kG. Partly because of the increase of the current to keep iota constant as a function of B, a very strong increase in the ion and electron temperatures with magnetic field is observed. Remarkably again, the ohmic heating power remains almost constant as a function of B, but the loss distribution changes, with electron pseudoclassical heat conduction dominating over convection at 10 kG, and vice versa at 25 kG. The energy replacement time is very strongly dependent on B (from 14 to 32 msec over this range).

f) Variation of n and Z_{eff} (case 10, Fig.24-26)

The electron temperature increases with increasing Z_{eff} (better ohmic heating), but the ion temperature remains almost constant with increasing impurity level, a consequence of the fact that, for our particular case of a fully ionized oxygen impurity, the impurity factor in W_{ei} and W_i^p is equal (see Appendix II). Although this is not the case for other Z and A of the impurity, the result may still hold roughly. The ohmic heating power increases over a factor 2 over the range considered.

VI) Calculations Including Additional Heating (case 6-9, Fig.27-37)

In these calculations, additional equal heating to the electrons and ions is included. This additional heating represents the power actually absorbed by the electrons or ions, exclusive of reflections, losses in the line etc., and also without regard to possible profile changes and changes in the impurity level as result of the heating. Also, homogeneous heating over the entire profile is assumed.

Heating in Phase I of WEGA operation (14.4. kG) is investigated in case 6 (Fig.27-30). It is seen in Fig.28 that a total additional power input into the plasma at 3.10^{13} of 200 kW (four times the initial ohmic heating power) just produces a heating factor of 2 for both electrons and ions (assuming, of course, as explained in Section I, a continued plateau for ion heat conduction). The electron heating factor obtainable remains remarkably constant as a function of density. The ion heating factor, and also the ion temperature, can be increased at constant additional heating power by lowering the density. However, as already explained in Section II, this is probably not possible because of difficulties with runaways in starting the discharge and because the recycling and the impurity levels are likely to increase as a function of the additional heating. The possibility of the occurrence of new loss mechanisms due to the application of the RF fields supplying the additional heating power is also not considered in this calculation. Therefore, the figure of 200 kW into the plasma should be taken as a lower limit for the input power into the plasma necessary to produce significant heating, i.e. by a factor of 2. (Note: It has been assumed here that equal additional power is absorbed by the ions and by the electrons, since no heating method is known which is able to transfer power only to the ions. Although the exact proportion depends on the particular heating method, the assumption of 50% each to ions and electrons may hold roughly for lower hybrid or, under some conditions, for neutral injection.)

The variation of the effect of the heating with magnetic field is shown in Fig.31 and 32. It is seen that, although higher temperatures are generally obtained

at the higher magnetic fields, the heating factor of the electrons relative to the relevant unheated case decreases with increasing magnetic field, and, while the ion heating factor increases somewhat with increasing magnetic field, it does so only very slowly (Fig.32). It is seen, therefore, that going to Phase II operation (25 kG) does not significantly affect the magnitude of the additional heating power necessary to produce the same ion heating factor.

One further point is to be noted. It is seen (e.g. Fig.30) that, because of the heating and the resultant increase in the electron temperature, the ohmic heating power decreases with additional heating power. For example, at 200 kW total additional power, the ohmic heating power is only 10 kW and,therefore, almost negligible. Therefore, the exact impurity level and/or anomalous resistivity induced by the RF fields are unimportant in the presence of the additional heating unless they become very large.

VII) Comparison of WEGA, W VII a and W VII b at same iota

Under the assumption of the same rotational transform, iota, density, and relative impurity level, as well as assuming a continued plateau for the ion heat conduction, a comparison of the three devices is given in Table V.

VIII) Conclusions

The detailed parameter study in this report has been carried out on the basis of the power balance equations in equilibrium, including ohmic heating, pseudo-classical and plateau regime losses, and additionl heating (from RF or neutral injection). Impurities and profile effects have been taken into account.

The main results are the following:

a) For phase I operation of WEGA (B up to 14.4. kG), reasonable plasma parameters, comparable to ST, can be achieved. Depending on the actual parameters, in the absence of additional heating, electron temperatures

TABLE V

COMPARISON OF WEGA, W VII a, AND W VII b

Parameter	WEGA	WVII a	WVII b
R (cm)	72	200	200
a (cm)	13	15	34
$iota_l$	0.355	0.355	0.355
$iota_0$	0.120	0.120	0.120
$iota_{tot}$	0.475	0.475	0.475
I (kA)	60	79.9	410
B (kG)	15	40	40
c^2_{pc}	3	3	3
Z_{eff} / Z_o /A_o	3/8/16	3/8/16	3/8/16
n (r = 0) (cm^{-3})	3.10^{13}	3.10^{13}	3.10^{13}
T_e (keV)	1.285	2.172	3.68
T_i (keV)	0.387	1.140	1.96
W_{OH} (kW)	49.44	83.2	193.8
W_e^{PC}	13.07	35.4	9.0
W_e^P	15.38	7.4	27.5
$W_i^P = W_{ei}$	21.00	40.6	158.0

at the peak of the profile between 1 and 2 keV may be expected. The ion temperatures should lie between 250 and 500 eV peak. The ohmic heating power level will lie between 50 and 100 kW.

b) Phase II operation of WEGA (B up to 25 kG) should permit electron temperature up to 3 keV and ion temperatures up to 550 eV.

c) Barring additional losses, an additional heating power into the plasma of 200 kW should permit an increase in electron and ion temperatures by a factor of 2. Assuming reasonably good efficiency and coupling, this means that the power level of the RF transmitter necessary should be at least 400 to 500 kW.

d) In the absence of additional heating, WEGA lies between W II b and W VII a in its plasma parameters and should therefore permit reasonable conclusions on scaling parameters.

IX) Acknowledgements

The author wishes to acknowledge his debt to valuable discussions with Dr. P.P. Lallia, C.E.N. Grenoble, and Dr. G.W. Pacher and J.-G. Wegrowe, MPI für Plasmaphysik, Garching. I would also like to express my thanks to Miss I. Weikmann for typing the manuscript, and to my wife, Mrs. Helga Pacher, for drawing the figures.

APPENDIX I - DERIVATION OF POWERS

1) Ohmic Heating Power

Spitzer (Ref.2) gives, for the resistivity:

$$\eta = 5.23 \cdot 10^{-3} \frac{\ln\Lambda}{T_e^{3/2}} \frac{n_i Z_i^2}{n_e} \quad [\Omega\text{-cm, eV}]$$

The heating power per unit volume is given by $\omega_{OH} = \eta j_{\parallel}^2$

, where, for uniform current distribution, $j_{\parallel} = \frac{I}{\pi a^2} = \frac{1}{\pi a^2} \cdot \frac{5a^2 B K_I}{R}$

Hence,

$$\omega_{OH} = 1.32 \cdot 10^{-2} \frac{B^2 K_I^2}{R^2} \frac{\ln\Lambda}{T_e^{3/2}} \frac{n_i Z^2}{n_e} \quad [\text{W/cm}^3, \text{eV, G, cm}]$$

Stix (Ref.3) multiplies this by a factor $\varepsilon_2 \varepsilon_3$ to take into account the anomalous resistivity resulting from neoclassical effects and the reduced current density from the bootstrap current effect. Here,

$$\varepsilon_2 = \left\langle \frac{1}{1 - 1.95\left(\frac{r}{R}\right)^{1/2} + 0.95\frac{r}{R}} \right\rangle$$

$$\varepsilon_3 = \left\langle 1 - 1.29\beta_\theta \left(\frac{r}{R}\right)^{1/2} \right\rangle$$

Hence, finally, in our units, the ohmic heating power per unit volume is given by

$$\omega_{OH} = 4.17 \cdot 10^{-10} \frac{B^2 K_I^2}{R^2} \frac{\ln\Lambda}{T_e^{3/2}} \frac{n_i Z^2}{n_e} \varepsilon_2 \varepsilon_3 \; , \left[\frac{kW}{cm^3}\right], [G, cm, keV]$$

2) Pseudoclassical Electron Heat Conduction

From Yoshikawa & Christofilos (Ref.4), the pseudoclassical diffusion coefficient is given by:

$$D^{PC} = C_{pc}^2 \cdot (D_{class})_{pol} = C_{pc}^2 \frac{R^2}{\kappa a^2} D_{class} = C_{pc}^2 \frac{R^2}{\kappa^2 a^2} \nu_{ei} r_{ce}^2$$

From Spitzer (Ref.2), the electron-ion collision time and electron Larmor radius are given by:

$$\frac{1}{\nu_{ei}} = 2.84 \cdot 10^5 \frac{A_i T_e^{3/2}}{n_i Z_i^2 \ln\Lambda} \; , \quad r_{ce} = 2.38 \sqrt{\frac{T_e}{B}} \quad [\text{sec, eV, cm, G}]$$

Then, since the power loss per unit volume is given by

$$\omega_e^{PC} = \frac{3}{2} kT_e \frac{\partial n_e}{\partial t} = \frac{3}{2} kT_e \left(-\nabla \cdot D^{PC} \nabla n\right)$$

replacing ∇ by $1/a$ (and taking the gradient dependence fully into account in Appendix III on profile factors), we obtain in our units for the power loss per unit volume

$$\omega_e^{PC} = 1.52 \cdot 10^{-25} C_{PC}^2 \frac{n_e n_i Z_i^2 \ln\Lambda}{A_i} \frac{R^2}{B^2 \kappa^2 a^4} T_e^{1/2} \left[\frac{kW}{cm^3}, cm, G, keV\right]$$

3) Plateau regime diffusion and heat conduction

From Galeev and Sagdeev (Ref.5)

$$D_e^P = 6 \cdot 10^8 \frac{T_e^{3/2}}{B^2 \kappa R} \qquad [sec, cm, eV, G]$$

The power loss per unit volume is then, calculated similarly as in 2) above, for the case of plateau regime electron convection:

$$\omega_e^P = 4.55 \cdot 10^{-6} \frac{n_e T_e^{5/2}}{B^2 \kappa R a^2} \left[\frac{kW}{cm^3}\right], [cm^{-3}, keV, G, cm]$$

The ion plateau regime heat conduction coefficient is given by Galeev and Sagdeev as:

$$K_i^P = \frac{3}{4} \left(\frac{T_i}{T_e}\right)^{3/2} \sqrt{\frac{m_i}{m_e}} \frac{n_i}{n_e} D_e^P$$

Hence the power loss per unit volume due to plateau regime ion heat conduction is

$$\omega_i^P = 1.47 \cdot 10^{-4} \frac{n_i T_i^{5/2} A_i^{1/2}}{B^2 \kappa R a^2} \left[\frac{kW}{cm^3}\right], [cm^{-3}, keV, G, cm]$$

4) Banana Regime Ion Heat Conduction

Again from Galeev and Sagdeev (Ref.5), the banana regime diffusion and heat conduction coefficients are given by:

$$D_e^b = 1.33 \cdot 10^{-4} \frac{n_i Z_i^2 \ln\Lambda}{T_e^{1/2} B^2 \kappa^2} \left(\frac{R}{a}\right)^{3/2}, \quad K_i^b = 0.079 \sqrt{\frac{T_e}{T_i}} \sqrt{\frac{m_i}{m_e}} D_e^b \; [cm, s, G, eV]$$

Hence, similar to 3) above, the power loss per unit volume due to banana regime ion heat conduction is given by:

$$\omega_i^b = 3{,}45 \cdot 10^{-24} \frac{n_i^2 z_i^2 A_i^{1/2} T_i^{1/2} \ln\Lambda}{B^2 R^2 \kappa^2} \left(\frac{R}{a}\right)^{7/2} \left[\frac{kW}{cm^3}, cm^{-3}, G, kev\right]$$

5) Electron-Ion Energy Exchange

From Spitzer (Ref. 6), the equilibration time between electrons and ions is

$$\tau_{ei}^{eq} = 7.33 \cdot 10^6 \frac{A_e A_i}{n_i z_e^2 z_i^2 \ln\Lambda} \cdot \left(\frac{T_e}{A_e} + \frac{T_i}{A_i}\right)^{3/2} \quad [sec, ev, cm^{-3}]$$

The power transferred per unit volume between species is

$$\omega_{ei} = \frac{3}{2} n k \frac{T_e - T_i}{\tau_{ei}^{eq}}$$

which becomes, in our units, since $A_e \ll A_i$

$$\omega_{ei} = 2.41 \cdot 10^{-32} \frac{n_e n_i z_i^2 \ln\Lambda}{A_i} \frac{T_e - T_i}{T_e^{3/2}} \quad \left[\frac{kW}{cm^3}, kev, cm^{-3}\right]$$

6) Other Quantities (Calculated for Parabolic Profile)

i) Energy Content

The energy content of the plasma is given by $\left(\hat{n} = \frac{n(r)}{n(0)}, u = \frac{r}{a}\right)$

$$E = \int \frac{3}{2} n k (T_e + T_i) dV = 4.73 \, Ra^2 n (T_e + T_i) \int_0^1 \hat{n} \tilde{T} du^2 \quad [joule, kev, cm^{-3}]$$

where, for a parabolic profile, the profile factor is

$$\int_0^1 \hat{n} \tilde{T} du^2 = \int_0^1 (1-u^2)^2 du^2 = \frac{1}{3}$$

Therefore, the energy content of the plasma for parabolic profile is

$$E = 1.58 \cdot 10^{-15} \, n (T_e + T_i) Ra^2 \quad [joule, kev, cm^{-3}, cm]$$

ii) Poloidal Beta β_θ

We calculate the poloidal beta, defined here as the average poloidal field pressure at the edge of the plasma. Hence,

$$\beta_\theta = \frac{\langle nk(T_e+T_i)\rangle}{B_p^2(a)/8\pi} = nk(T_e+T_i)\cdot 8\pi \left(\frac{R}{\kappa a B}\right)^2 \cdot \int_0^1 \tilde{n}\tilde{T}\, du^2$$

Similar to i) above, the profile factor is 1/3, so that

$$\beta_\theta = 1.34\cdot 10^{-8}\,\frac{n(T_e+T_i)R^2}{\kappa^2 a^2 B^2} \qquad [cm^{-3},\ kell,\ cm,\ G)$$

iii) Energy Replacement Time τ_E''

We define the total energy replacement time as the ratio of energy content to total input power. Hence,

$$\tau_E'' = \frac{E}{W_{OH} + W_e^h + W_i^h} \qquad [msec,\ joule,\ keV]$$

APPENDIX II - THE EFFECT OF IMPURITIES

In this appendix, the effect of impurities with Z and A different from 1 on the transport coefficients is derived. We choose to define the impurity concentration in terms of the effective charge Z_{eff}. Let the main species ions be denoted by the subscript i, the impurity ions be denoted by o, then Z_{eff} is defined by

$$Z_{eff} = \frac{1}{n_e} \cdot \sum n_i Z_i^2 = \frac{n_i Z_i^2 + n_o Z_o^2}{n_e}$$

Charge neutrality demands that the electron density equals

$$n_e = n_i Z_i + n_o Z_o$$

Hence, the main ion and impurity ion concentrations are given by

$$\frac{n_i}{n_e} = \frac{Z_o - Z_{eff}}{Z_i (Z_o - Z_i)} \quad ; \quad \frac{n_o}{n_e} = \frac{Z_{eff} - Z_i}{Z_o (Z_o - Z_i)}$$

a) Equilibration between electrons, main ions, and impurities

From Spitzer, (Ref. 6), the equilibration rate between two species is given by

$$\nu_{12}^{eq} = 1.36 \cdot 10^{-7} \frac{n_2 Z_1^2 Z_2^2 \ln\Lambda}{A_1 A_2 (T_1/A_1 + T_2/A_2)^{3/2}} \quad [eV, cm^{-3}, sec^{-1}]$$

The power transferred between the two species per unit volume is then

$$P_{12} = \frac{3}{2} n_1 k (T_1 - T_2) \nu_{12}^{eq}, \text{ or}$$

$$P_{12} = 3.26 \cdot 10^{-26} \frac{n_1 n_2 Z_1^2 Z_2^2 \ln\Lambda}{A_1 A_2} \frac{T_1 - T_2}{(T_1/A_1 + T_2/A_2)^{3/2}} \quad [W/cm^3, eV, cm^{-3}]$$

If we let P_{ei}' be the power that would be transferred between electrons and ions in a pure electron-hydrogen plasma, i.e.,

$$P_{ei}' = 3.26 \cdot 10^{-26} n_e^2 \ln\Lambda \frac{T_e - T_i}{T_e^{3/2}} A_e^{1/2} \quad [W/cm^3, eV, cm^{-3}]$$

we may write the power transferred between the various species for general main ion species and impurity ions as

$$P_{ei} = \frac{Z_o - Z_{eff}}{Z_o - Z_i} \frac{Z_i}{A_i} P_{ei}'$$

$$P_{eo} = \frac{Z_{eff} - Z_i}{Z_o - Z_i} \frac{Z_o}{A_o} P_{ei}' \cdot \frac{T_e - T_o}{T_e - T_i}$$

$$P_{io} = \frac{(Z_o - Z_{eff})(Z_{eff} - Z_i)}{(Z_o - Z_i)^2} \frac{Z_o Z_i}{A_o A_i A_e^{1/2}} \frac{T_e^{3/2}}{\left(\frac{T_i}{A_i} + \frac{T_o}{A_o}\right)^{3/2}} \frac{T_i - T_o}{T_e - T_i} P_{ei}'$$

If ohmic heating is assumed to be the only energy input, the complete power balance equations may be written

$$P_{OH} = P_e^{loss} + P_{ei} + P_{eo}$$
$$P_{ei} = P_i^{loss} + P_{io}$$
$$P_{eo} = P_o^{loss} - P_{io}$$

From these equations, since the inputs and losses are positive, it is clear that

$$|P_{io}| \leq \max \{P_{ei}, P_{eo}\}$$

If we substitute the powers derived above, and further assume reasonably that

$$\left(\frac{\frac{T_i}{A_i} + \frac{T_o}{A_o}}{T_e}\right)^{3/2} < \left(\frac{1}{3}\right)^{3/2}, \text{ and } \frac{T_e - T_o}{T_e - T_i} \sim 1$$

this inequality may be written as

$$\left|\frac{T_i - T_o}{T_e - T_i}\right| \leq 4.5 \cdot 10^{-3} \cdot \max\left\{\frac{z_o - z_i}{z_{eff} - z_i}\frac{A_o}{z_o}, \frac{z_o - z_i}{z_o - z_{eff}}\frac{A_i}{z_i}\right\}$$

We now calculate some examples of typical cases that might occur in WEGA operation:

i) i = hydrogen, $Z_i = 1$, $A_i = 1$, o = oxygen, $Z_o = 8$, $A_o = 16$, $Z_{eff} = 3$

$$\left|\frac{T_i - T_o}{T_e - T_i}\right| < \frac{1}{32}$$

ii) i = hydrogen, $Z_i = 1$, $A_i = 1$, o = oxygen, $Z_o = 5$, $A_o = 16$, $Z_{eff} = 2.2$

$$\left|\frac{T_i - T_o}{T_e - T_i}\right| < \frac{1}{21}$$

iii) i = hydrogen, $Z_i = 1$, $A_i = 1$, o = iron, $Z_o = 22$, $A_o = 56$, $Z_{eff} = 5$

$$\left|\frac{T_i - T_o}{T_e - T_i}\right| < \frac{1}{17}$$

From these examples, it is clear that for reasonable cases

$$\left|\frac{T_i - T_o}{T_e - T_i}\right| < \frac{1}{10} \ll 1$$

Hence, as is already reasonable from the large mass difference between ions and electrons, the energy transfer between main ions and impurity ions is much more effective than the transfer between ions and electrons. Therefore, we are justified in setting $T_i = T_o$ in all the calculations.

b) Impurity Multiplier Factors

Following the result of a) above, we may set the main and impurity ion temperatures equal. If we now express the various loss powers as the power that would be lost in an ideal electron-hydrogen plasma at the same electron density n multiplied by an impurity factor ζ, these impurity factors are given by

i) Electron Collision Frequency

The total electron collision frequency is given by

$$\nu_e = \nu_{ei} + \nu_{eo} \sim \frac{\sum n_i z_i^2}{n_e} \nu_{ei}$$

Hence,

$$\zeta_{\nu_e} = z_{eff}$$

ii) Ohmic heating

The ohmic heating power is proportional to

$$W_{OH} \propto \eta j_{\parallel}^2 \sim \nu_e$$

Hence,

$$\zeta_{OH} = z_{eff}$$

iii) Pseudoclassical electron heat conduction

This is proportional to

$$W_e^{PC} \propto n_e \nu_e$$

Hence,

$$\zeta_e^{PC} = z_{eff}$$

iv) Plateau Regime electron convection

This is independent of collision frequency. Hence,

$$\zeta_e^{P} = 1$$

v) Electron-Ion Exchange

From a) above, the total power exchanged between electrons and ions is proportional to

$$W_{ei} \propto n_e \sum \frac{n_i z_i^2}{A_i}$$

Hence,

$$\zeta_{ei} = \frac{z_0 - z_{eff}}{z_0 - z_i} \frac{z_i}{A_i} + \frac{z_{eff} - z_i}{z_0 - z_i} \frac{z_0}{A_0}$$

vi) Plateau Regime ion heat conduction

This is proportional to

$$W_i^P \propto \Sigma n_i A_i^{1/2}$$

Hence,

$$\zeta_i^P = A_i^{1/2} \frac{Z_0 - Z_{eff}}{Z_i (Z_0 - Z_i)} + A_0^{1/2} \frac{Z_{eff} - Z_i}{Z_0 (Z_0 - Z_i)}$$

vii) Banana Regime ion heat conduction

This is proportional to

$$W_i^b \propto \Sigma n_i \nu_{ii} \propto \Sigma \frac{n_i^2 Z_i^4}{A_i^{1/2}}$$

Hence,

$$\zeta_i^b = \left(\frac{Z_0 - Z_{eff}}{Z_0 - Z_i}\right)^2 \frac{Z_i^2}{A_i^{1/2}} + \left(\frac{Z_{eff} - Z_i}{Z_0 - Z_i}\right)^2 \frac{Z_0^2}{A_0^{1/2}}$$

These results are given again in Table II-1. Numerical values for these impurity factors for some typical cases are plotted as a function of Z_{eff} in Fig. II-1.

TABLE II - 1

EXPRESSIONS FOR IMPURITY FACTORS

Ohmic Heating	$\zeta_{OH} = Z_{eff}$
Pseudocl. Electron Cond.	$\zeta_e^{PC} = Z_{eff}$
Plateau Reg. Electron Conv.	$\zeta_e^{P} = 1$
Electron-Ion Transfer	$\zeta_{ei} = \frac{Z_i}{A_i}\frac{Z_0 - Z_{eff}}{Z_0 - Z_i} + \frac{Z_0}{A_0}\frac{Z_{eff} - Z_i}{Z_0 - Z_i}$
Plateau Reg. Ion Cond.	$\zeta_i^{P} = \frac{A_i^{1/2}}{Z_i}\frac{Z_0 - Z_{eff}}{Z_0 - Z_i} + \frac{A_0^{1/2}}{Z_0}\cdot\frac{Z_{eff} - Z_i}{Z_0 - Z_i}$
Banana Reg. Ion Cond.	$\zeta_i^{b} = \frac{Z_i^2}{A_i^{1/2}}\left(\frac{Z_0 - Z_{eff}}{Z_0 - Z_i}\right)^2 + \frac{Z_0^2}{A_0^{1/2}}\left(\frac{Z_{eff} - Z_i}{Z_0 - Z_i}\right)^2$

IMPURITY FACTORS, VARIOUS CASES

Hydrogen Plasma $Z_i=1$
$A_i=1$
Oxygen Impurity $Z_o=8$
$(T_e \geq 1keV)$ $A_o=16$

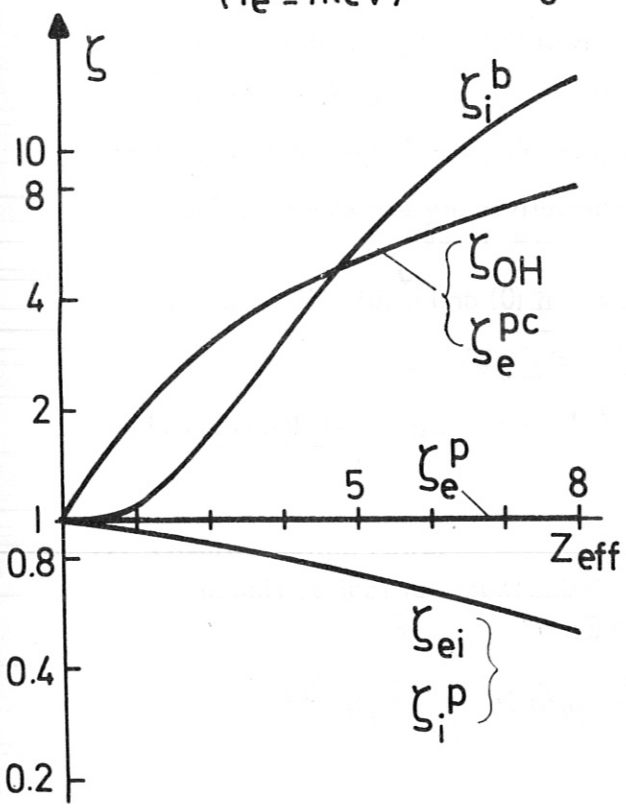

Hydrogen Plasma $Z_i=1$
$A_i=1$
Oxygen Impurity $Z_o=5$
$(T_e \sim 150eV)$ $A_o=16$

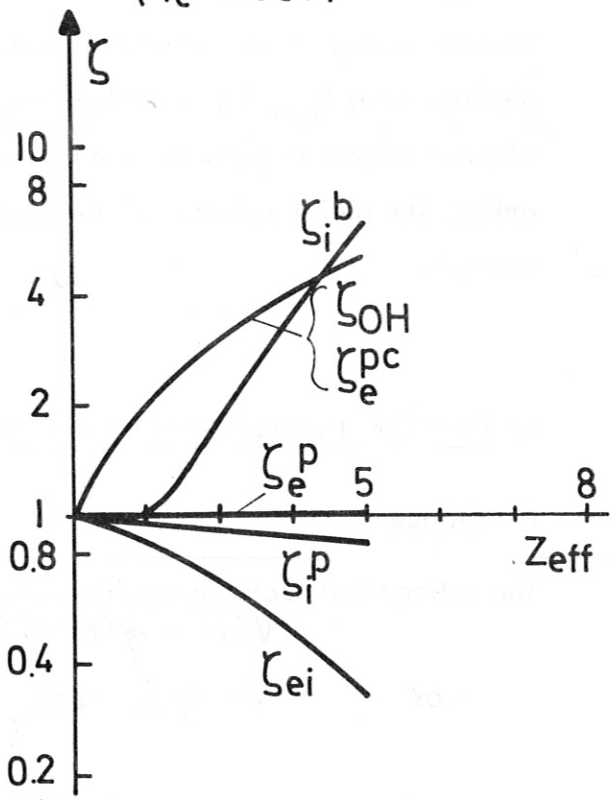

Hydrogen Plasma $Z_i=1$
$A_i=1$
Iron Impurity $Z_o=22$
$A_o=56$

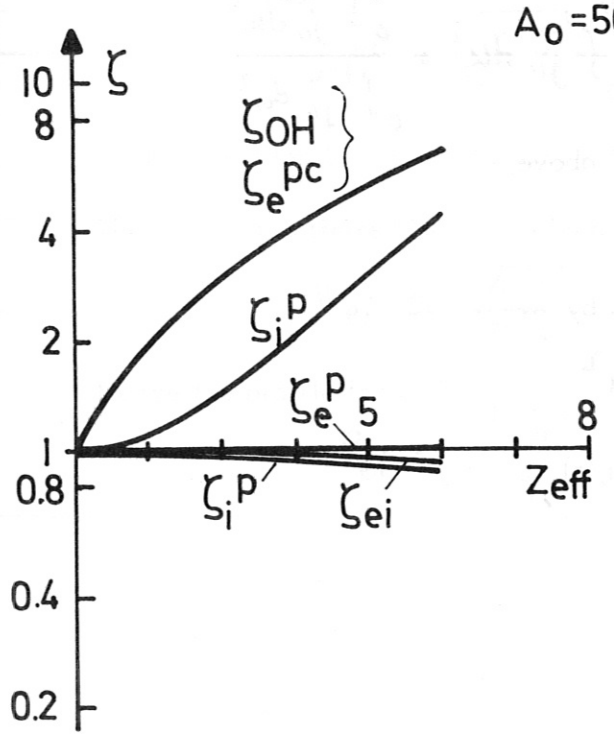

Deuterium Plasma $Z_i=1$ $A_i=2$
Oxygen Impurity $Z_o=8$ $A_o=16$

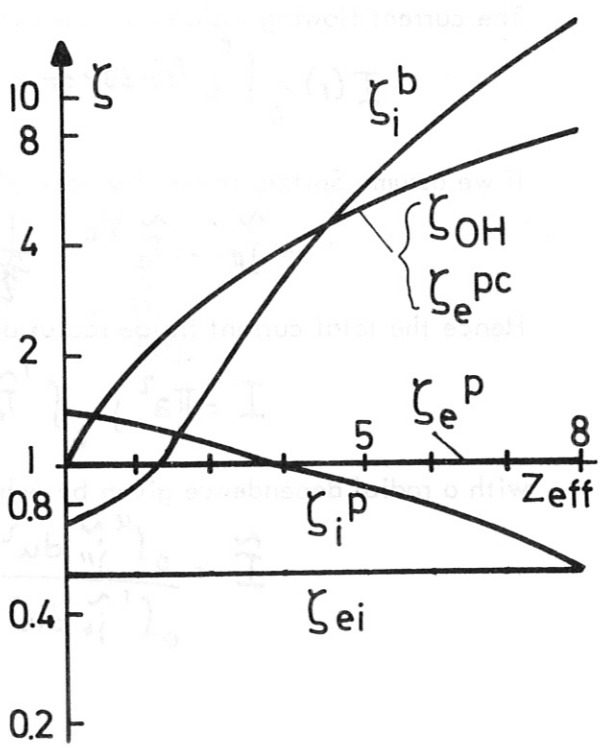

Fig. II-1

APPENDIX III - PROFILE FACTORS

In order to include the effect of radial variations of the various quantities, the profile factors P_{OH} & c are calculated, where P = 1 refers to a uniform profile or, where gradients of quantities are involved, a gradient scale length of a, the minor radius. The radial variation of the quantities themselves are expressed as, for example,

$$n(r) = n \cdot \tilde{n}(r), \text{ where } n = n(0) \text{ and } \tilde{n}(0) = 1$$

a) Profile Factors for General Profile and Spitzer Resistivity

i) Voltage

The voltage is inductively applied, and hence independent of radius. Hence,

$$V(r) = \eta(r) \cdot j_{\parallel}(r) \cdot 2\pi R = V \quad , \quad \tilde{V} = 1$$

or $$V = \eta J_{\parallel} \cdot 2\pi R, \quad \eta(r)\, j_{\parallel}(r) = \eta(0)\, j_{\parallel}(0)$$

i.e. the product of resistivity and current density is a constant.

ii) Current, Current Profile

The current flowing inside a radius r is given by

$$I(r) = \int_0^r j_{\parallel}(r) \cdot 2\pi r\, dr = \pi a^2 j_{\parallel} \int_0^1 \tilde{j}_{\parallel}\, du^2 \cdot \frac{\int_0^u \tilde{j}_{\parallel}\, du^2}{\int_0^1 \tilde{j}_{\parallel}\, du^2}$$

If we assume Spitzer resistivity, and also use i) above,

$$\tilde{j}_{\parallel} = \tilde{T}_e^{3/2} = \frac{1}{\tilde{\eta}}$$

Hence the total current inside radius a is given by

$$I = \pi a^2 j_{\parallel} \int_0^1 \tilde{T}_e^{3/2}\, du^2$$

with a radial dependence given by (where u = r/a)

$$\tilde{I} = \frac{\int_0^u \tilde{j}_{\parallel}\, du^2}{\int_0^1 \tilde{j}_{\parallel}\, du^2}$$

iii) Rotational Transform

The rotational transform due to the current is given by

$$\iota_I(r) = \frac{RI(r)}{5r^2B}$$

Letting ι_I be the rotational transform due to the current at the edge (r = a), ι_0 be the helical rotational transform, then the total rotational transform at the edge of the plasma is given by

$$\iota = \iota_I + \iota_0$$

with a radial variation:

$$\tilde{\iota} = \frac{\iota_I \frac{\tilde{I}}{u^2} + \iota_0}{\iota_I + \iota_0}$$

iv) Ohmic Heating Power

The power input from the ohmic heating is given by

$$W_{OH} = \int \eta j_{\parallel}^2 \, dV$$

Using i) above, as well as ii), this may be written:

$$W_{OH} = \eta j_{\parallel}^2 \int \tilde{j}_{\parallel} dV = \eta I^2 \cdot \frac{2\pi R}{\pi a^2} \cdot \frac{1}{\int_0^1 \tilde{T}_e^{3/2} du^2}$$

Hence the profile factor (relative to uniform distribution) is

$$P_{OH} = \frac{1}{\int_0^1 \tilde{T}_e^{3/2} du^2}$$

v) Electron-Ion Energy Exchange

The power transferred between electrons and ions is proportional to

$$W_{ei} \propto \frac{\tilde{n}^2(r)}{T_i^{1/2}(r)} \quad ; \quad \tilde{W}_{ei} = \frac{\tilde{n}^2}{\tilde{T}_i^{1/2}}$$

Hence the profile factor is

$$P_{ei} = \int_0^1 \frac{\tilde{n}^2}{\tilde{T}_i^{1/2}} du^2$$

vi) Convective Losses

All convective losses may be written as

$$W_{conv} = \int \frac{3}{2} kT \frac{\partial n}{\partial t} dV = \int \frac{3}{2} kT \left(-\nabla \cdot D \nabla n\right) dV$$

which, after integration by parts and assuming $TD \frac{dn}{dr}\Big|_{r=a} = 0$

$$W_{conv} = \frac{3}{2} k \cdot 4\pi^2 R \int r D \frac{dn}{dr} \frac{dT}{dr} dr$$

Hence the profile factor is

$$P_{conv} = {}_0\int^1 \tilde{D} \frac{d\tilde{n}}{du} \frac{d\tilde{T}}{du} du^2$$

Specifically, for intermediate regime electron convection,

$$\tilde{D}_e^{\,P} = \frac{\tilde{T}_e^{\,3/2}}{\tilde{\kappa}}$$

$$P_e^{\,P} = 2 {}_0\int^1 u \frac{\tilde{T}_e^{\,3/2}}{\tilde{\kappa}} \frac{d\tilde{n}}{du} \frac{d\tilde{T}_e}{du} du$$

vii) Heat Conduction Losses

This is the same as convective losses, vi), except $D \longrightarrow K$.

For plateau regime ion heat conduction, then,

$$\tilde{K}_i^{\,P} = \tilde{T}_i^{\,3/2} / \tilde{\kappa}$$

$$P_i^{\,P} = 2 {}_0\int^1 u \frac{\tilde{T}_i^{\,3/2}}{\tilde{\kappa}} \cdot \frac{d\tilde{n}}{du} \cdot \frac{d\tilde{T}}{du} du$$

For pseudoclassical electron heat conduction, the profile factor results as

$$\tilde{K}_e^{\,Pc} = \frac{\tilde{n}}{\tilde{T}_e^{\,1/2} \tilde{\kappa}^2}$$

$$P_e^{\,Pc} = 2 {}_0\int^1 u \frac{\tilde{n}}{\tilde{T}_e^{\,1/2} \tilde{\kappa}^2} \frac{d\tilde{n}}{du} \frac{d\tilde{T}}{du} du$$

viii) Banana Regime Heat Conduction

Stix (Ref.3) give the profile factor for banana regime heat conduction of the ions as

$$P_i^{\,b} = \left\langle -\frac{r}{T(r)} \frac{dT(r)}{dr} \left(\frac{a}{r}\right)^{3/2} \right\rangle$$

b) Expressions for Uniform Profile

$$\tilde{n} = \tilde{T}_e = \tilde{T}_i = 1$$

i) Voltage $\tilde{\eta} = 1$, $\tilde{j}_{||} = 1$

ii) Current $I = \pi a^2 j_{||}$, $\tilde{I} = u^2$

iii) Iota $\tilde{\iota} = 1$

iv) - vii) Profile cannot be uniform since then no diffusion or heat conduction.

But assume $\frac{d\tilde{n}}{du}$ = const, then $P = 1$.

c) Expressions for Parabolic Profile

$$\tilde{n} = \tilde{T}_e = \tilde{T}_i = (1-u^2)$$

$$I = \pi a^2 j_{||} \int_0^1 (1-u^2)^{3/2} du^2 \longrightarrow I = \frac{2}{5} \pi a^2 j_{||}$$

$$\tilde{I} = \frac{\int_0^u (1-u^2)^{3/2} du^2}{\frac{2}{5}} \longrightarrow \tilde{I} = 1 - (1-u^2)^{5/2}$$

$$\tilde{\iota} = \frac{\iota_I \cdot \frac{\tilde{I}}{u^2} + \iota_0}{\iota_I + \iota_0} \longrightarrow \tilde{\iota} = \frac{\iota_I \cdot \frac{1-(1-u^2)^{5/2}}{u^2} + \iota_0}{\iota_I + \iota_0}$$

$$P_{OH} = \frac{1}{\int_0^1 (1-u^2)^{3/2} du^2} \longrightarrow P_{OH} = \frac{5}{2}$$

$$P_{ei} = \int_0^1 \frac{\tilde{n}^2}{\tilde{T}_i^{1/2}} du^2 = \int_0^1 (1-u^2)^{3/2} du^2 \longrightarrow P_{ei} = \frac{2}{5}$$

$$P_e{}^P = 2 \int_0^1 u \frac{(1-u^2)^{3/2}}{\tilde{\iota}} \cdot (2u)^2 du \longrightarrow P_e{}^P = 4 \int_0^1 \frac{(1-u^2)^{3/2}}{\tilde{\iota}} u^2 du^2$$

$$P_i{}^P = 2 \int_0^1 u \frac{(1-u^2)^{3/2}}{\tilde{\iota}} (2u)^2 du \longrightarrow P_i{}^P = P_e{}^P$$

$$P_e{}^{Pc} = 2 \int_0^1 u \frac{\tilde{n}}{\tilde{T}_e^{1/2} \tilde{\iota}^2} \frac{d\tilde{n}}{du} \frac{d\tilde{T}}{du} du \longrightarrow P_e{}^{Pc} = 4 \int_0^1 \frac{(1-u^2)^{1/2}}{\tilde{\iota}^2} u^2 du^2$$

$$P_i{}^b = \left\langle -\frac{r}{1-u^2} (-2u) \cdot \frac{1}{u^{3/2}} \right\rangle = \left\langle \frac{2u^{1/2}}{1-u^2} \right\rangle \longrightarrow P_i{}^b = 1.886$$

The expressions given here for a parabolic profile are the ones quoted in Table I of the main text, and used throughout the calculation. The variation of various quantities, particularly the power densities, as a function of radius are plotted for a parabolic profile in Fig. III-1.

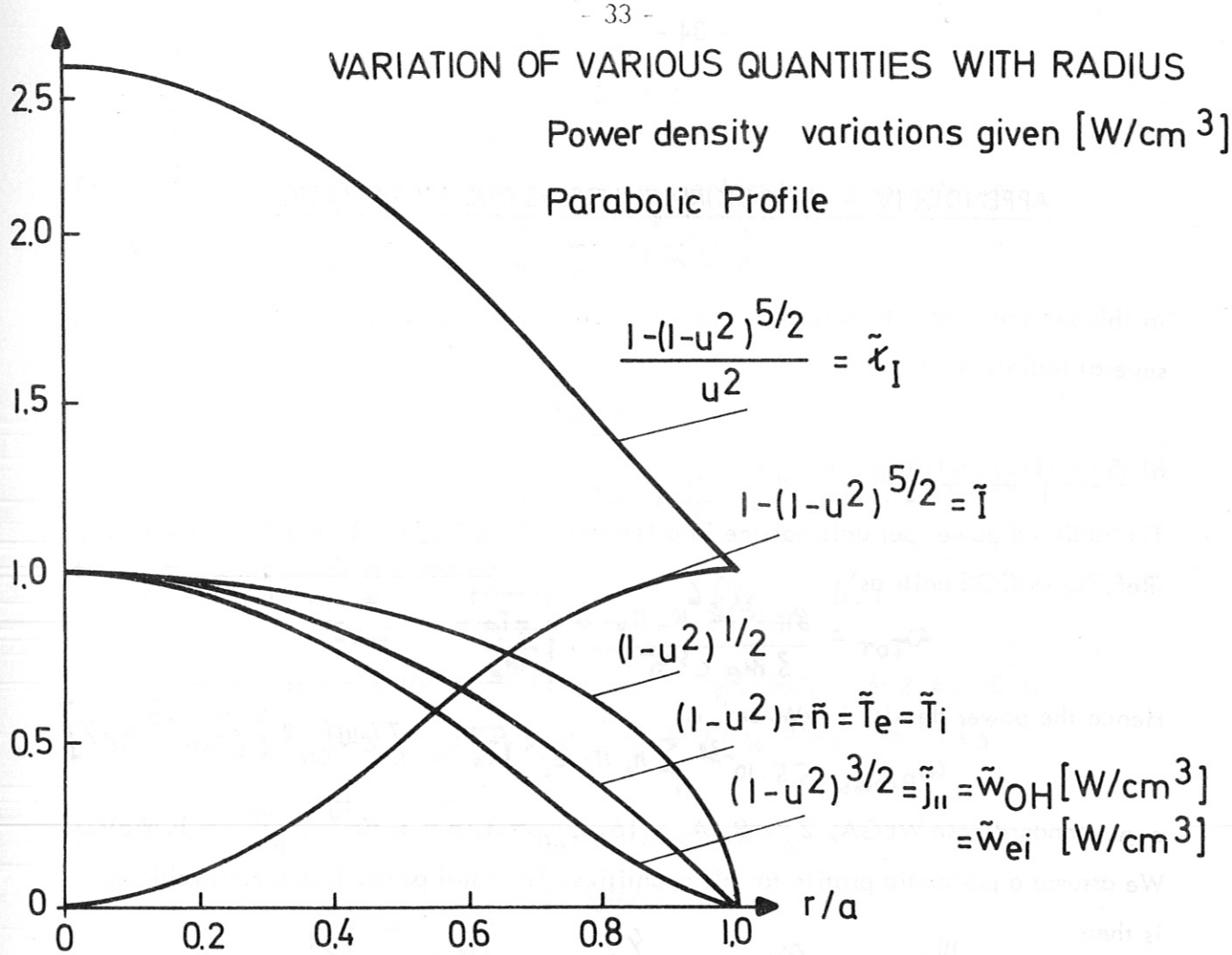
VARIATION OF VARIOUS QUANTITIES WITH RADIUS
Power density variations given [W/cm 3]
Parabolic Profile
$\frac{1-(1-u^2)^{5/2}}{u^2} = \tilde{\iota}_I$
$1-(1-u^2)^{5/2} = \tilde{I}$
$(1-u^2)^{1/2}$
$(1-u^2) = \tilde{n} = \tilde{T}_e = \tilde{T}_i$
$(1-u^2)^{3/2} = \tilde{j}_{II} = \tilde{w}_{OH}$ [W/cm 3]
$= \tilde{w}_{ei}$ [W/cm 3]
r/a
0
0.2
0.4
0.6
0.8
1.0
0.5
1.0
1.5
2.0
2.5

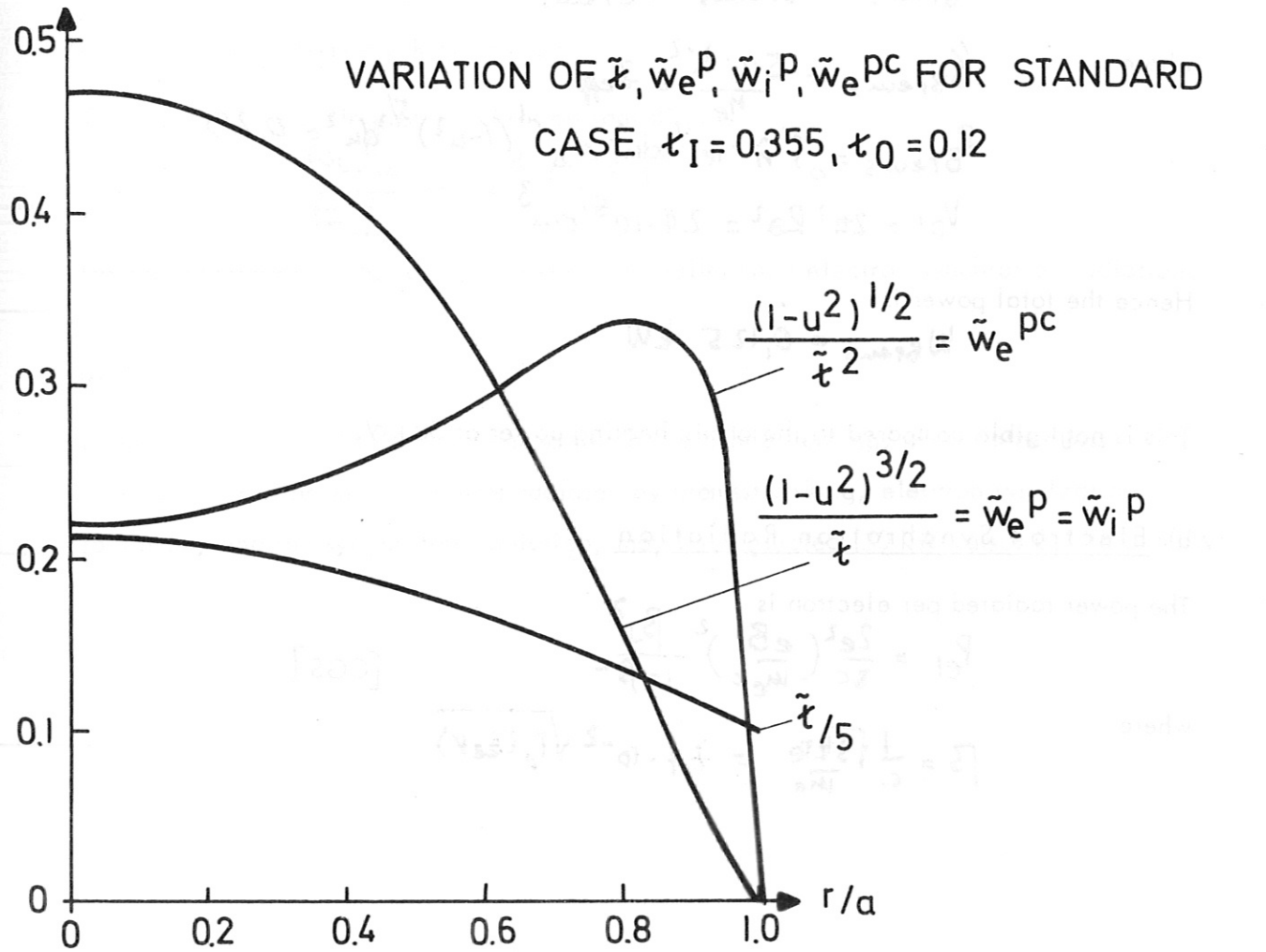
VARIATION OF $\tilde{\iota}, \tilde{w}_e{}^p, \tilde{w}_i{}^p, \tilde{w}_e{}^{pc}$ FOR STANDARD
CASE $\iota_I = 0.355, \iota_0 = 0.12$
$\frac{(1-u^2)^{1/2}}{\tilde{\iota}^2} = \tilde{w}_e{}^{pc}$
$\frac{(1-u^2)^{3/2}}{\tilde{\iota}} = \tilde{w}_e{}^p = \tilde{w}_i{}^p$
$\tilde{\iota}/5$
r/a
0
0.2
0.4
0.6
0.8
1.0
0.1
0.2
0.3
0.4
0.5

Fig. III-1

APPENDIX IV - APPROXIMATE LOSSES DUE TO RADIATION

In this section, we calculate the order of magnitude of the power lost due to several radiation effects.

a) Bremsstrahlung

The radiated power per unit volume into bremsstrahlung is given by Boyd & Saunderson, (Ref.7), in CGS units as

$$\omega_{TOT} = \frac{8\pi}{3} \frac{\hbar^2 e^6}{m_e c^3 \hbar} n_- n_+ \cdot \sqrt{\frac{kT_e}{m_e}} \qquad [CGS]$$

Hence the power density in kW/cm^3 is

$$\omega_{Brems} = 5.5 \cdot 10^{-34} \sum_i n_e n_i Z_i^2 \sqrt{T_e} \qquad [kW/cm^3] \; [cm^{-3}, keV]$$

e.g. standard case WEGA, $Z_o = 8$, $A_o = 16$, $Z_{eff} = 3$, $n = 3.10^{13}$, $T_e^{max} = 1.5 keV$.

We assume a parabolic profile for all quantities. The total power into bremsstrahlung is then

$$W_{Brems} = \omega_{Brems} \cdot \zeta_{Brems} \cdot P_{Brems} \cdot V_{01}$$

where

$$\zeta_{Brems} = \frac{\sum n_i Z_i^2}{n_e} = Z_{eff}$$

$$P_{Brems} = {}_0\int^1 \tilde{n}^2 T_e^{1/2} du^2 = {}_0\int^1 (1-u^2)^{5/2} du^2 = 0.29$$

$$V_{01} = 2\pi^2 R a^2 = 2.4 \cdot 10^5 \; cm^3$$

Hence the total power is

$$W_{Brems} = 0.125 \; kW$$

This is negligible compared to the ohmic heating power of 50 kW.

b) Electron Synchrotron Radiation

The power radiated per electron is

$$P_{el} = \frac{2e^2}{3c} \left(\frac{eB}{m_e c} \right)^2 \frac{\beta_\perp^2}{1-\beta^2} \qquad [CGS]$$

where

$$\beta = \frac{1}{c} \sqrt{\frac{3kT_e}{m_e}} = 7.7 \cdot 10^{-2} \sqrt{T_e (keV)}$$

For $T_e < 10$ keV, $\frac{1}{1-\beta^2} < 1.06$. Hence we can neglect this factor. Hence,

$$\langle P_{el} \rangle = \frac{2}{3} \frac{e^2}{c^3} \left(\frac{eB}{m_e c}\right)^2 \langle v_\perp^2 \rangle$$

and the power radiated per unit volume is

$$\omega_{sync}^{e} = \frac{4}{3} \frac{e^4 B^2}{c^5 m_e^3} n k T_e \qquad [\text{CGS}]$$

This may be rewritten as

$$\omega_{sync}^{e} = 6.18 \cdot 10^{-28} B^2 n T_e \quad [kW/cm^3][G, cm^{-3}, keV]$$

Hence the total power is given by

$$W_{sync}^{e} = \omega_{sync} \cdot \zeta_{sync} \cdot P_{sync} \cdot Vol$$

e.g. standard case $n = 3.10^{13}$, $B = 14.4$ kG, $T_e = 1.5$ keV, $Vol = 2.4 \cdot 10^5$ cm.

$$P_{sync} = {}_0\int^1 \tilde{n} \tilde{T}_e \, du^2 = {}_0\int^1 (1-u^2)^2 du^2 = 0.33$$

$$\zeta_{sync} = 1$$

Hence the total power due to electron synchrotron radiation is

$$W_{sync}^{e} = 0.46 \text{ kW}$$

c) Ion Synchrotron Radiation

The ratio of ion to electron synchrotron radiation is

$$\frac{\omega_{sync}^{i}}{\omega_{sync}^{e}} = Z^4 \left(\frac{m_e}{m_i}\right)^3$$

Hence, because $m_e/m_i \ll 1$, this is much smaller than electron synchrotron radiation.

d) Conclusion

It has been shown that, in comparison with the ohmic heating, or the other loss levels, in equilibrium, the power radiated by bremsstrahlung, electron synchrotron radiation, and ion synchrotron radiation, may be neglected (50 kW versus 0.1 to 0.5 kW).

References

1. Grieger, G., H.Hacker, G.Pacher, H.Renner, H.Ringler, E.Würsching, Proc. Sixth European Conf. on Controlled Fusion and Plasma Physics, Moscow (1973), p.101.

2. Spitzer, Lyman Jr., Physics of Fully Ionized Gases, Interscience Publishers Ltd., London (1956), p.83.

3. Stix, Thomas H., Proc. Symposium on Plasma Heating and Injection, Varenna, Italy (1972), p.1.

4. Yoshikawa, S., and N.Christofilos, Proc. Fourth International Conf. on Plasma Physics and Controlled Nuclear Fusion Research, IAEA, Vienna (1971), Vol.II, p.357.

5. Galeev, A.A., and R.Z.Sagdeev, Zh.Eksp. Teor.Fiz. 53 (1967), 348 (Translation: Sov. Phys. - JETP 26 (1968) 233 .

6. Spitzer, Lyman Jr., ibid., p.80.

7. Boyd, T.J.M., and J.J.Saunderson, Plasma Dynamics, Thomas Nelson & Sons Ltd., London (1969), pp. 211 ff.

Figure Captions

"Standard Case" refers to the input parameters given in Table III.

Fig.1 and 2 Case 1 & 2. Variation of a from 10-16cm [and I from 35,5 - 90,9 kA to keep κ constant] . Other input parameters as in standard case (Table III).

Fig.3 Case 1 & 2. Variation of a from 10-16cm [and I from 35,5 - 90,9 kA to keep κ constant] and n from 7.10^{12} to 5.10^{13}. Other inputs as in Table III.

Fig.4 Case 1 & 2. Variation of n from 7.10^{12} to 5.10^{13} for a = 13cm [I = 60 kA] and a = 16cm [I = 90,9 kA] . Other inputs as in Table III.

Fig.5 - 10 Case 1 & 2. Variation of n from 7.10^{12} to 5.10^{13}, a from 10-16cm [and I from 35,5 to 90 kA, to keep κ constant] . Other inputs as in Table III.

Fig.11 Case 3. Variation of I from 40 - 120 kA [κ_I from 0,23 - 0,7] for κ_o = 0 - 0,3 [κ = 0,23 - 1.0]. Other inputs as in Table III.

Fig.12, 13 Case 3. Variation of I from 40 - 120 kA [κ_I from 0,23 - 0,7] for κ_o = 0,1 [κ = 0,33 - 0,8]. Other inputs as in Table III.

Fig.14 Case 4. Variation at constant κ = 0,5 of κ_I from 0,1 - 0,5, and κ_o from 0,0 to 0,4 [I = 16,9 - 84,5 kA] for n = 1 - 3.10^{13} cm^{-3}. Other inputs as in Table III.

Fig.15, 16 Case 4. Variation at constant κ = 0,5 of κ_I from 0,1 - 0,5 and κ_o from 0,0 to 0,4 [I = 16,9 - 84,5 kA]. Other inputs as in Table III.

Fig.17 Case 5. For c^2pc = 10 and Z_{eff} = 5, variation of a from 10-16cm [and I from 35,5 - 90,9 kA to keep κ constant] for n from 1 - 3.10^{13} cm^{-3}. Other inputs as in Table III.

Fig.18, 19 Case 5. For c^2pc = 10 and Z_{eff} = 5, variation of a from 10-16cm [and I from 35,5 - 90,9 kA]. Other inputs as in Table III.

Fig.20 Case 5. For c^2pc = 10 and Z_{eff} = 5, results for a = 13cm [I = 60 kA] and a = 16cm [I = 90,9 kA]. Other inputs as in Table III.

Fig.21 Case 6 - 9. Variation of B from 10 - 25 kG [and I from 41,7 - 104 kA to keep κ constant] for n = 1 - 3 . 10^{13} cm^{-3}. Other inputs as in Table III.

Fig.22, 23 Case 6 - 9. Variation of B from 10 - 25 kG [and I from 41,7 - 104 kA to keep κ constant]. Other inputs as in Table III.

Fig.24 Case 10. Variation of Z_{eff} from 1 - 8 for n = 1 - 3.10^{13} cm^{-3}. Other inputs as in Table III.

Fig.25, 26 Case 10. Variation of Z_{eff} from 1 - 8 . Other inputs as in Table III.

Fig.27, 28 Case 6. Variation of W_e^h and W_i^h from 0 - 100 kW for n = 1 - 3.10^{13} cm^{-3}. Other inputs as in Table III.

Fig.29 Case 6. Variation of W_e^h and W_i^h from 0 - 100 kW. Other inputs as in Table III.

Fig.30 Case 6. Variation of W_e^h and W_i^h from 0 - 100 kW for n = 1.10^{13} cm^{-3}. Other inputs as in Table III.

Fig.31, 32 Cases 6 - 9. Variation of W_e^h and W_i^h from 0 - 100 kW for B = 10 - 25 kG [and I = 41,7 - 104 kA to keep κ_i constant]. Other inputs as in Table III.

Fig.33 Case 9. Variation of W_e^h and W_i^h from 0 - 100 kW fro n = 1 - 3.10^{13} cm^{-3} and B = 25 kG [I = 104 kA]. Other inputs as in Table III.

Fig.34 Case 9. Variation of W_e^h and W_i^h from 0 - 100 kW for B = 25 kG [I = 104 kA]. Other inputs as in Table III.

Fig.35 Case 6. Variation of W_e^h and W_i^h from 0 - 100 kW. Other inputs as in Table III.

Fig.36 Case 7. Variation of W_e^h and W_i^h from 0 - 100 kW for B = 10 kG [I = 41,7 kA]. Other inputs as in Table III.

Fig.37 Case 9. Variation of W_e^h and W_i^h from 0 - 100 kW for B = 25 kG [I = 104 kA]. Other inputs as in Table III.

CASE 1+2 a) Loss Distribution vs a, $n = 3 \cdot 10^{13} cm^{-3}$

b) T_e vs T_i for various a and n

Fig. 1

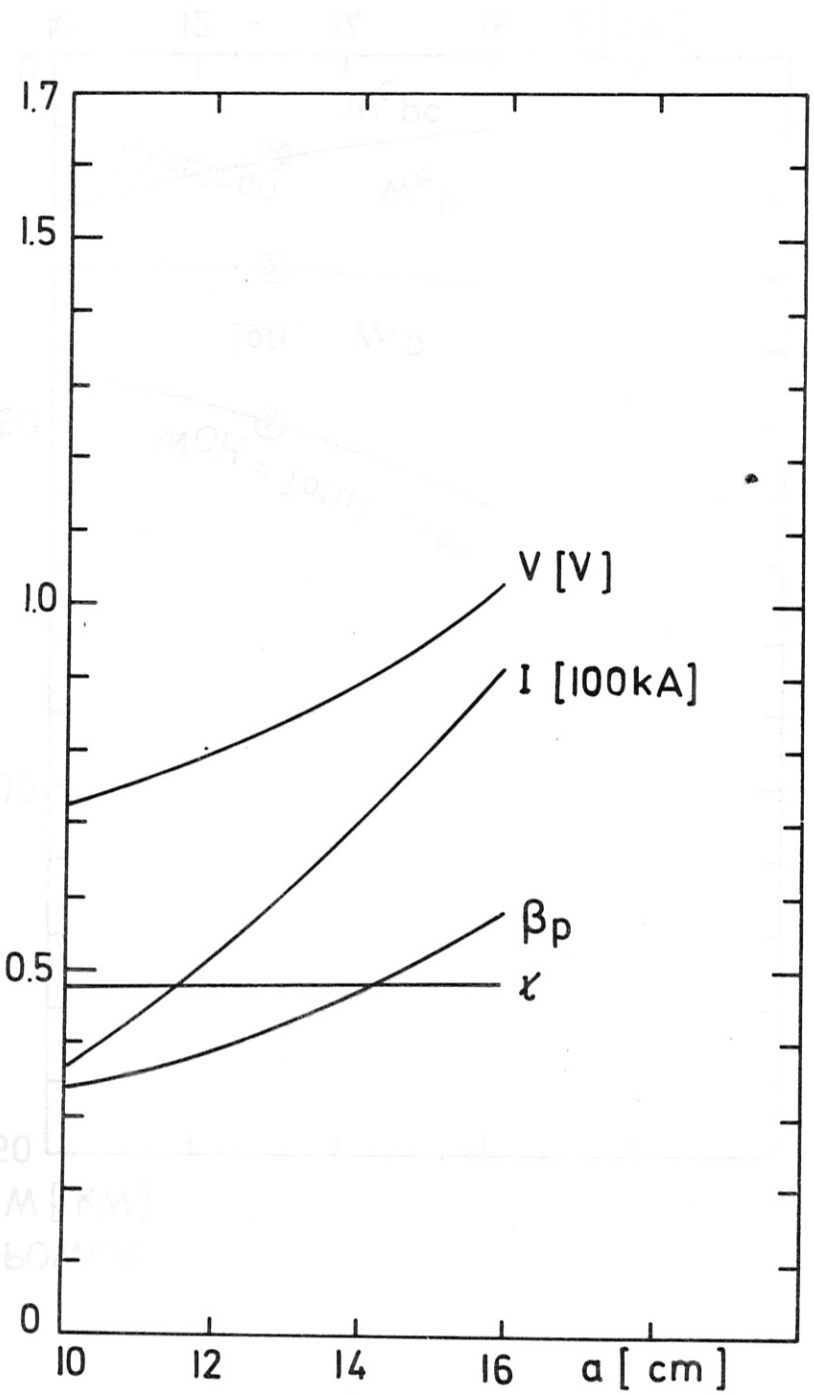

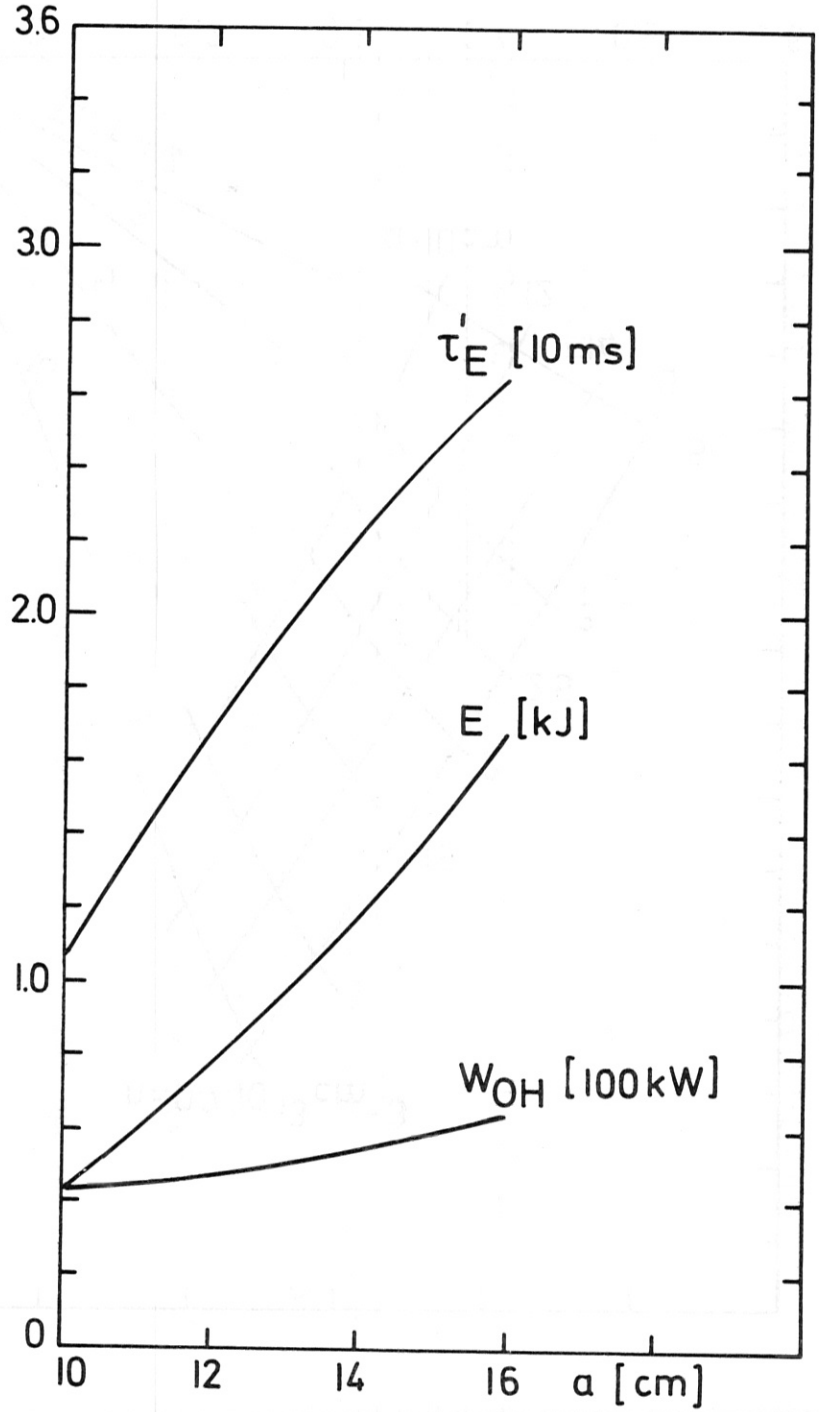

CASE 1+2

a Variation

$n = 3 \cdot 10^{13} cm^{-3}$

Fig. 2

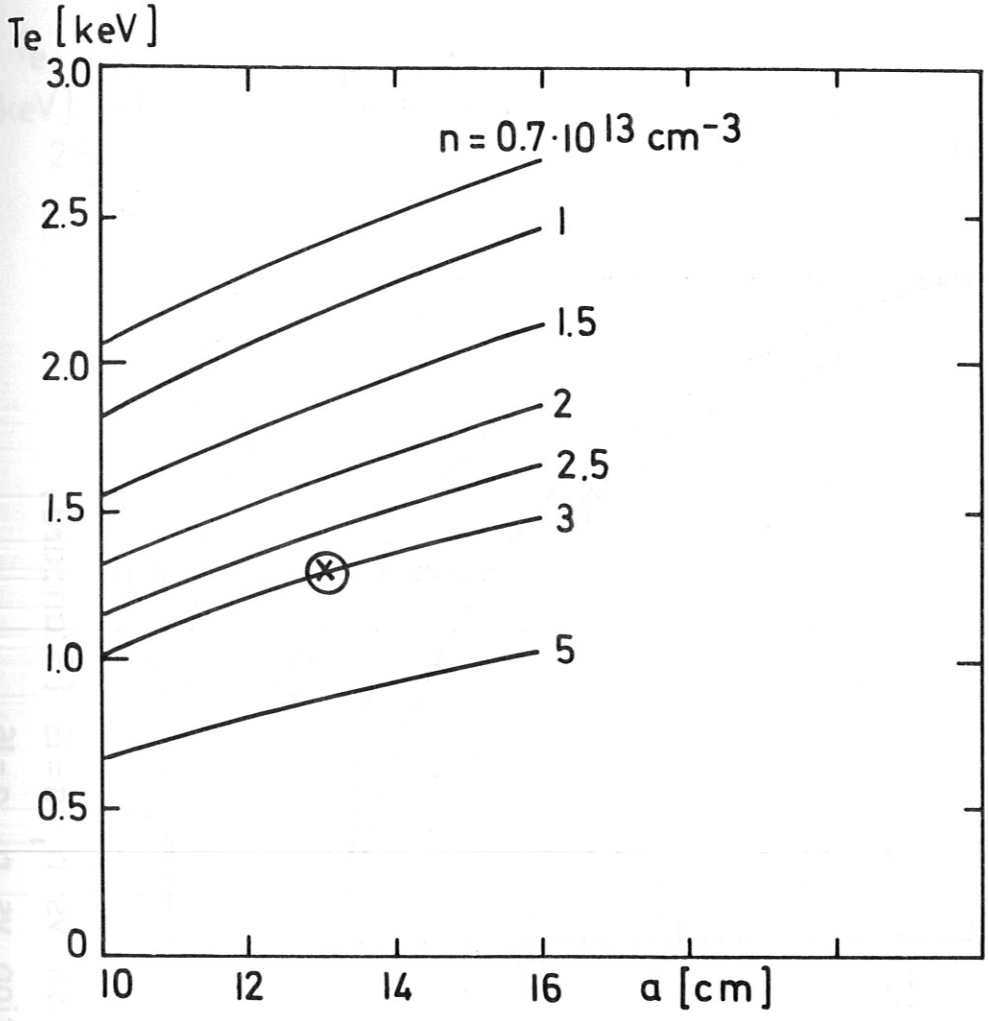

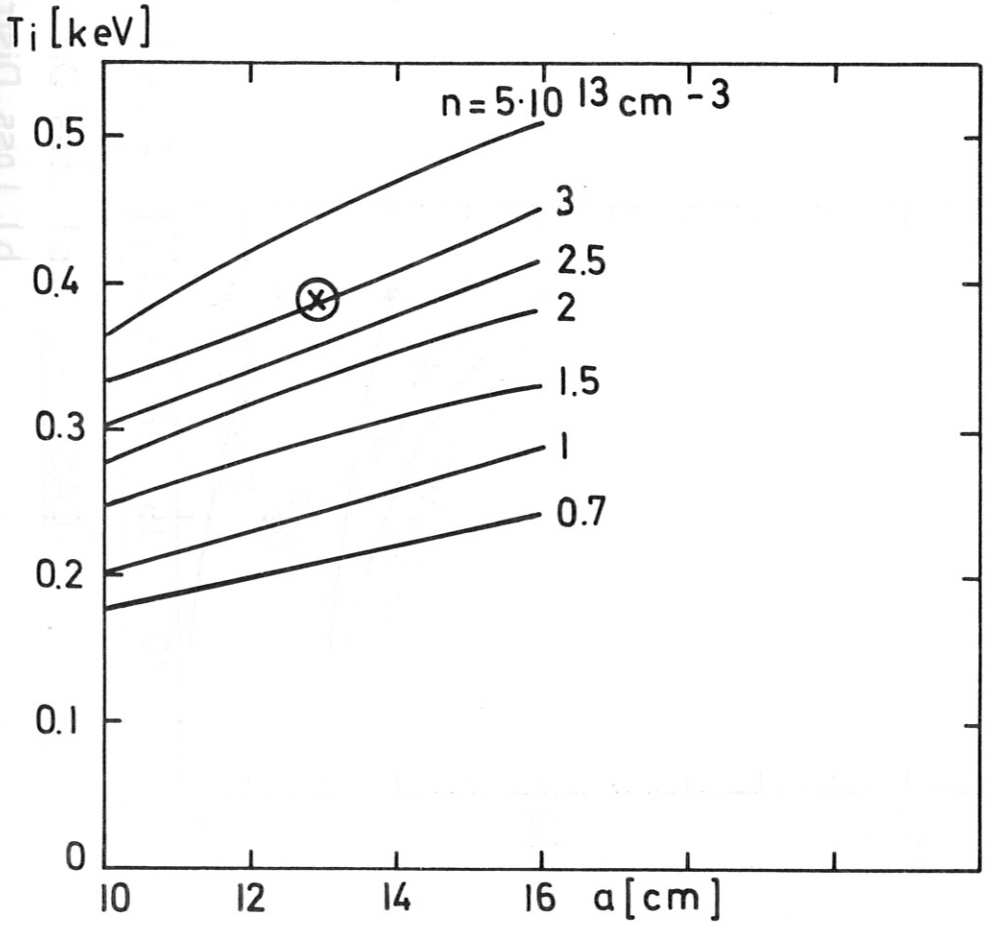

Fig. 3

CASE 1+2

T_e and T_i vs a and n

κ = const

⊗ = Standard Case

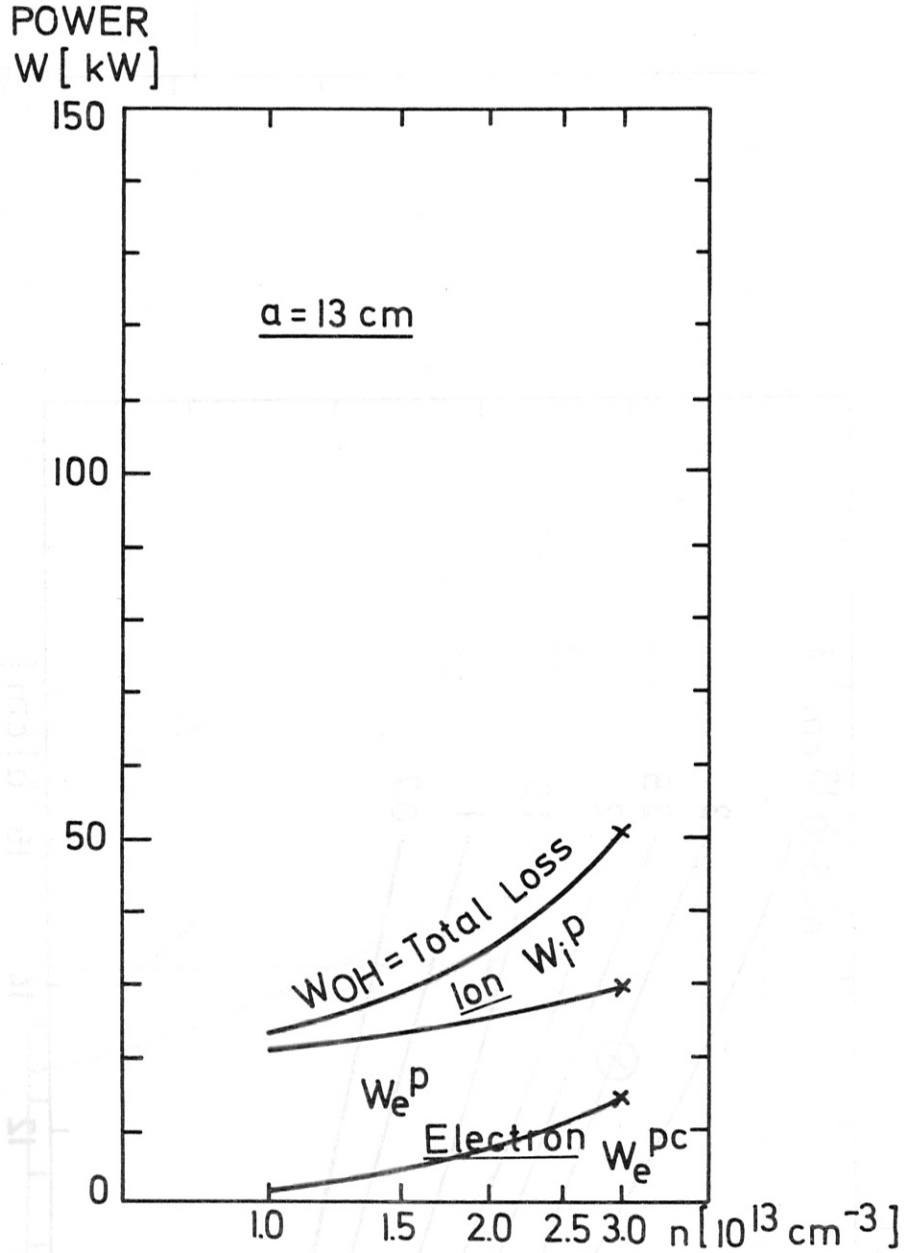

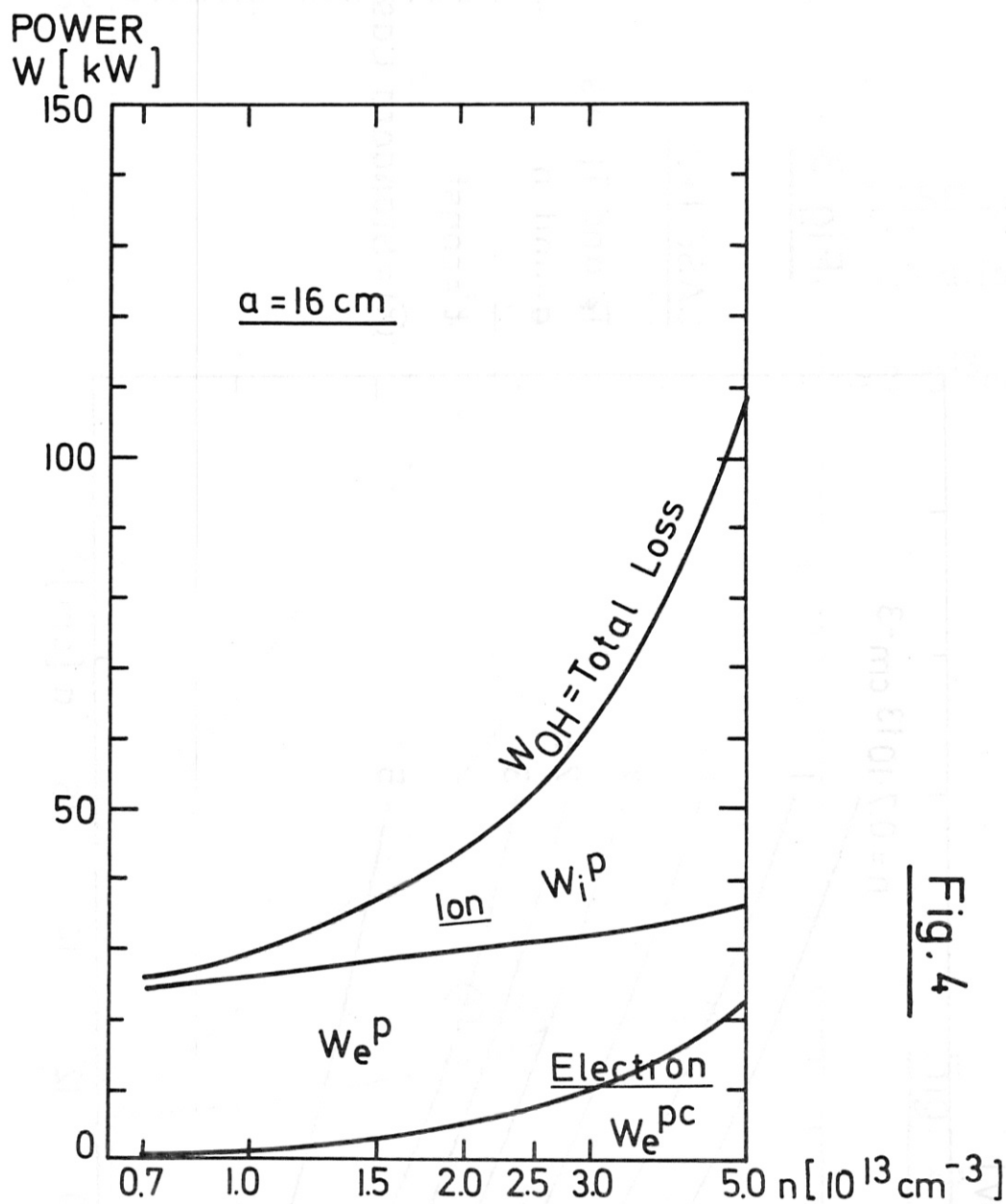

Fig. 4

CASE 1+2 a) Loss Distribution vs n_1 a = 13 (Standard)
b) Loss Distribution vs n_1 a = 16

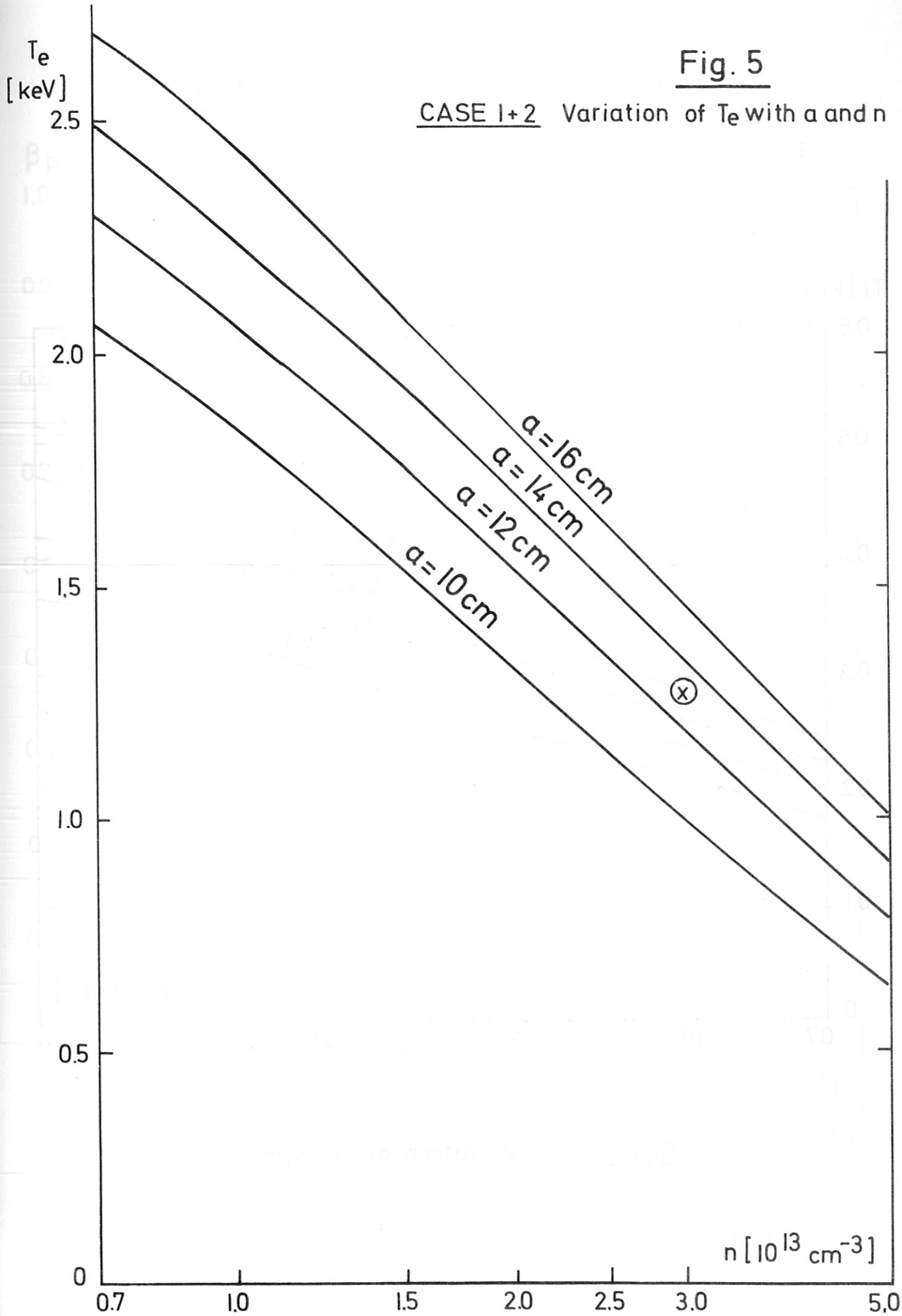
Fig. 5
CASE 1+2 Variation of T_e with a and n
T_e [keV]
2.5
2.0
1.5
1.0
0.5
0
a = 16 cm
a = 14 cm
a = 12 cm
a = 10 cm
n [10^{13} cm^{-3}]
0.7
1.0
1.5
2.0
2.5
3.0
5.0

Fig. 6

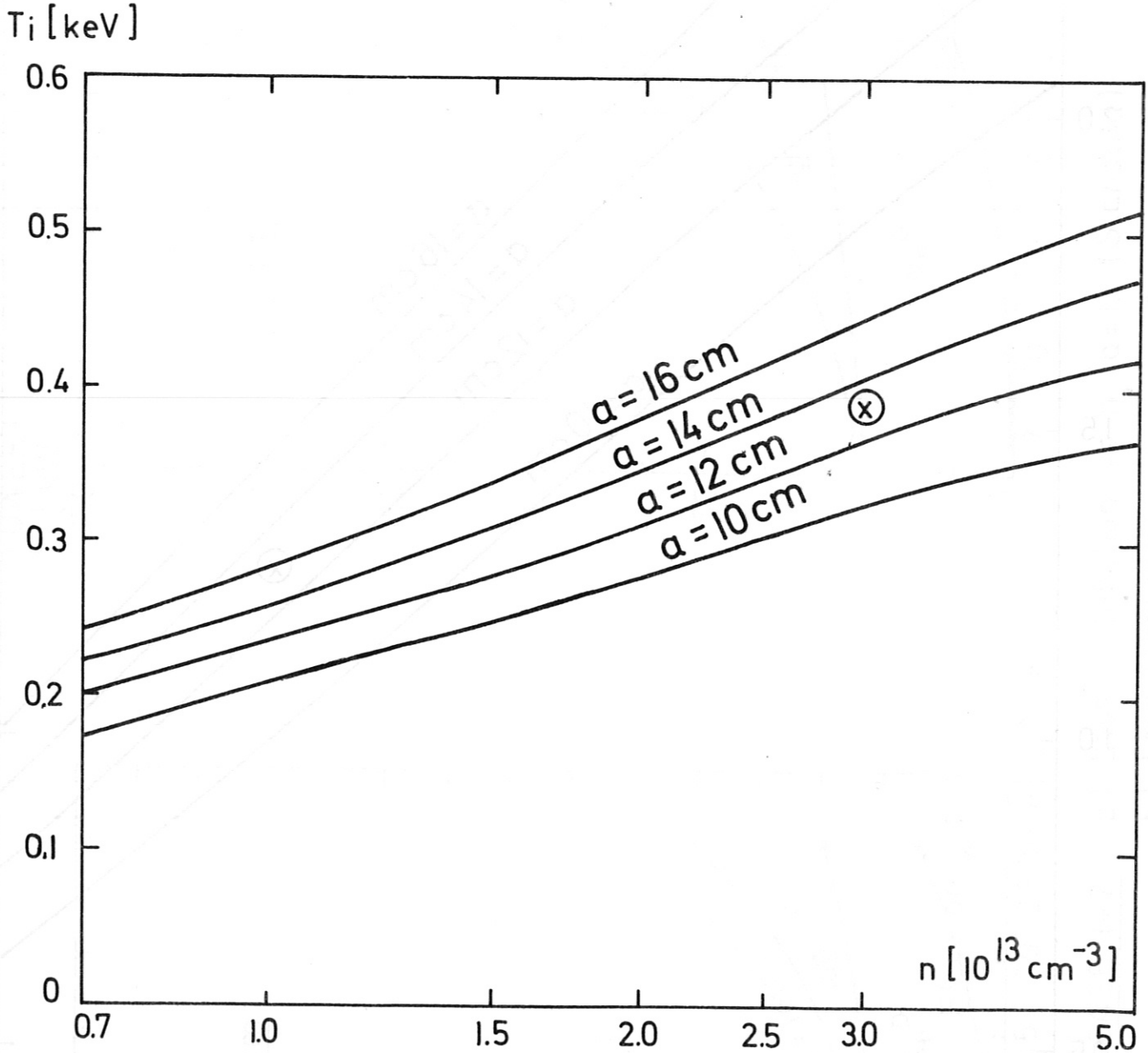

CASE 1+2 Variation of T_i with a and n

Fig. 7

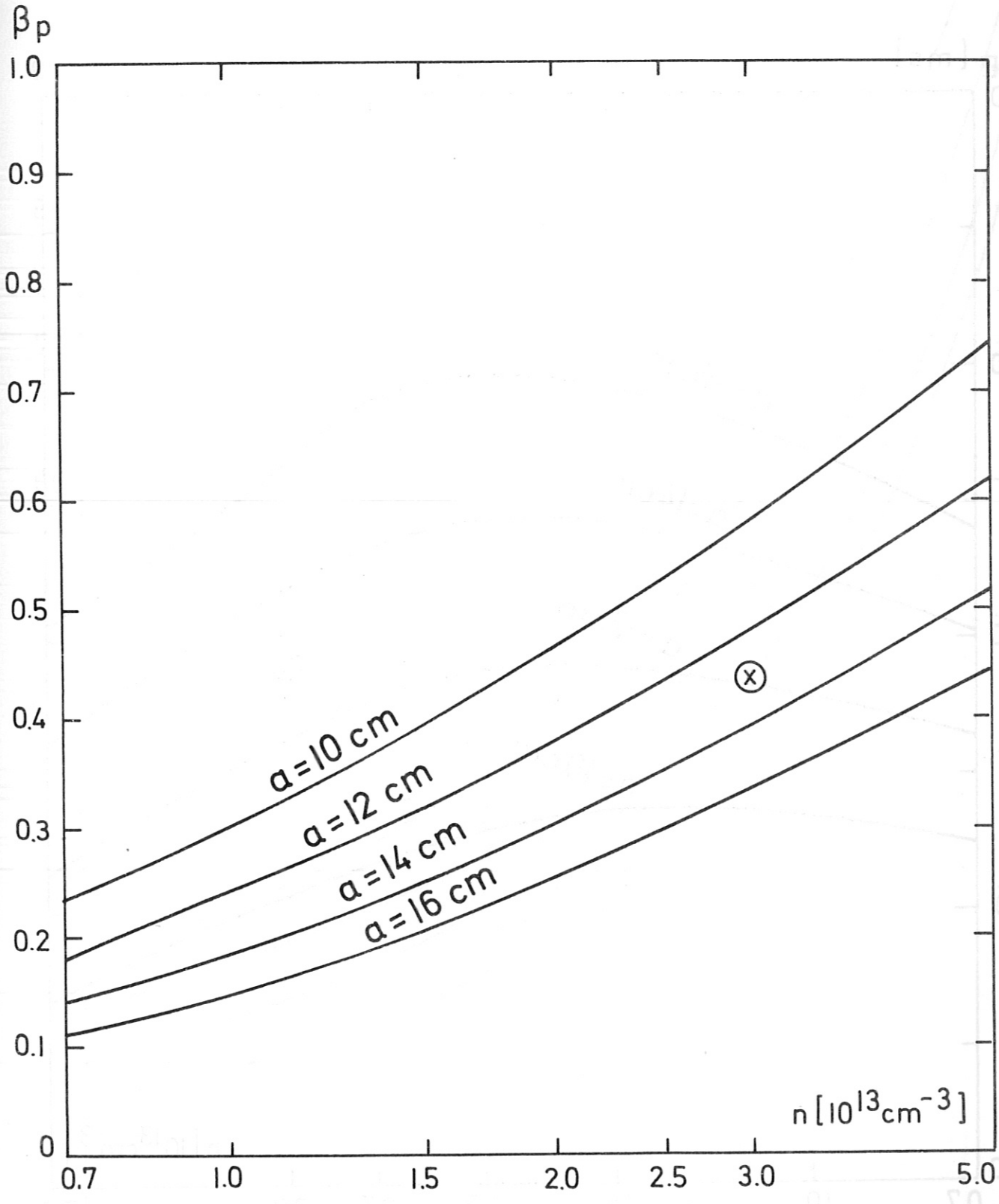

CASE 1+2 Variation of β_p with a and n

Fig. 8

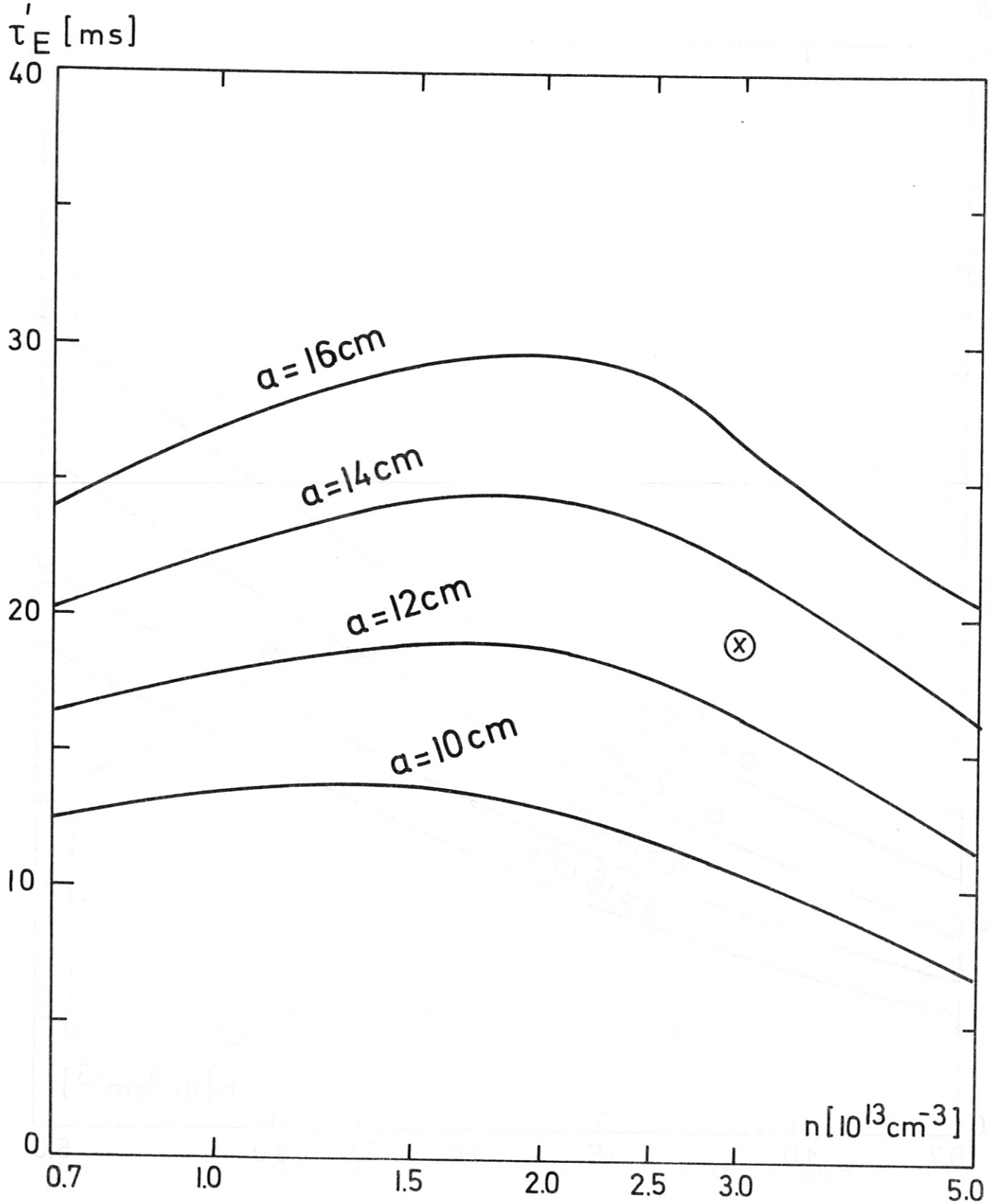

CASE 1+2 Variation of τ'_E with a and n

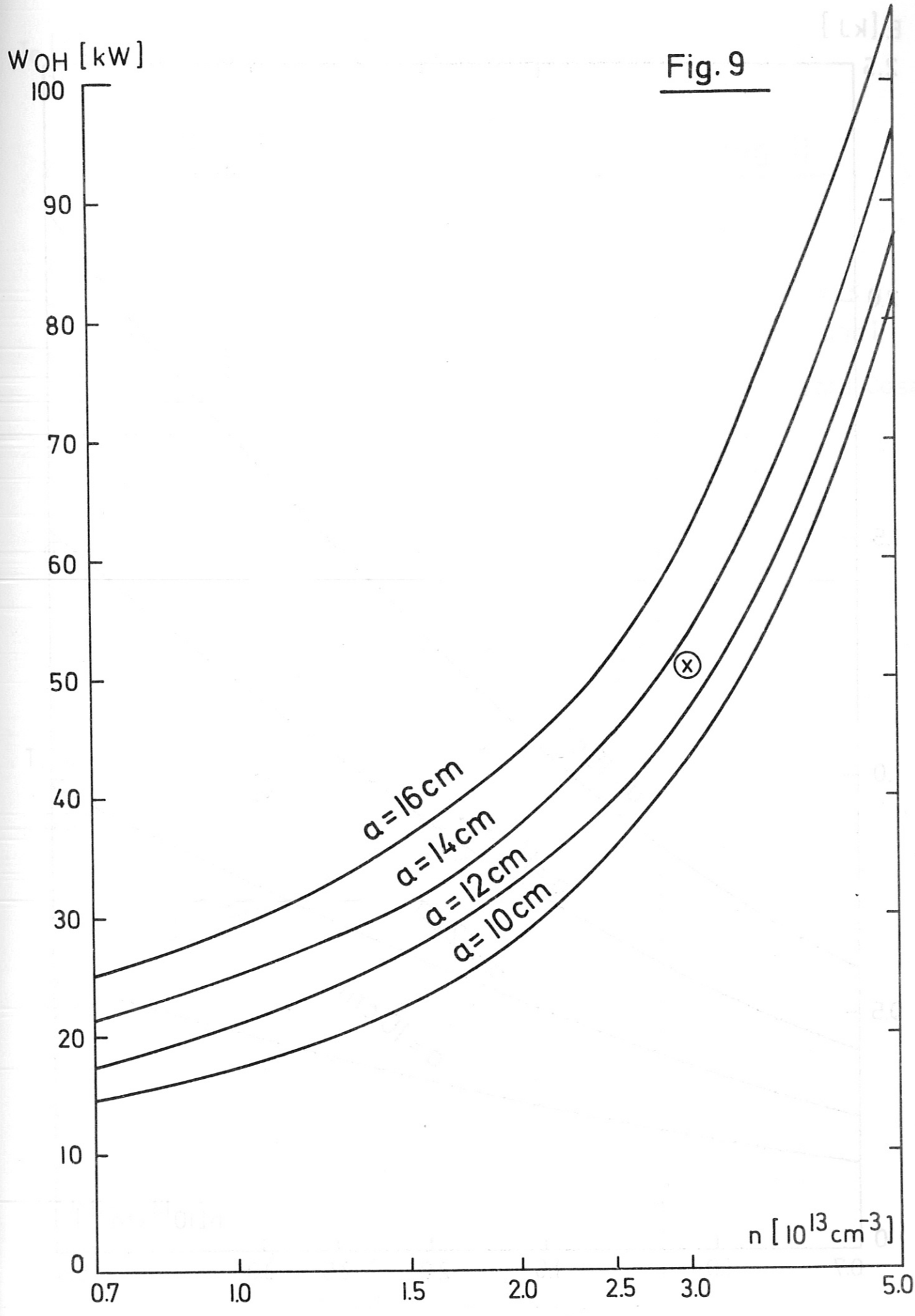

Fig. 9

CASE 1+2 Variation of W_{OH} with a and n

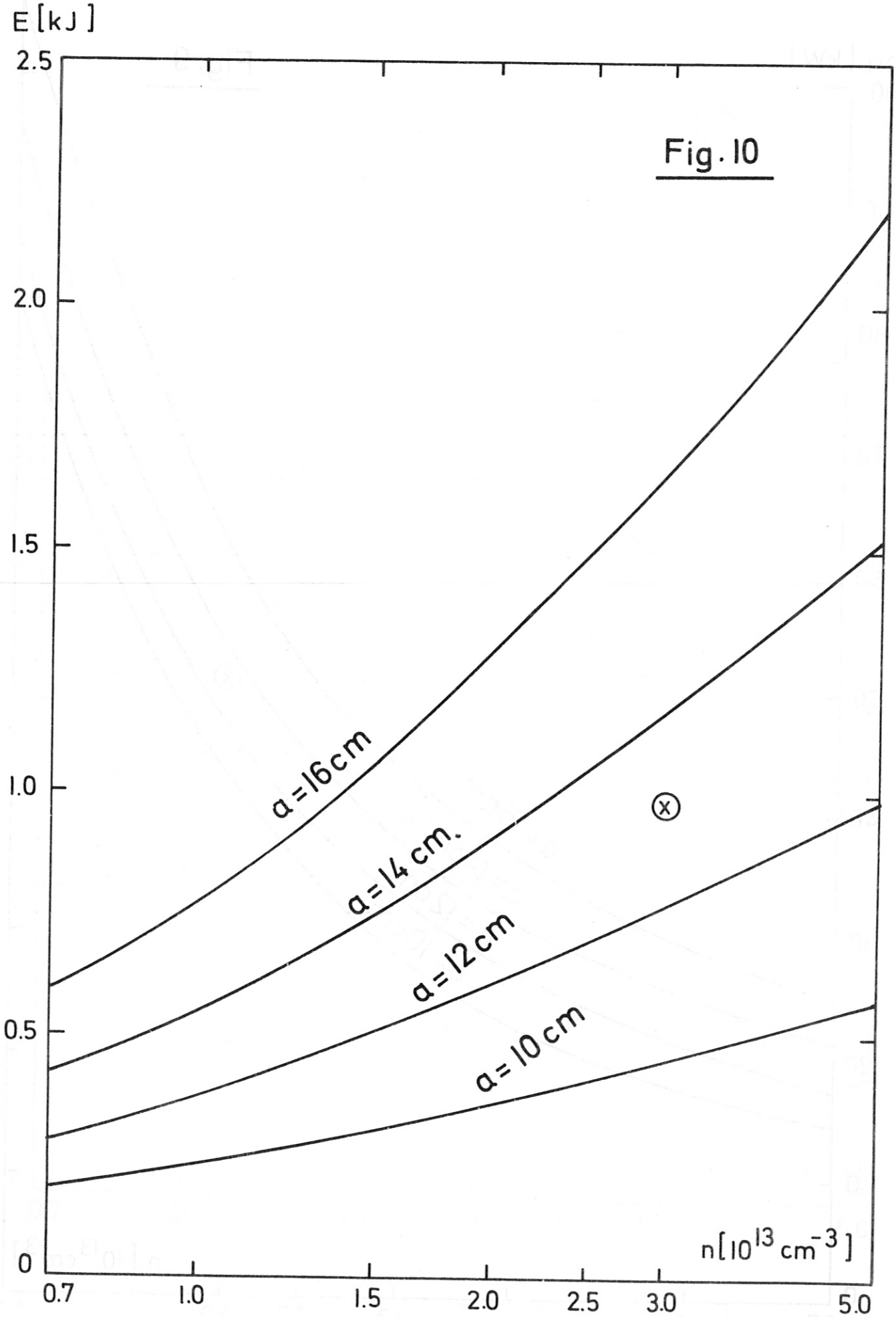

CASE 1+2 Variation of Energy content E vs n and a

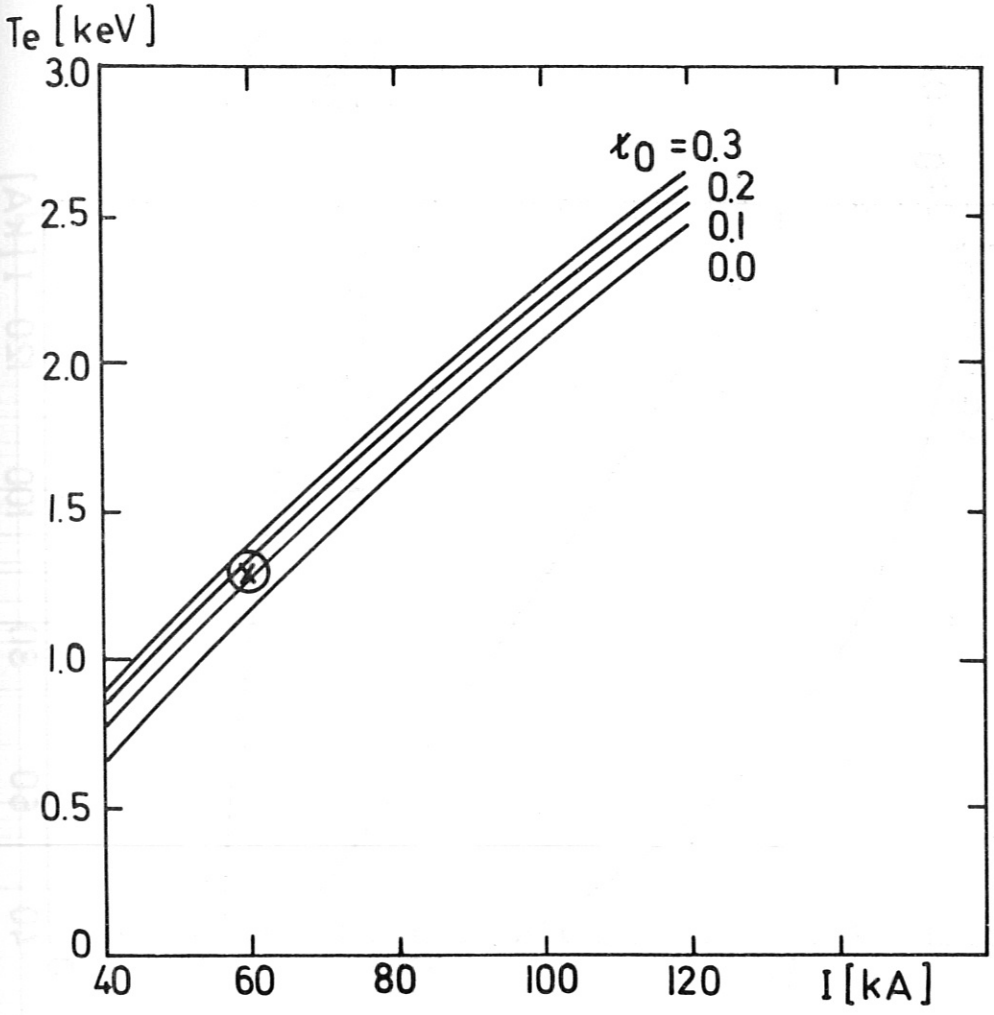

Fig. II

CASE 3

T_e and T_i vs τ_0 and I

⊗ = Standard Case

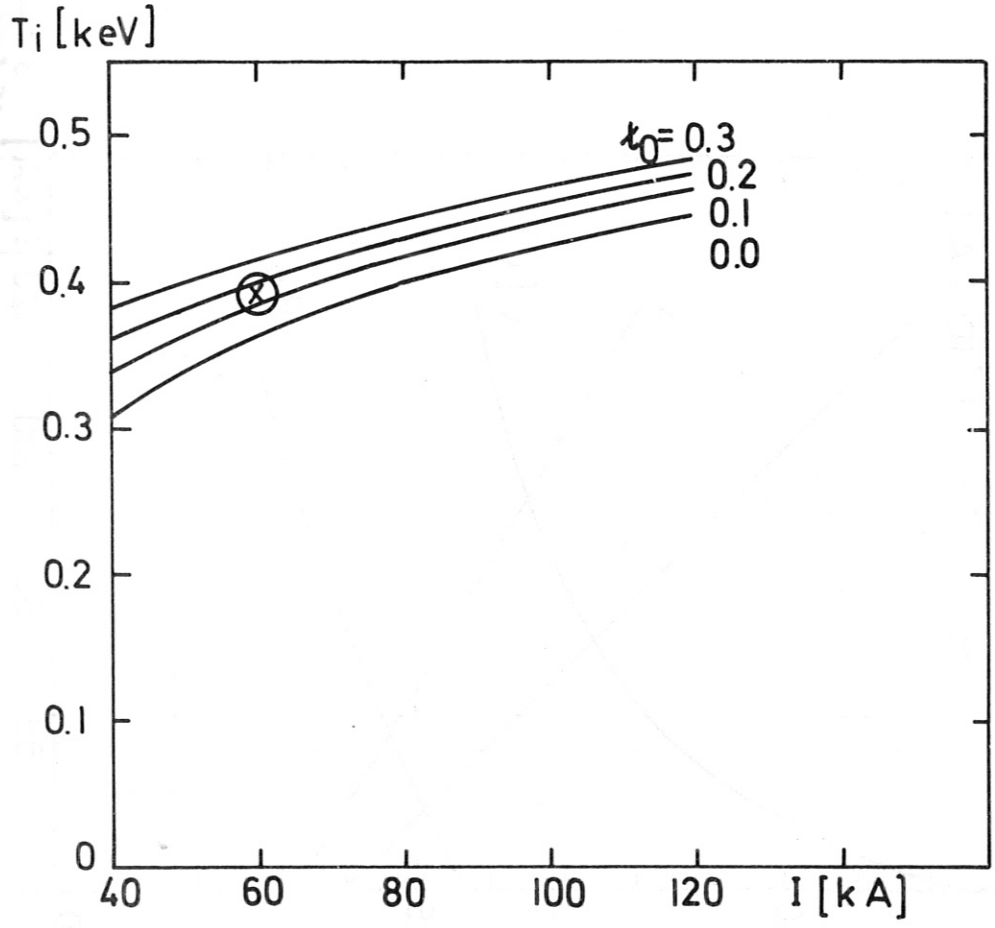

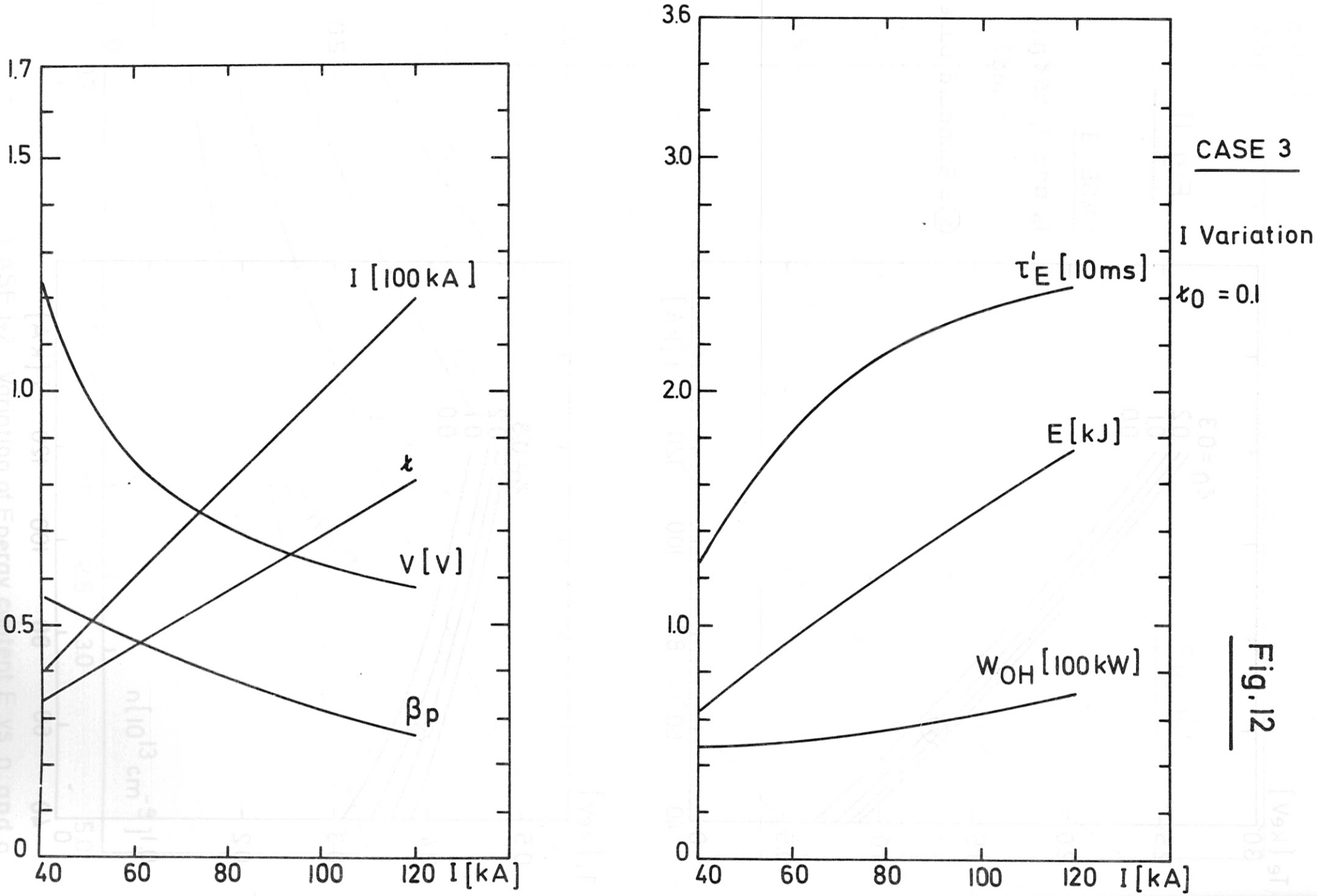
1.7
1.5
1.0
0.5
0
I [100 kA]
ι
V [V]
βp
40
60
80
100
120 I [kA]
3.6
3.0
2.0
1.0
0
τ'E [10ms]
E [kJ]
WOH [100 kW]
40
60
80
100
120 I [kA]
CASE 3
I Variation
ι0 = 0.1

Fig. 12

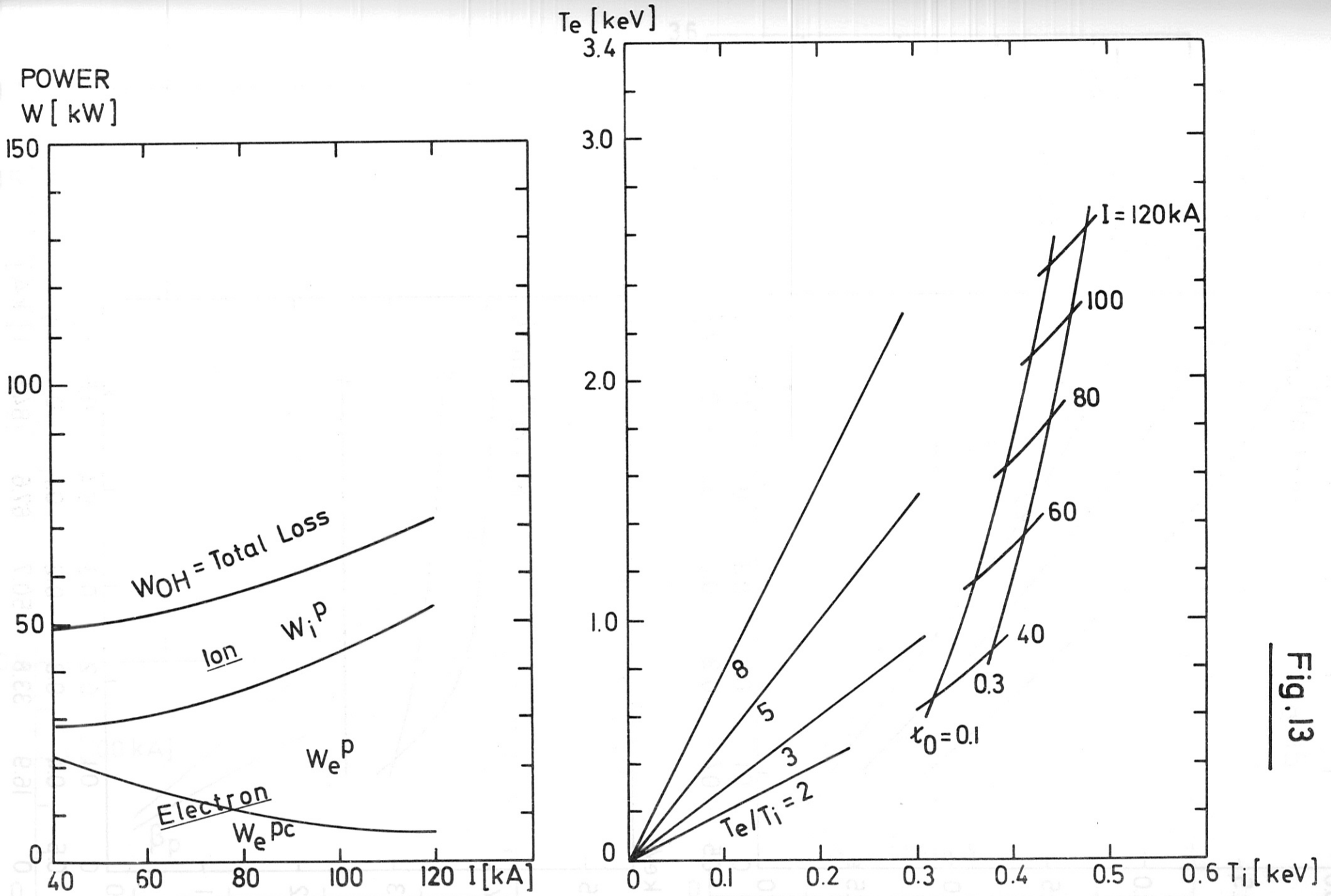

Fig. 13

CASE 3 a) Loss Distribution vs I, $\tau_0 = 0.1$
b) T_e vs T_i for various τ_0, I

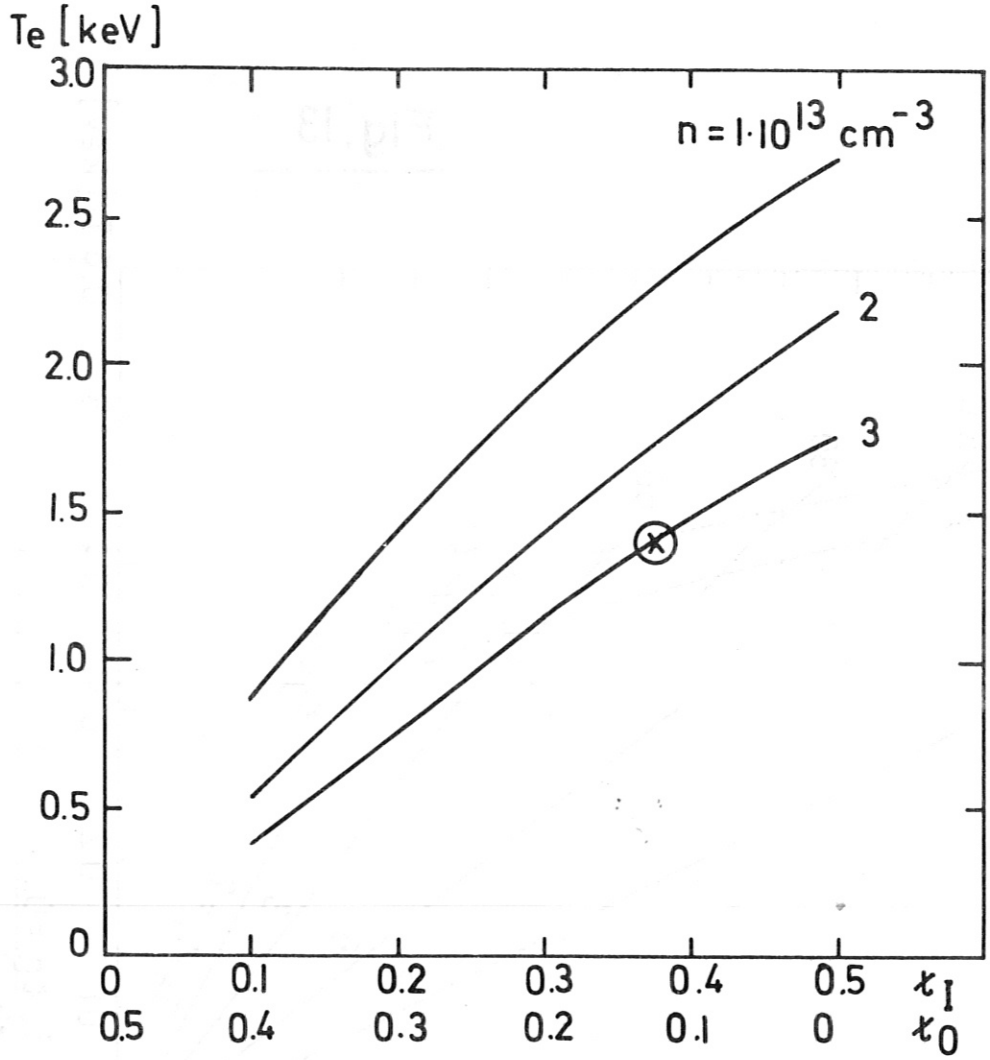

Fig. 14

CASE 4

Te and Ti vs $\frac{t_I}{t_0}$

$t = 0.5 = \text{const}$

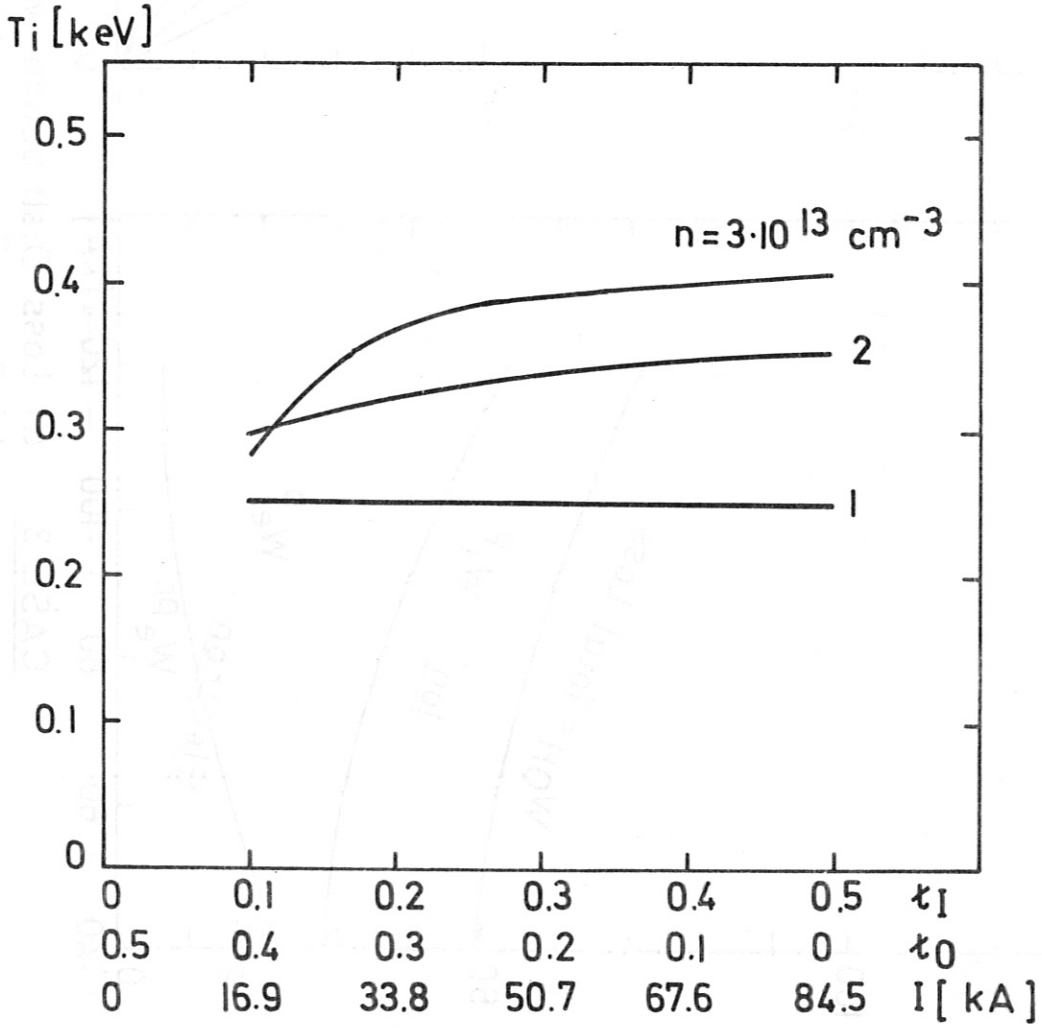

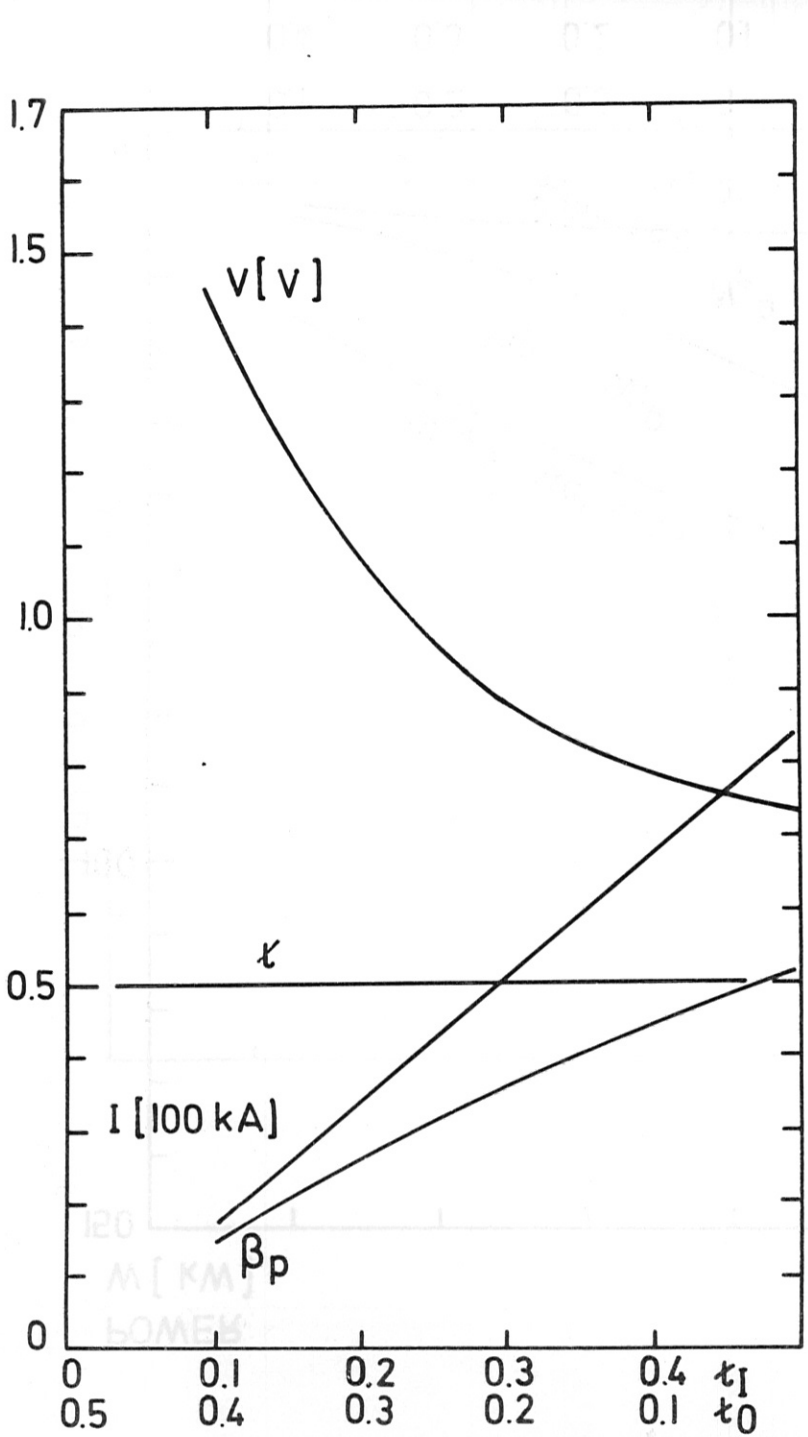

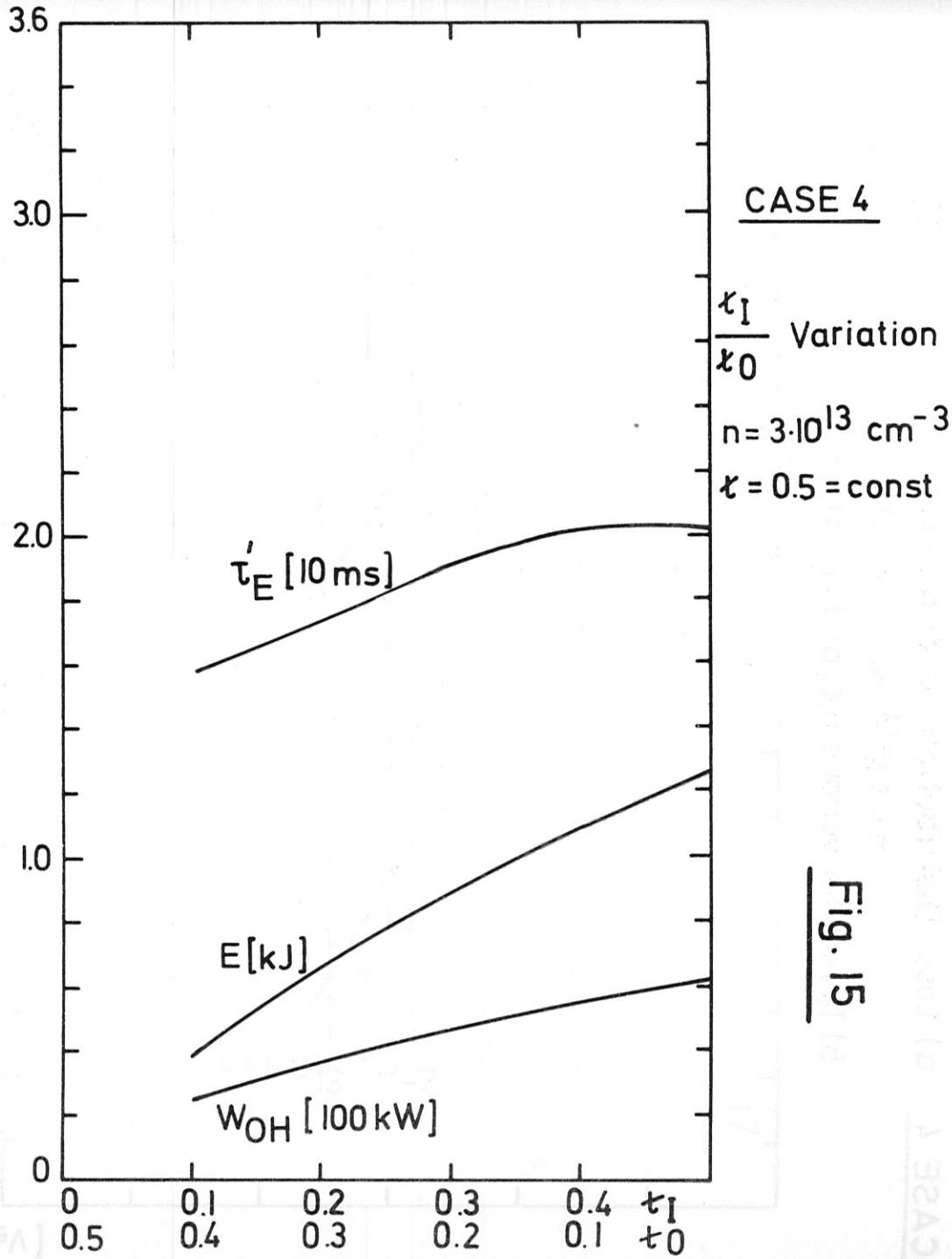

CASE 4

$\frac{\iota_I}{\iota_0}$ Variation

$n = 3 \cdot 10^{13}$ cm^{-3}

$\iota = 0.5 = \text{const}$

Fig. 15

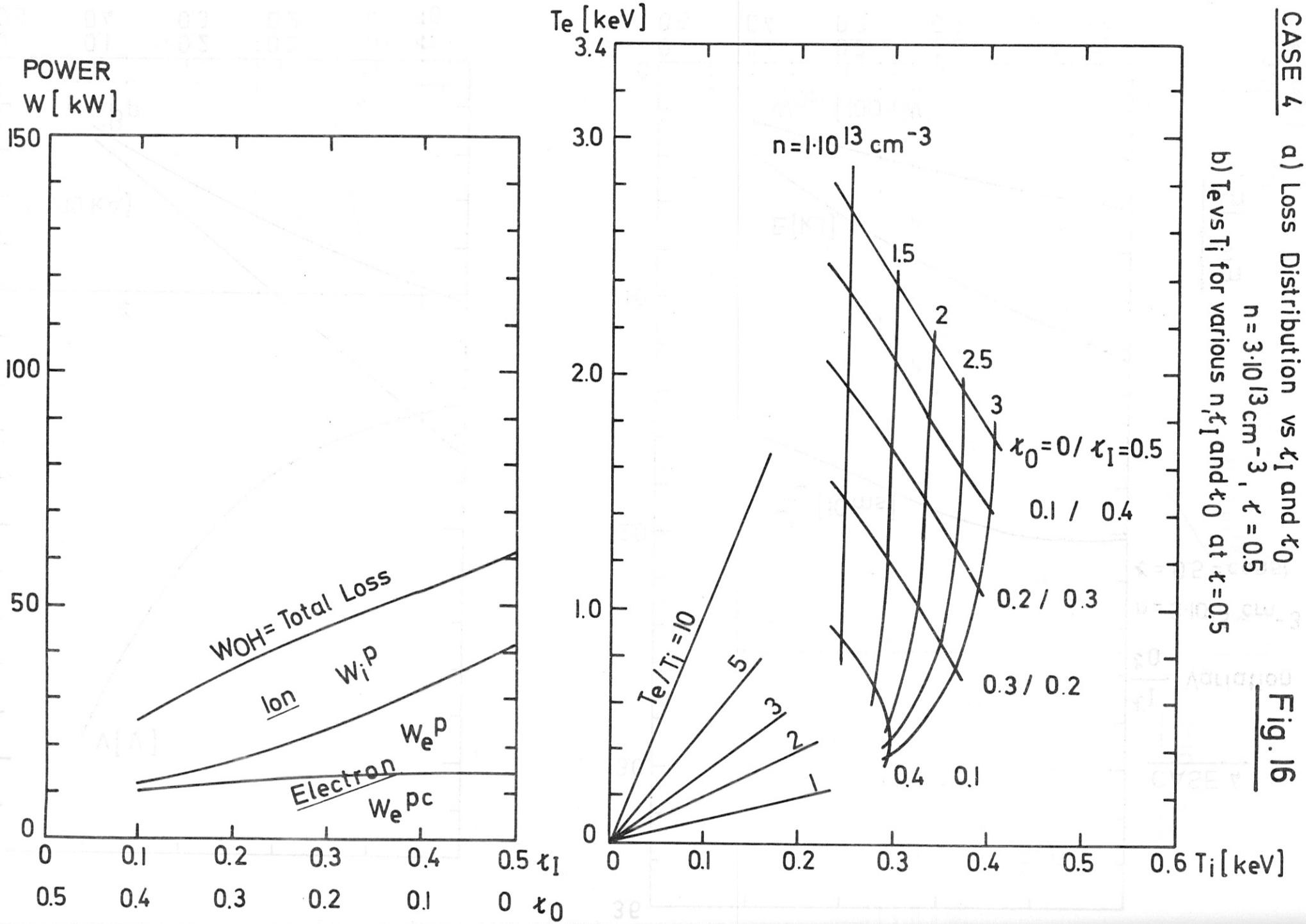

CASE 4 a) Loss Distribution vs τ_I and τ_0
$n = 3 \cdot 10^{13}\ cm^{-3}$, $\tau = 0.5$
b) Te vs Ti for various n, τ_I and τ_0 at $\tau = 0.5$

Fig. 16

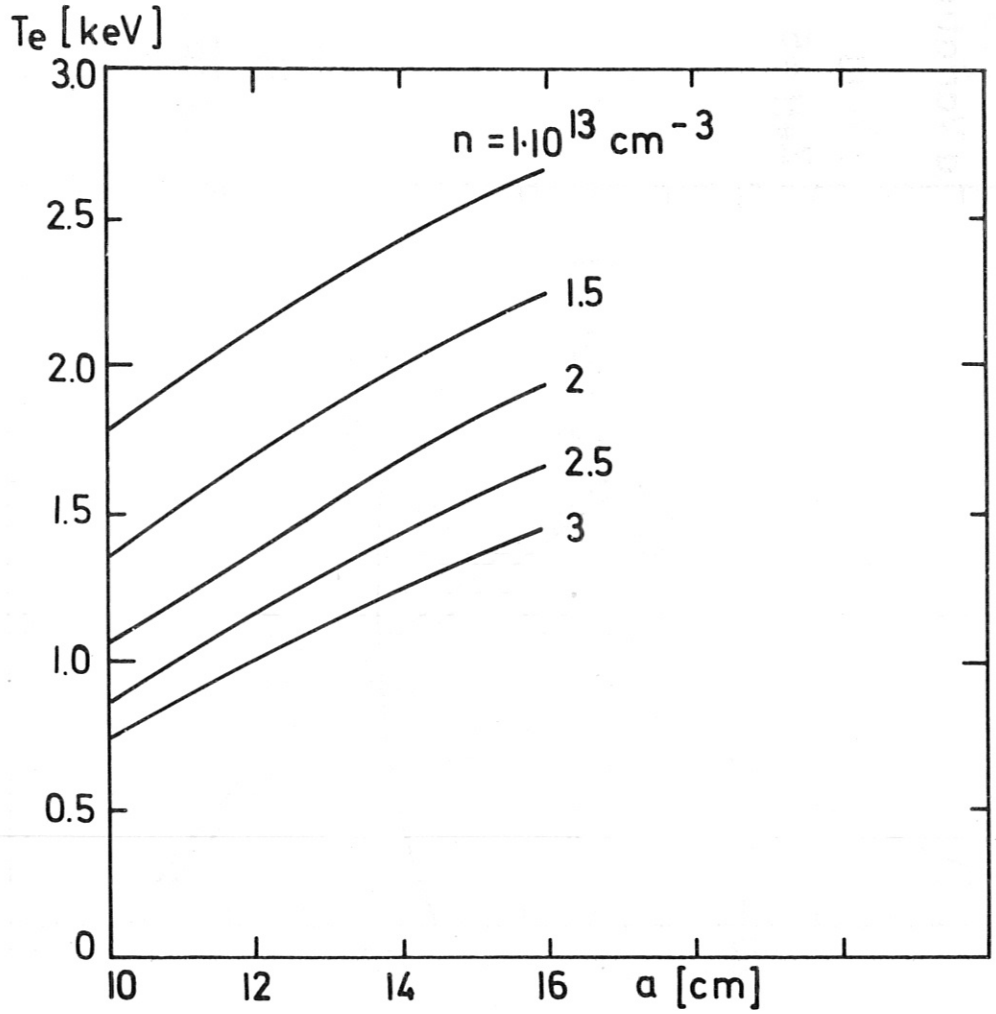

Fig. 17

CASE 5

T_e and T_i vs a and n

$Z_{eff} = 5$
$c^2 = 10$
ι = const

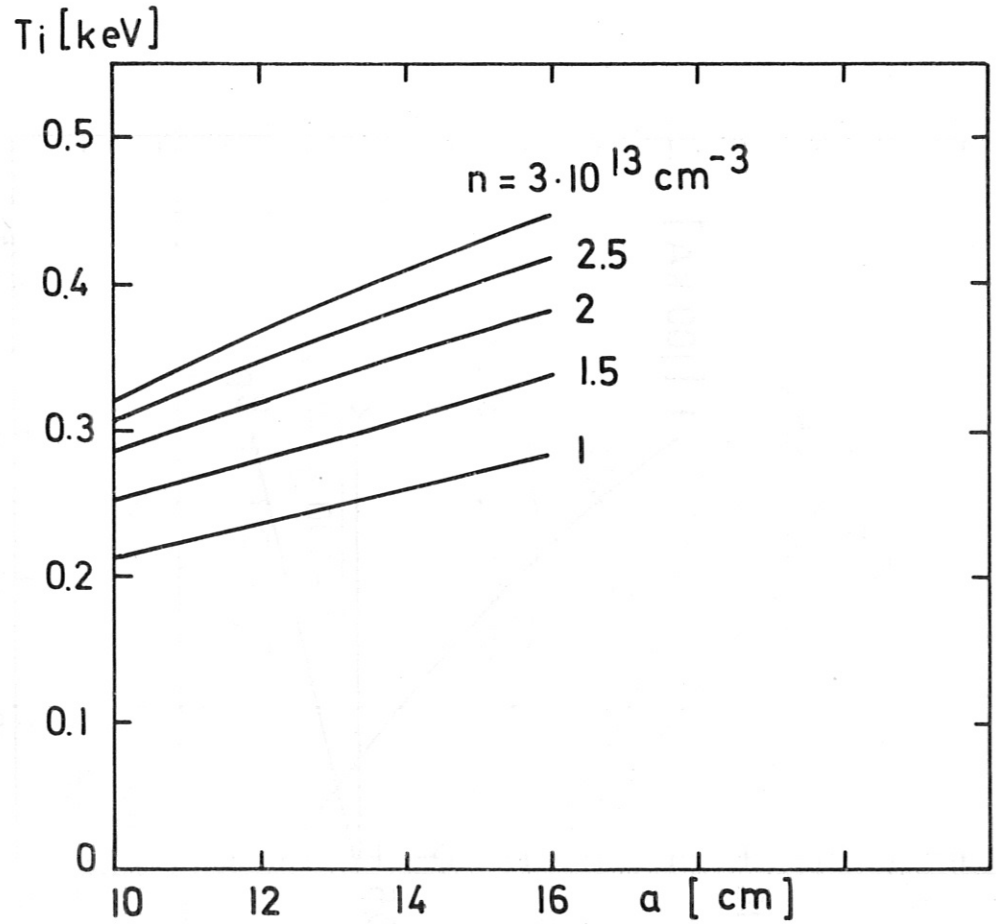

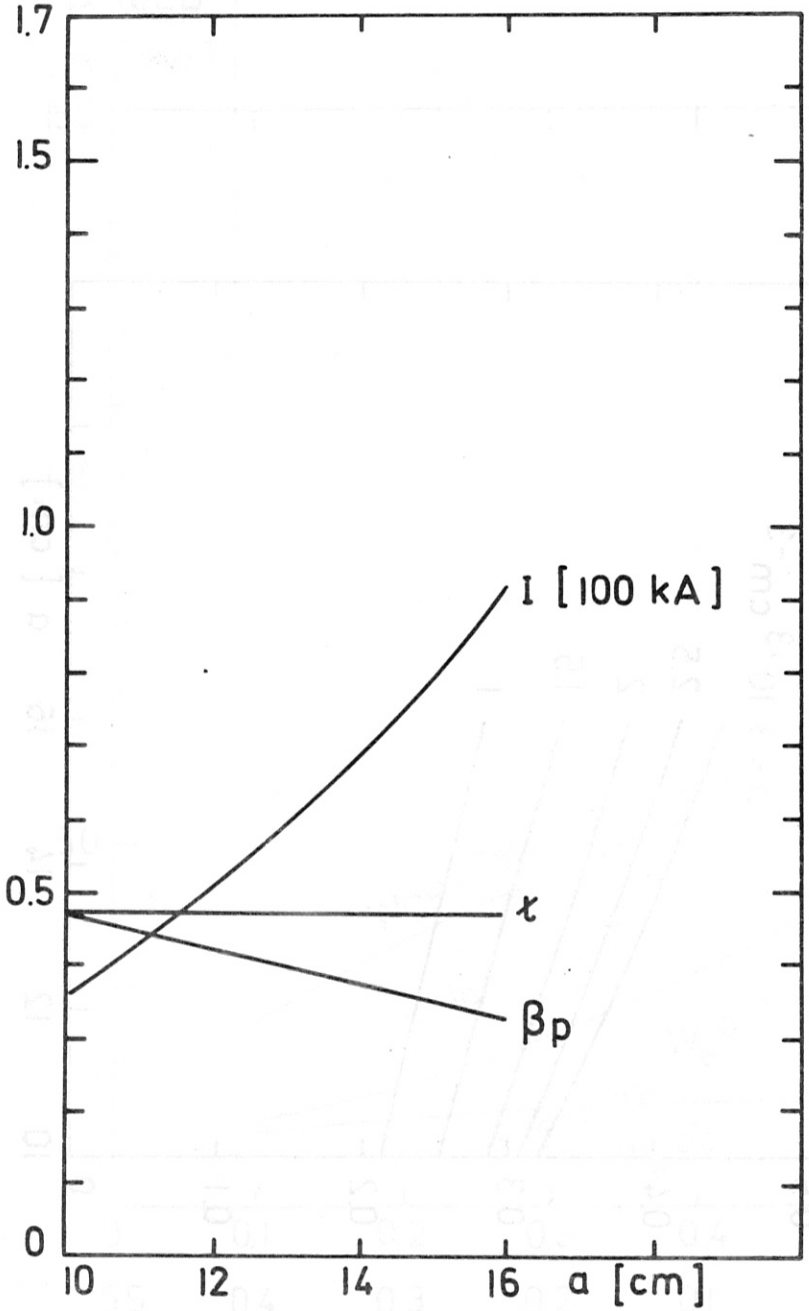

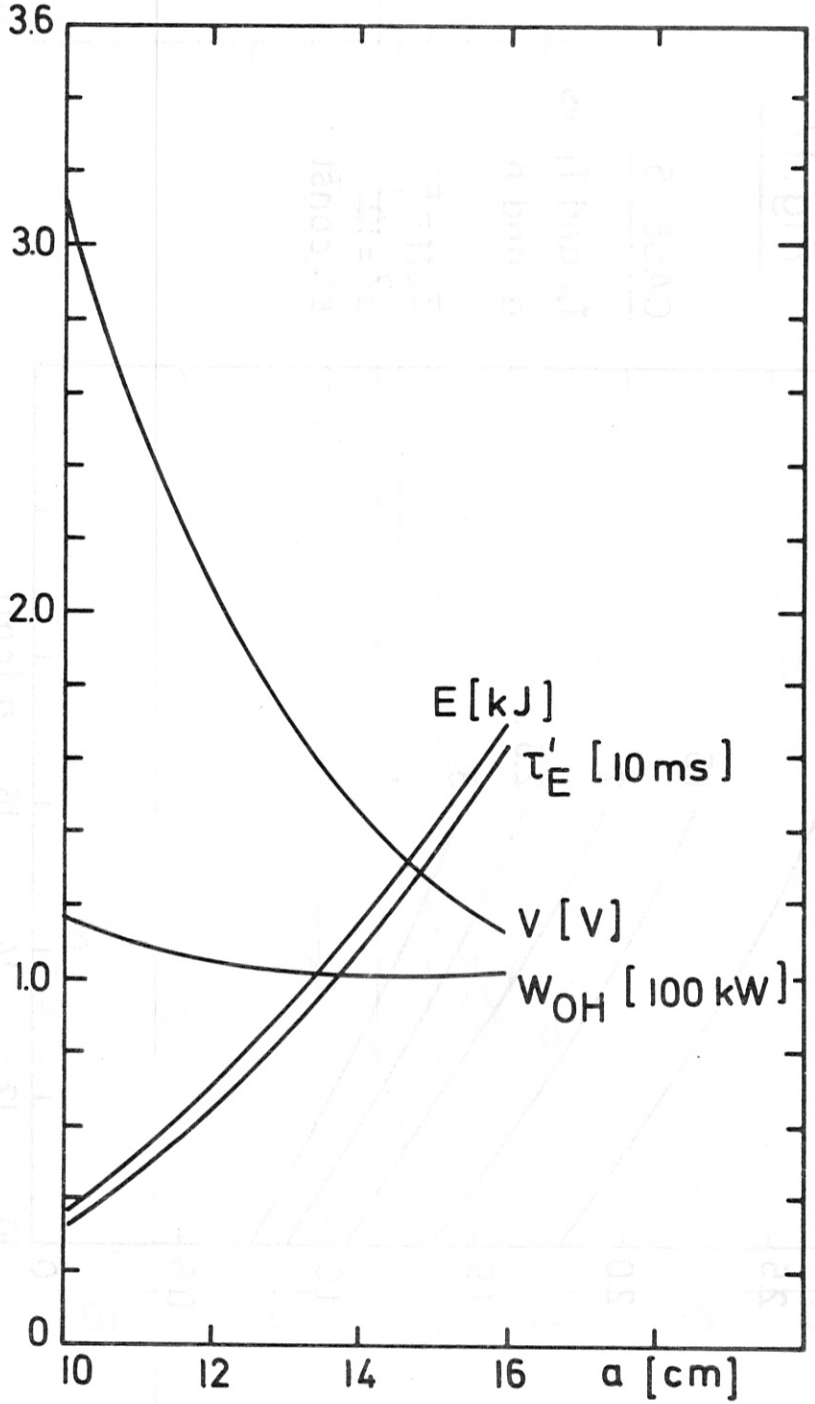

CASE 5

$n = 3 \cdot 10^{13}\ cm^{-3}$

a Variation

$c^2 = 10$

$Z_{eff} = 5$

Fig. 18

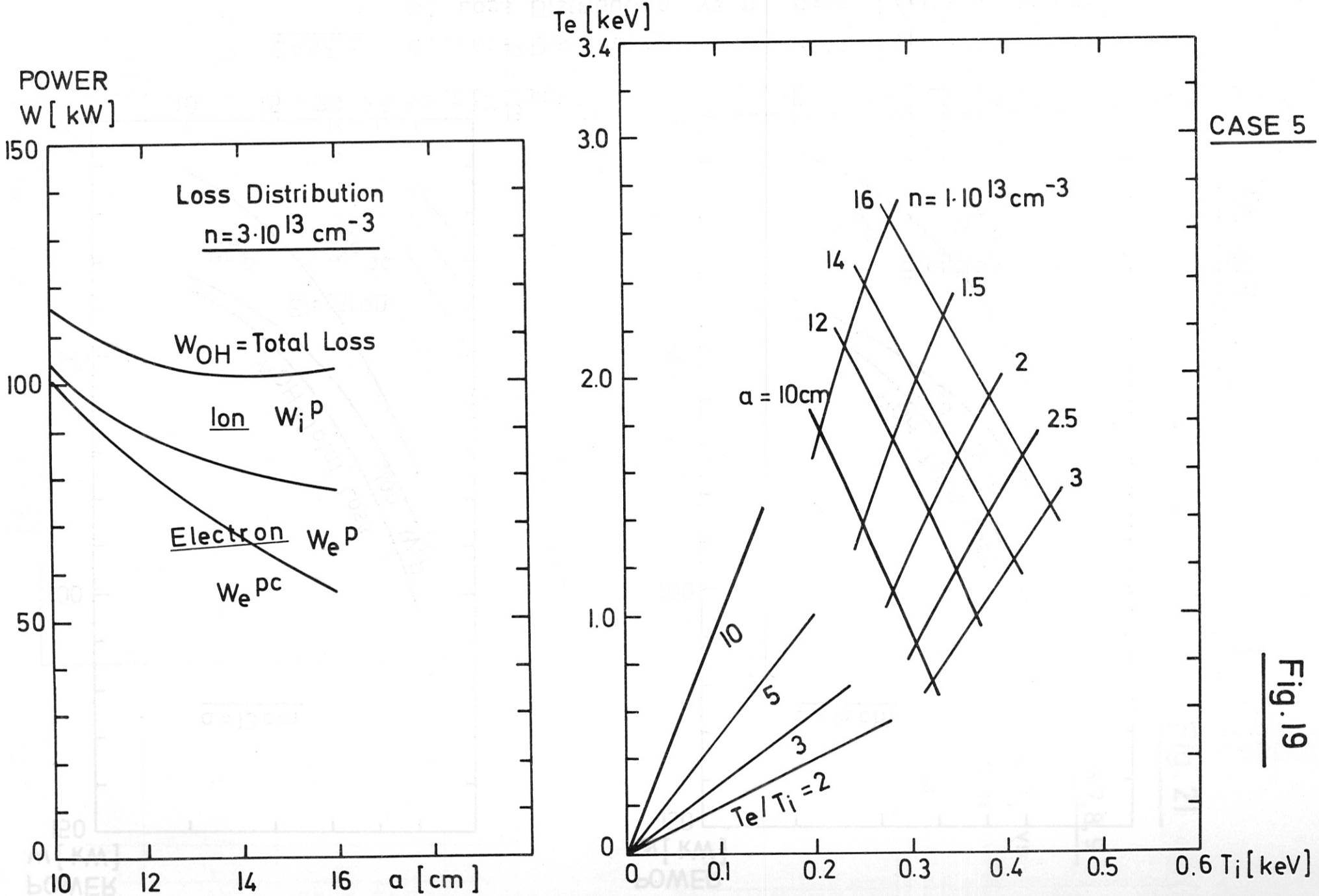
POWER
W [kW]
150
100
50
0
Loss Distribution
n=3·10 13 cm -3
W OH = Total Loss
Ion W i P
Electron W e P
W e Pc
10
12
14
16
a [cm]
Te [keV]
3.4
3.0
2.0
1.0
0
16
n= 1·10 13 cm -3
14
12
1.5
2
2.5
3
a = 10cm
10
5
3
Te / Ti = 2
0
0.1
0.2
0.3
0.4
0.5
0.6 Ti [keV]
CASE 5

Fig. 19

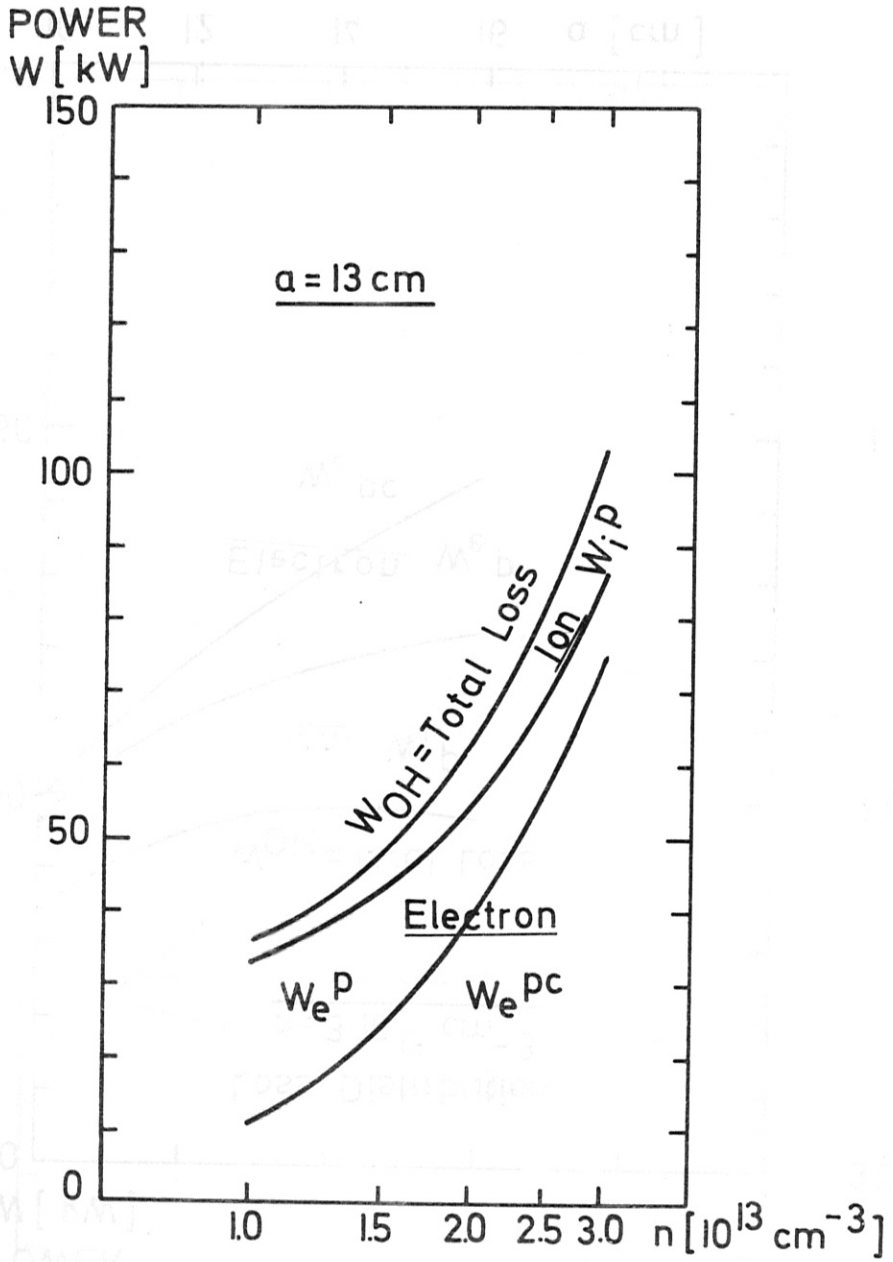

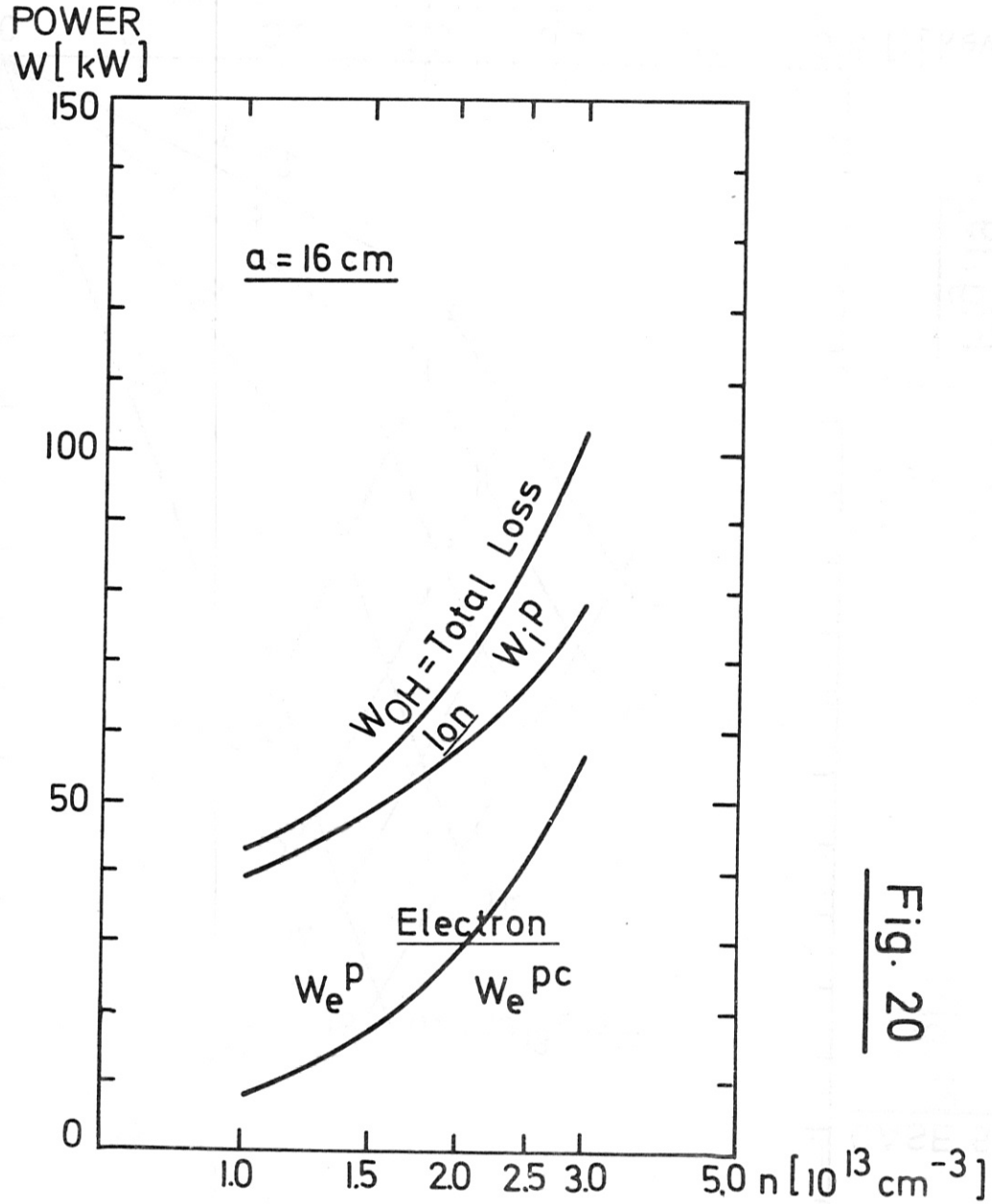

Fig. 20

CASE 5 a) Loss Distribution vs n, a=13 (Z_{eff} = 5, c^2 = 10)
b) Loss Distribution vs n, a=16 (Z_{eff} = 5, c^2 = 10)

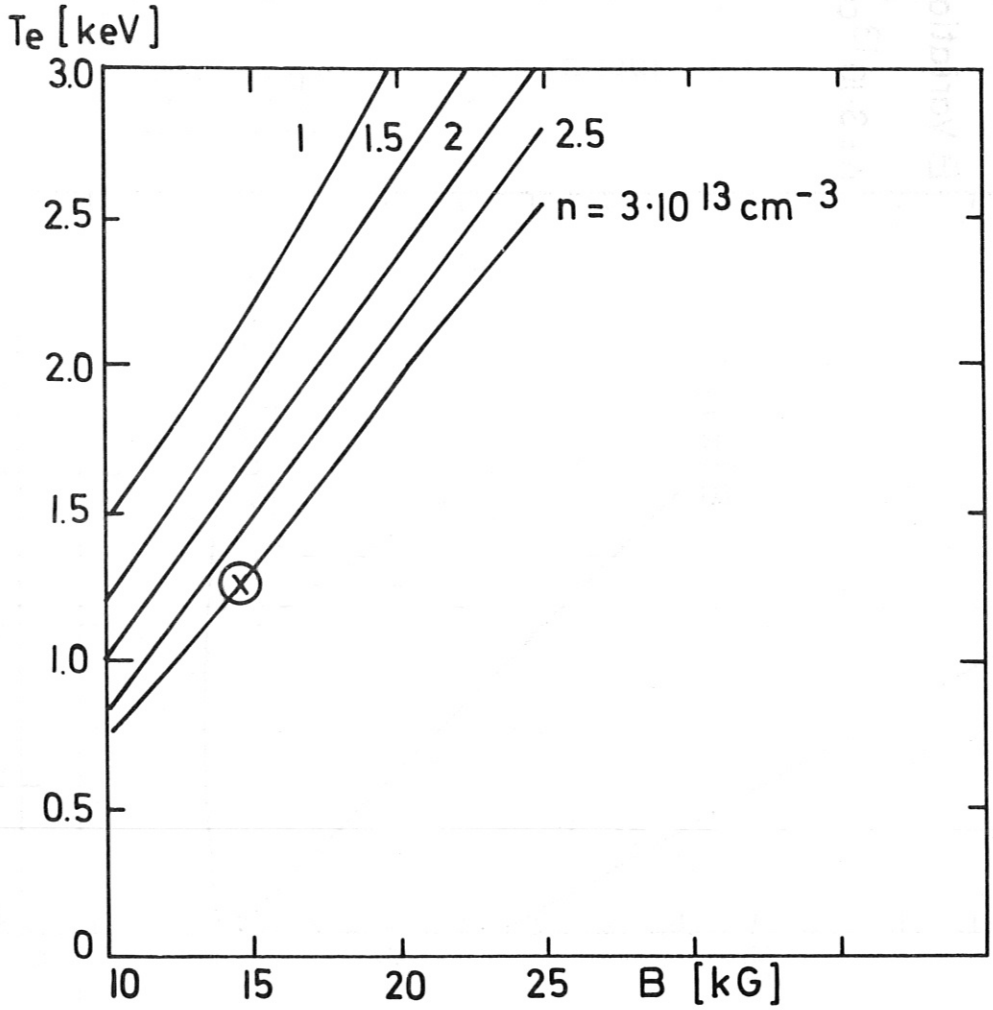

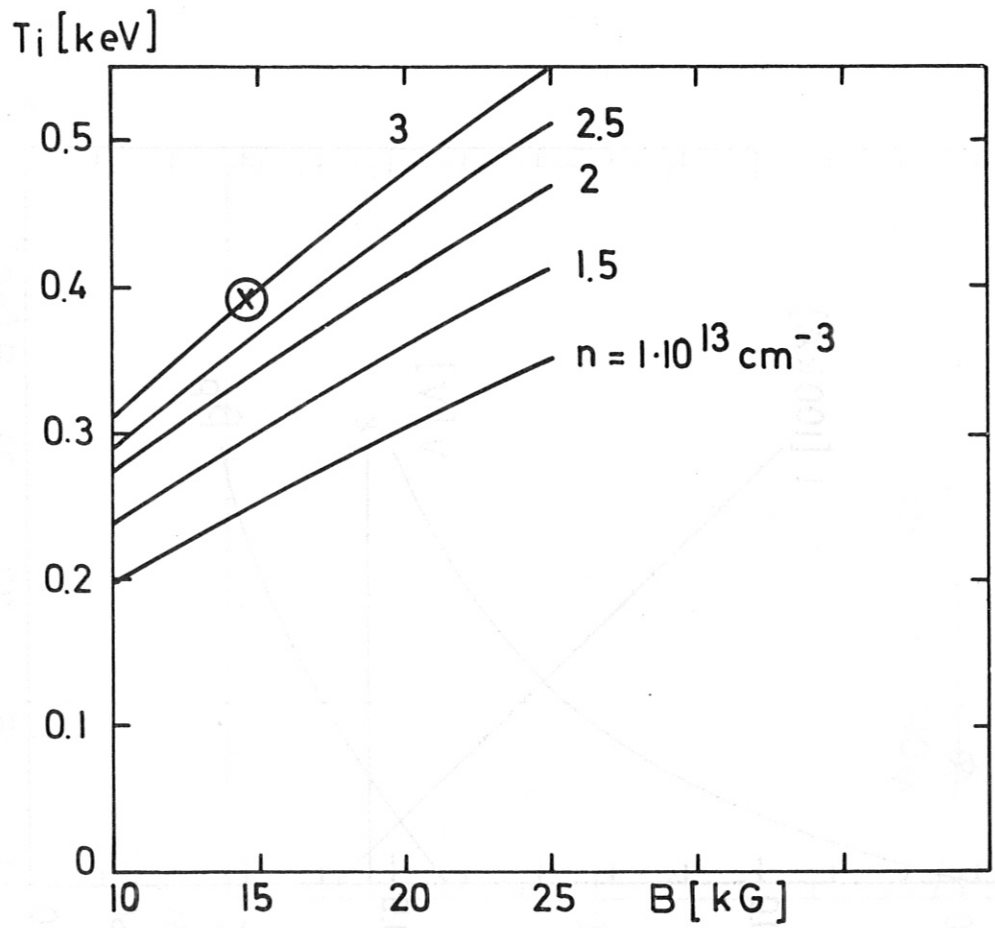

Fig. 21

CASE 6,7,8,9

T_e and T_i vs B and n

ℓ = const

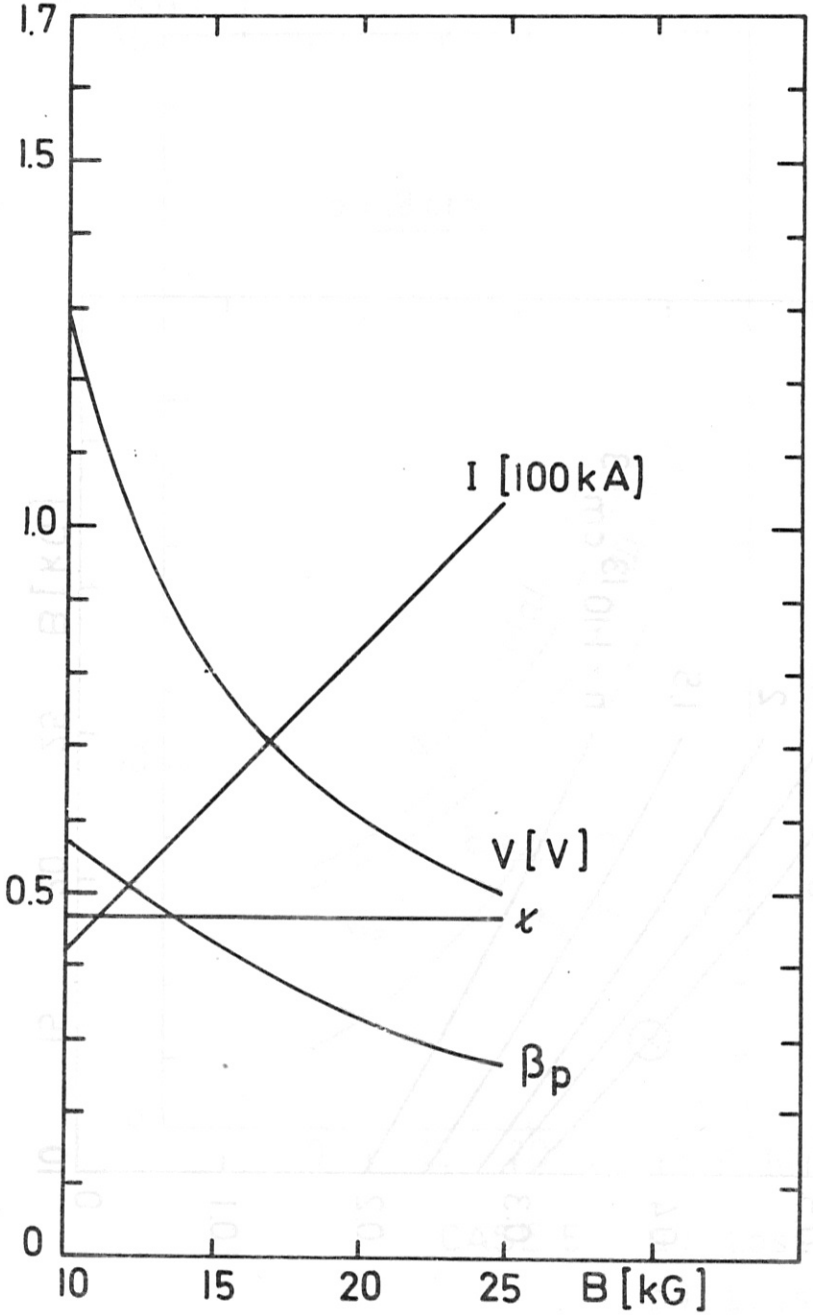

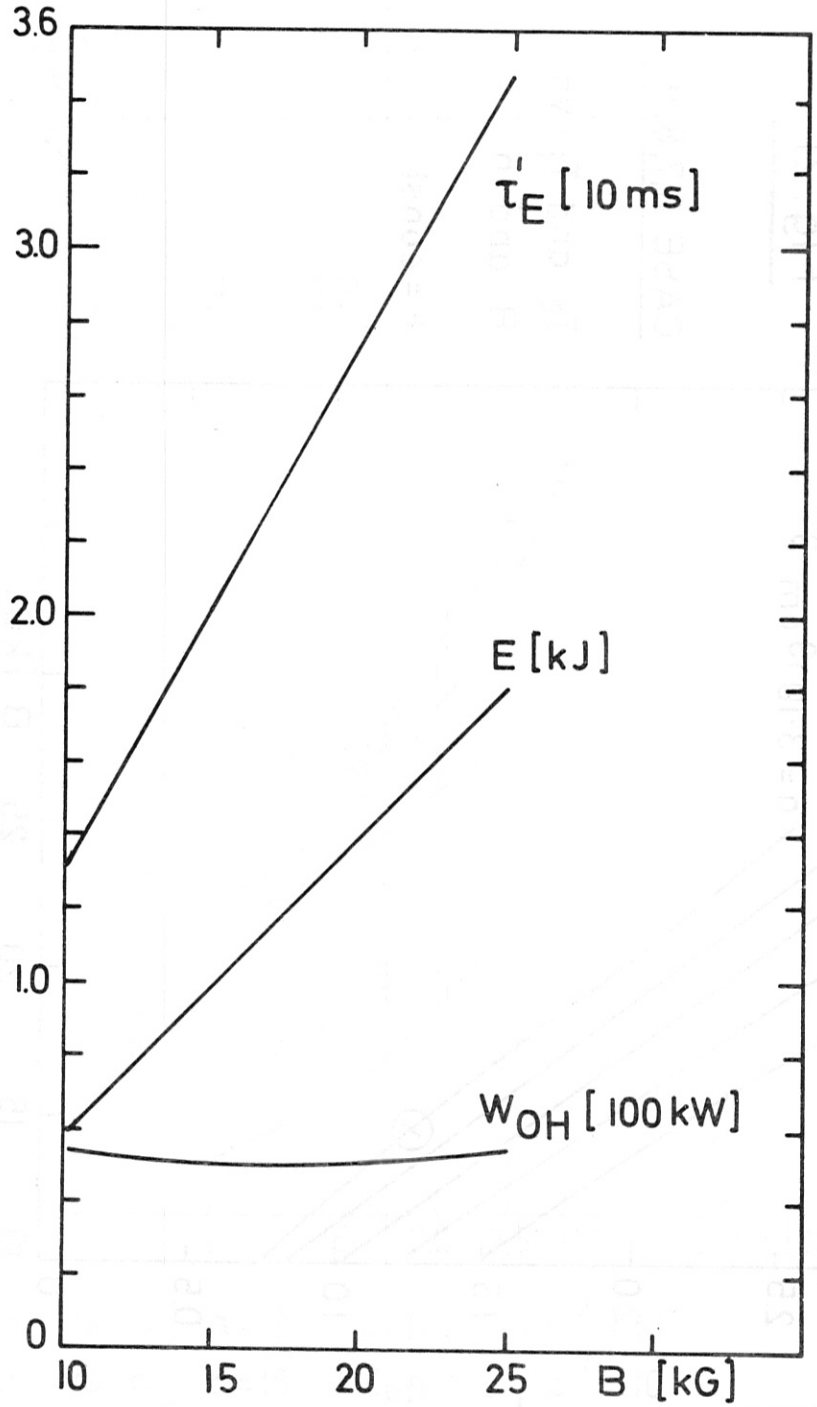

CASE 6,7,8,9

no Heating

B Variation

$n = 3 \cdot 10^{13} cm^{-3}$

Fig. 22

CASE 6,7,8,9 a) Loss Distribution vs $B_1 n = 3 \cdot 10^{13} cm^{-3}$

b) T_e vs T_i for various $B_1 n$

Fig. 23

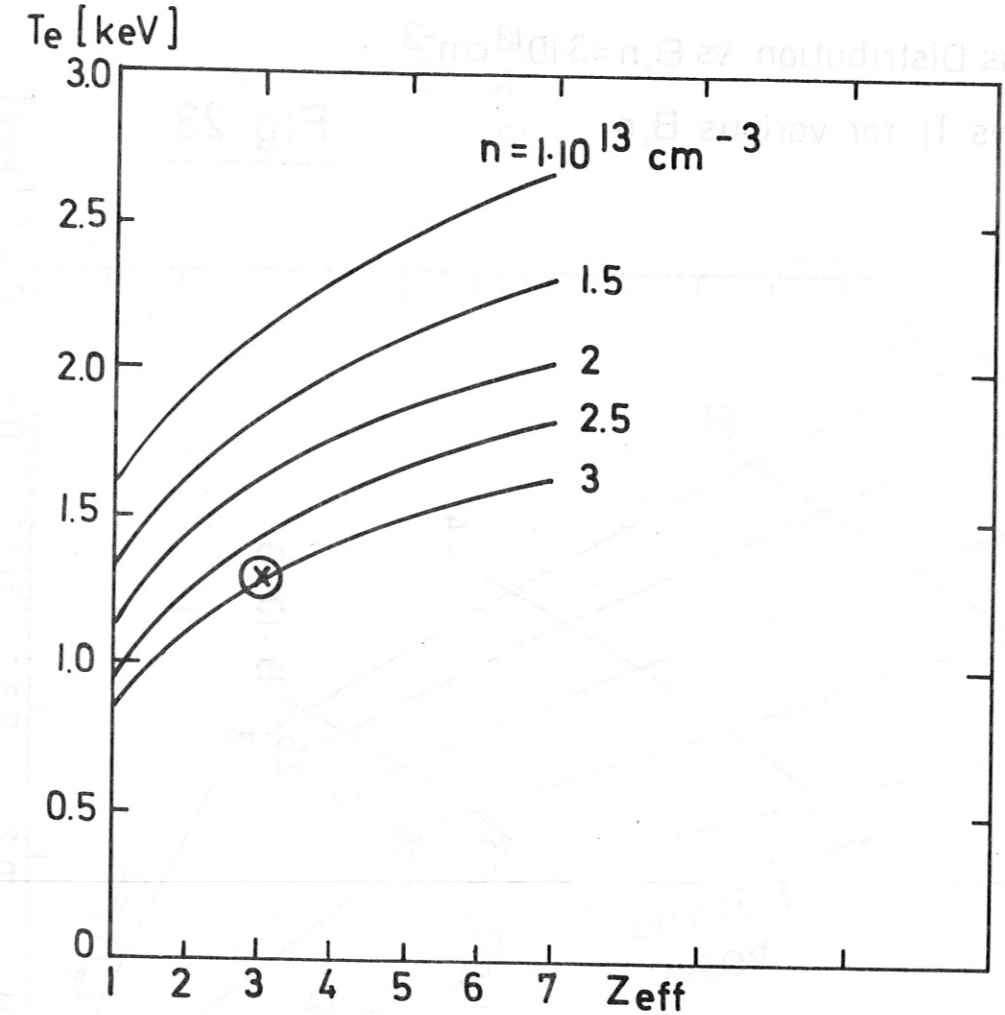

Fig. 24

CASE 10

T_e and T_i vs n and Z_{eff}

⊗ = Standard Case

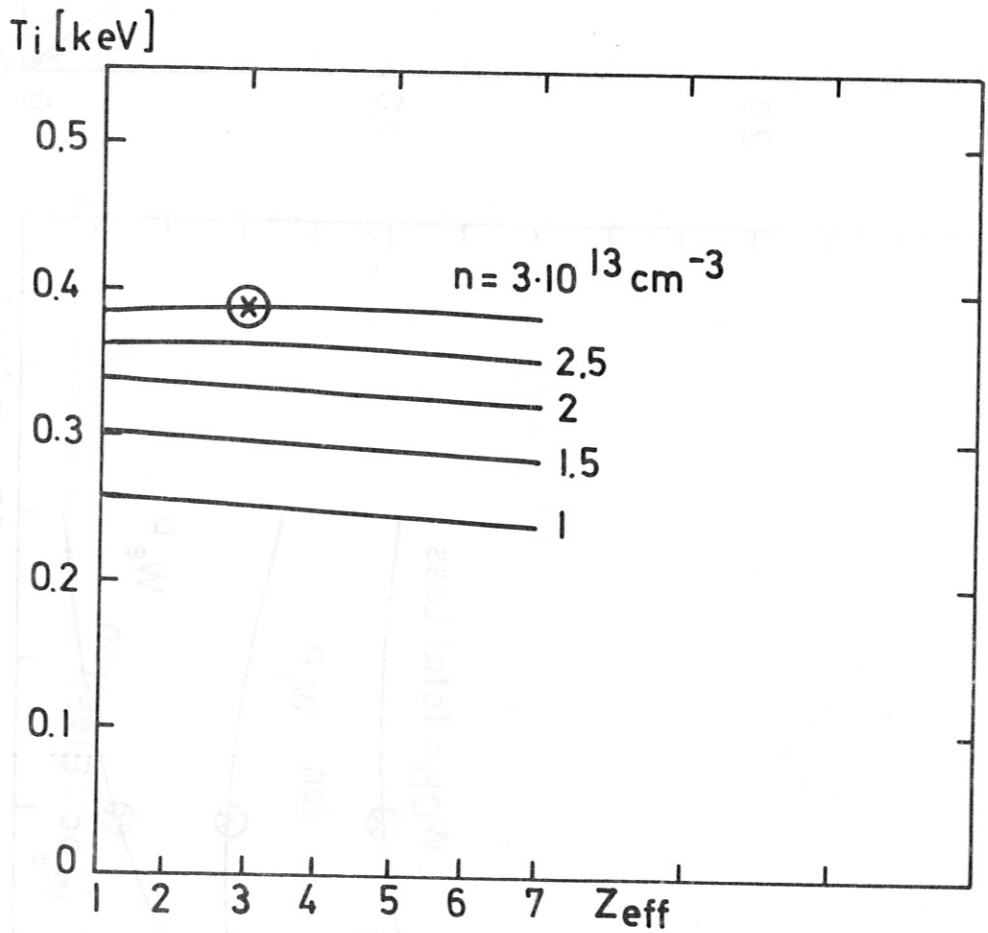

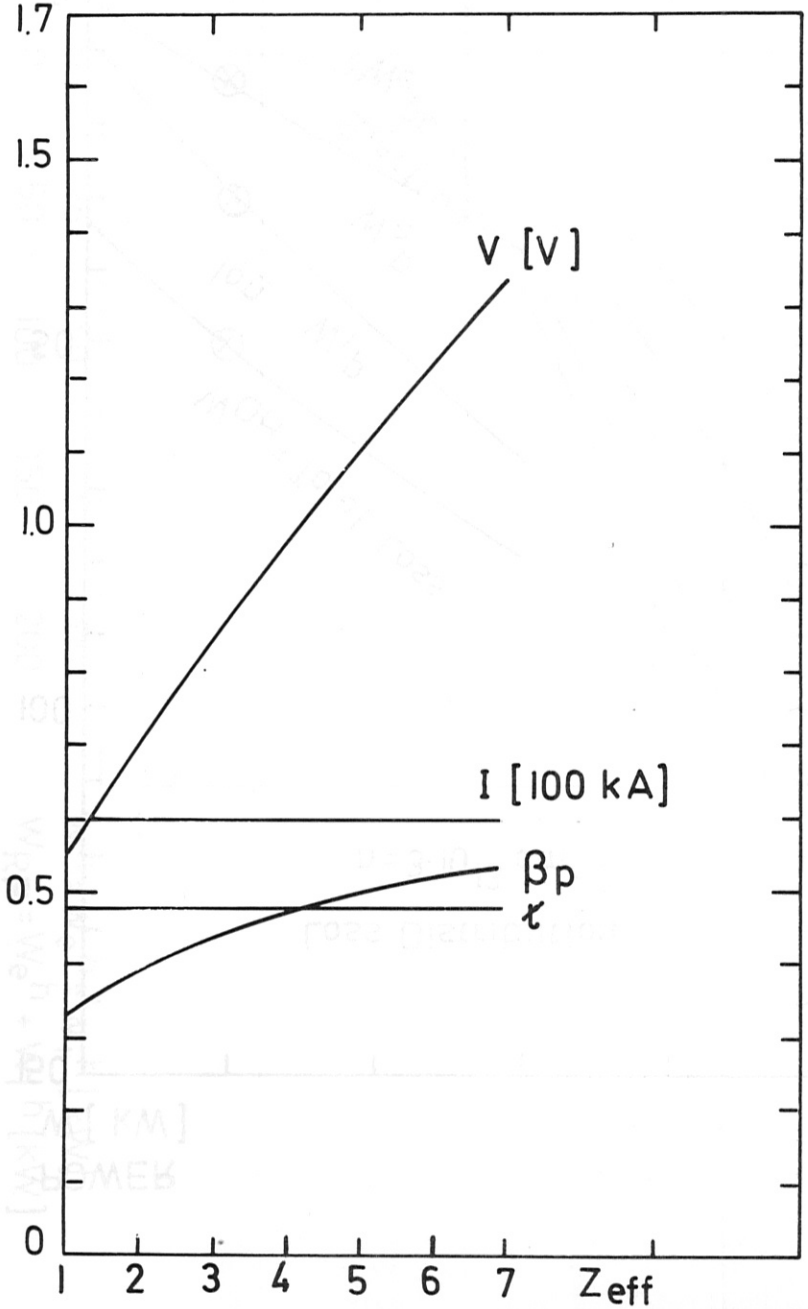

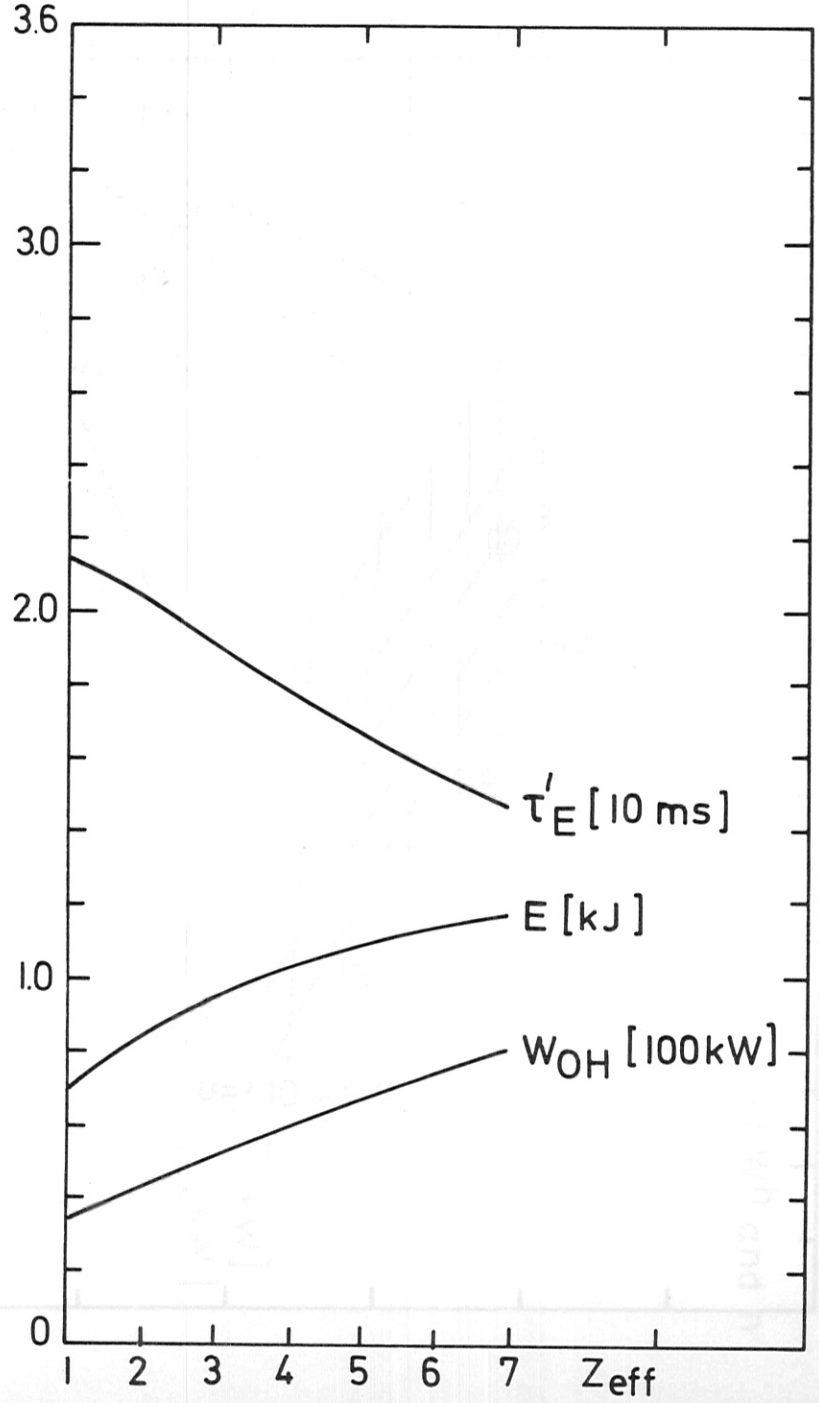

CASE 10

Z_{eff} Variation

$n=3\cdot10^{13}cm^{-3}$

Fig. 25

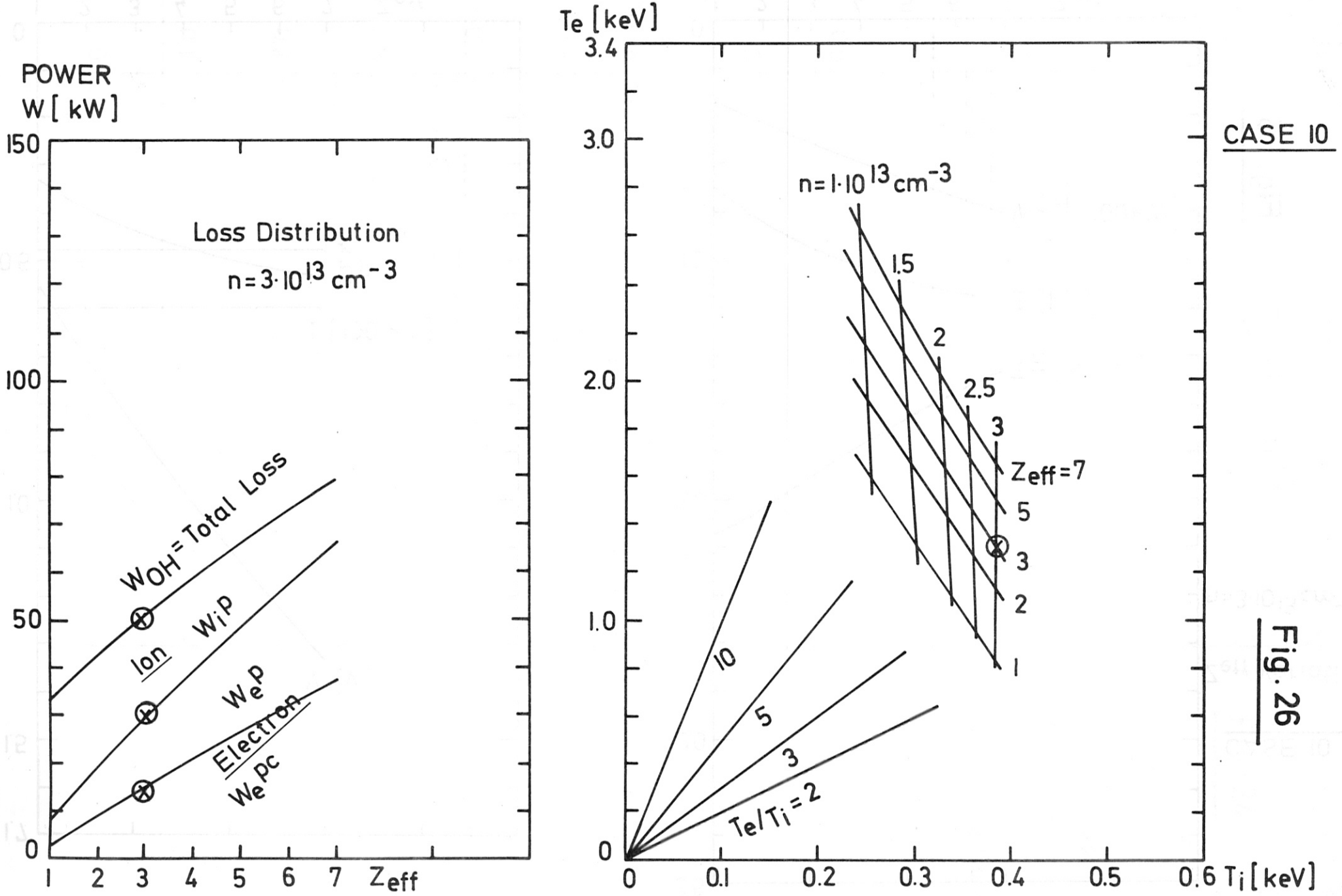
POWER
W [kW]
150
100
50
0
Loss Distribution
n = 3·10^13 cm^-3
W_OH = Total Loss
Ion W_i^p
W_e^p
Electron W_e^pc
1 2 3 4 5 6 7 Z_eff
Te [keV]
3.4
3.0
2.0
1.0
0
n = 1·10^13 cm^-3
1.5
2
2.5
3
Z_eff = 7
5
3
2
1
10
5
3
Te/Ti = 2
0 0.1 0.2 0.3 0.4 0.5 0.6 Ti [keV]
CASE 10

Fig. 26

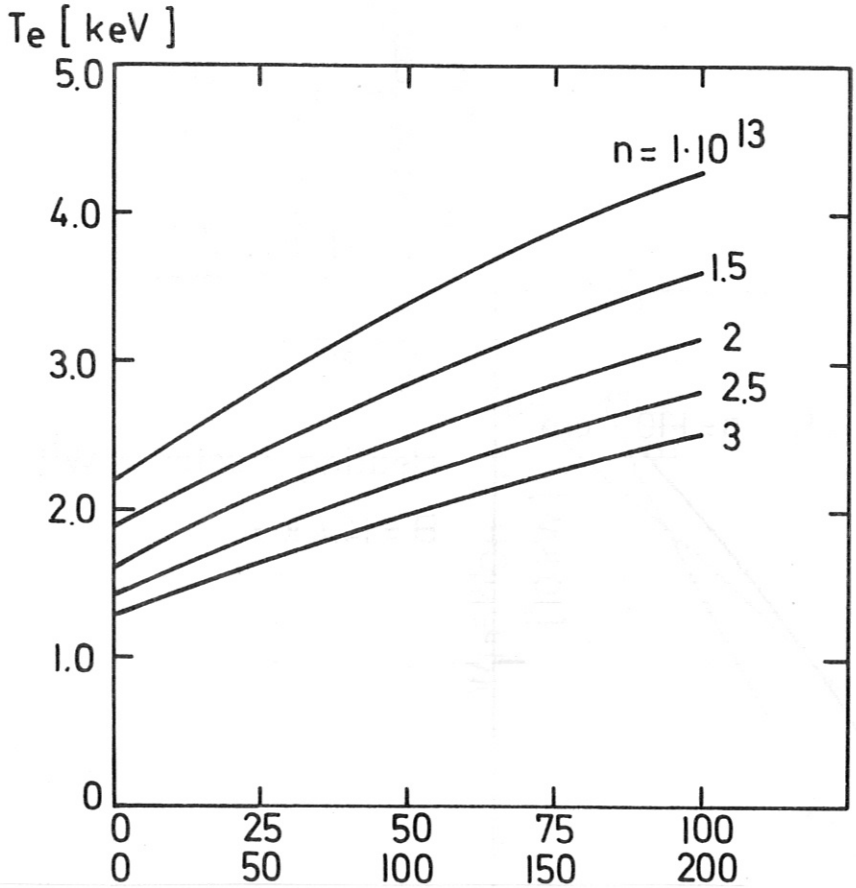

Fig. 27

CASE 6

Variation of W^h and n

B = 14.4 kG

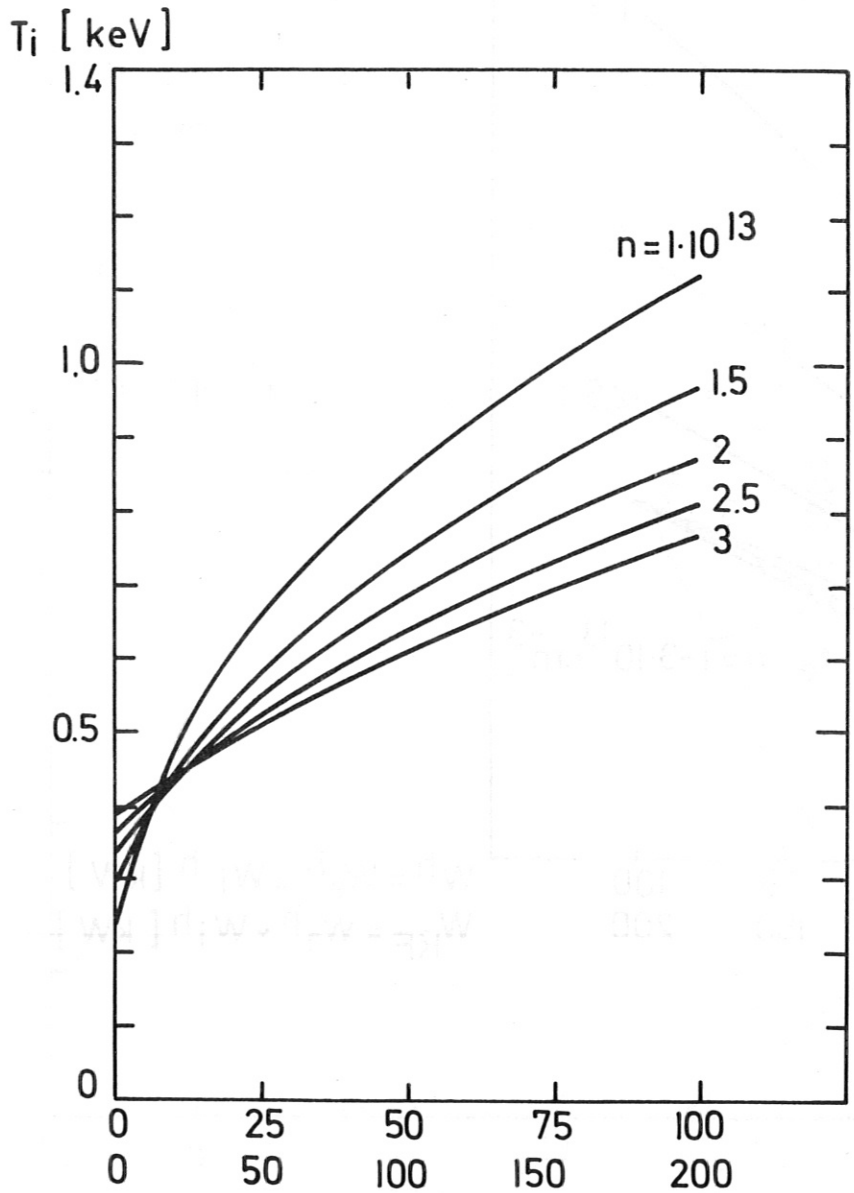

Fig. 28

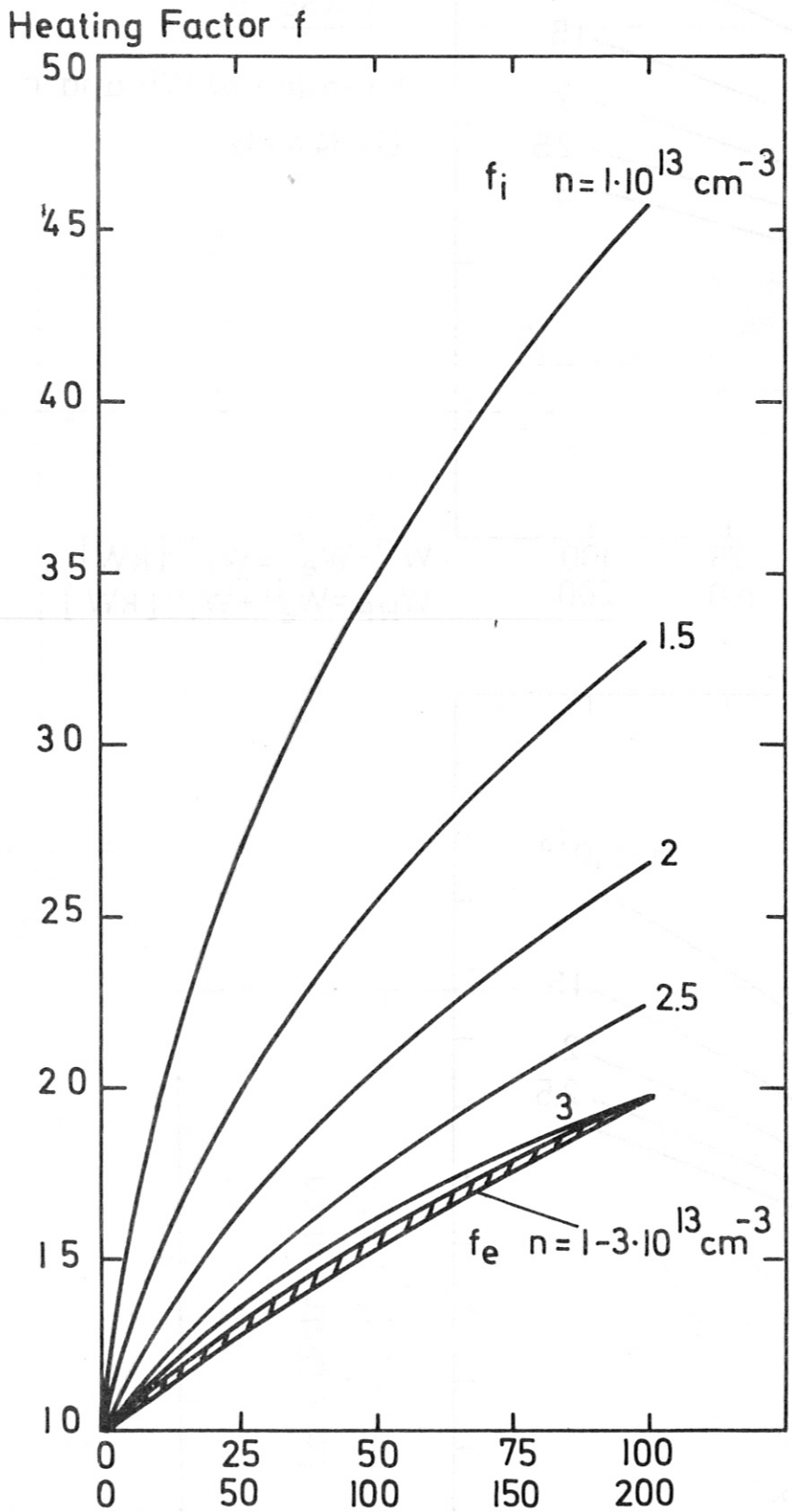

CASE 6

Heating Factor vs W^h, n

B = 14.4 kG

$W^h = W_e{}^h = W_i{}^h$ [kW]

$W_{RF} = W_e{}^h + W_i{}^h$ [kW]

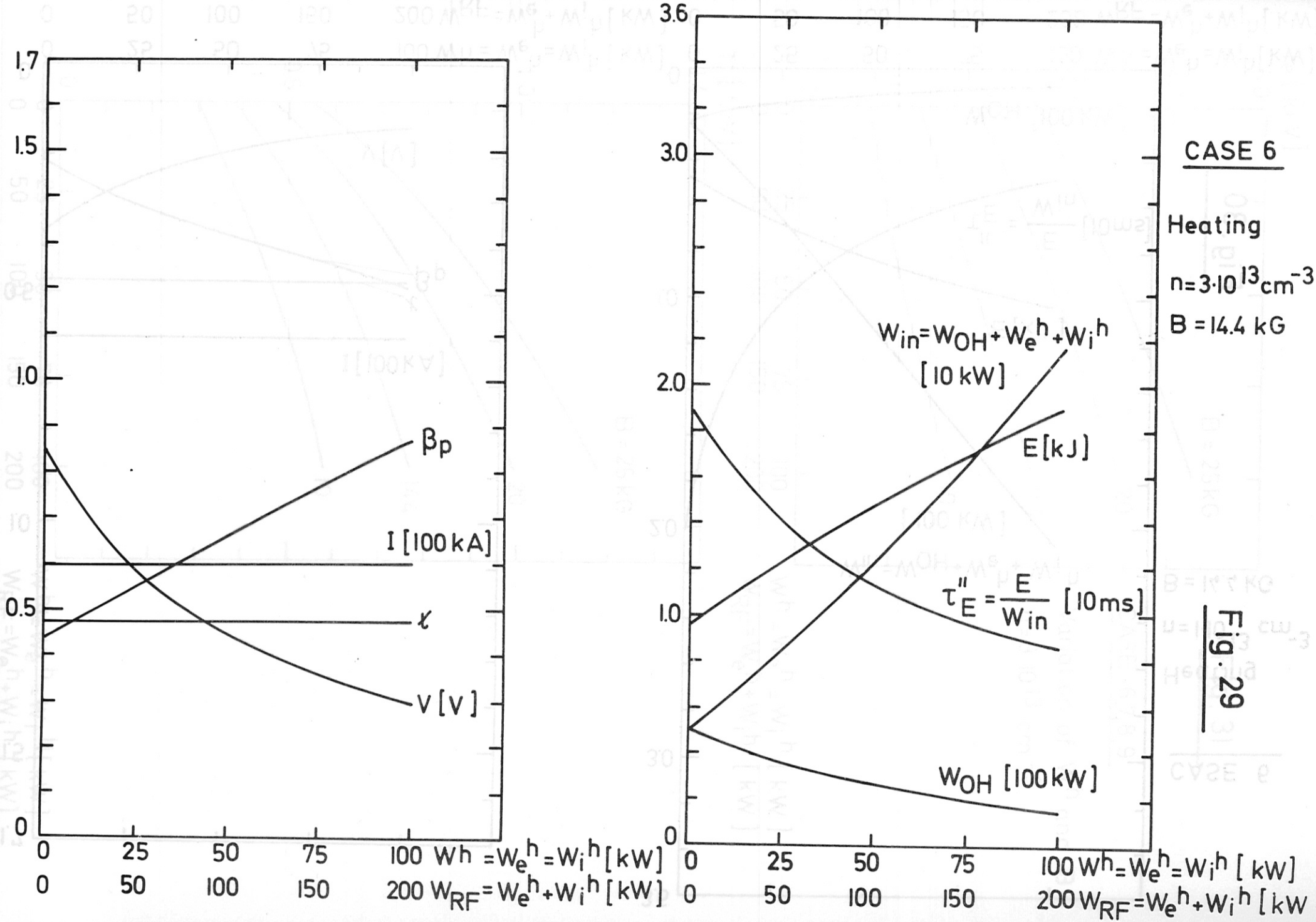
CASE 6
Heating
n=3·10^13 cm^-3
B = 14.4 kG
Win=WOH+We^h+Wi^h
[10 kW]
E[kJ]
τ"E = E/Win [10ms]
WOH [100 kW]
βp
I [100 kA]
ℓ
V [V]
Wh = We^h = Wi^h [kW]
WRF = We^h + Wi^h [kW]
Fig. 29

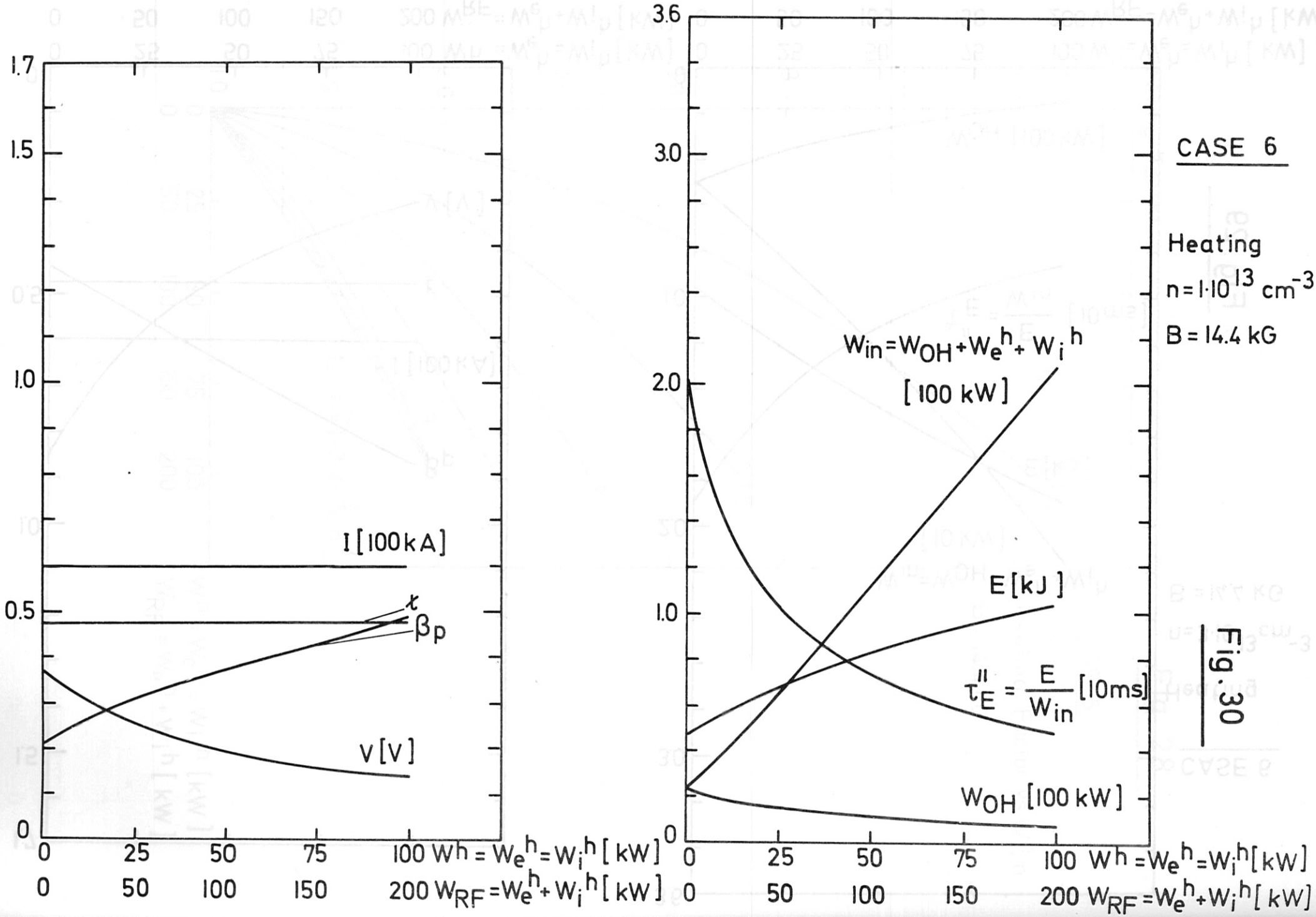
CASE 6
Heating
n = 1·10^13 cm^-3
B = 14.4 kG
I [100 kA]
V [V]
x
βp
Win = WOH + We^h + Wi^h
[100 kW]
E [kJ]
τE'' = E / Win [10ms]
WOH [100 kW]
Wh = We^h = Wi^h [kW]
WRF = We^h + Wi^h [kW]

Fig. 30

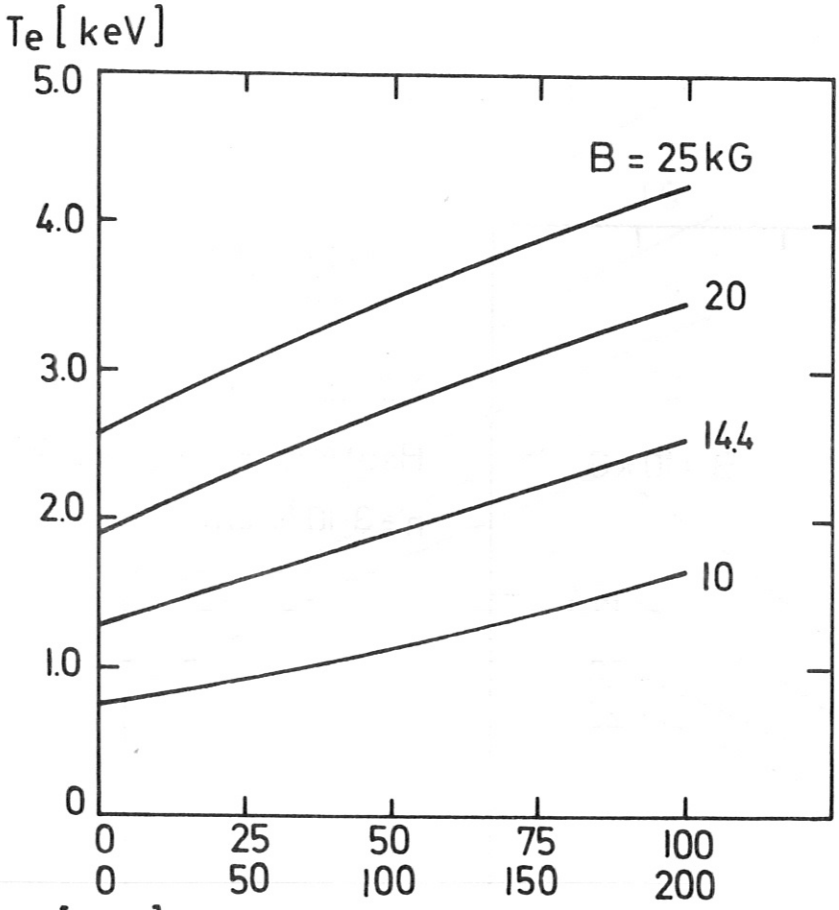

Fig. 31

CASE 6,7,8,9

Variation of W^h and B

$n = 3 \cdot 10^{13}$ cm $^{-3}$

$W^h = W_e{}^h = W_i{}^h$ [kW]

$W_{RF} = W_e{}^h + W_i{}^h$ [kW]

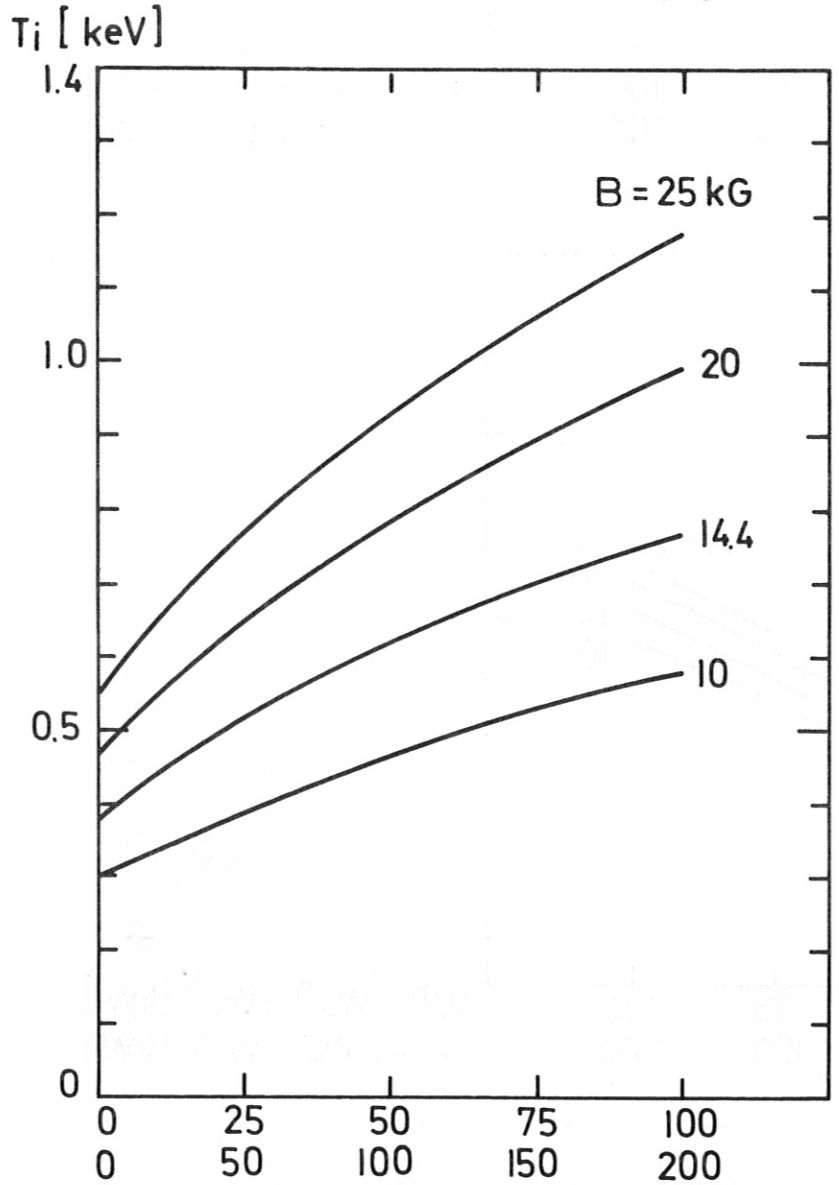

$W^h = W_e{}^h = W_i{}^h$ [kW]

$W_{RF} = W_e{}^h + W_i{}^h$ [kW]

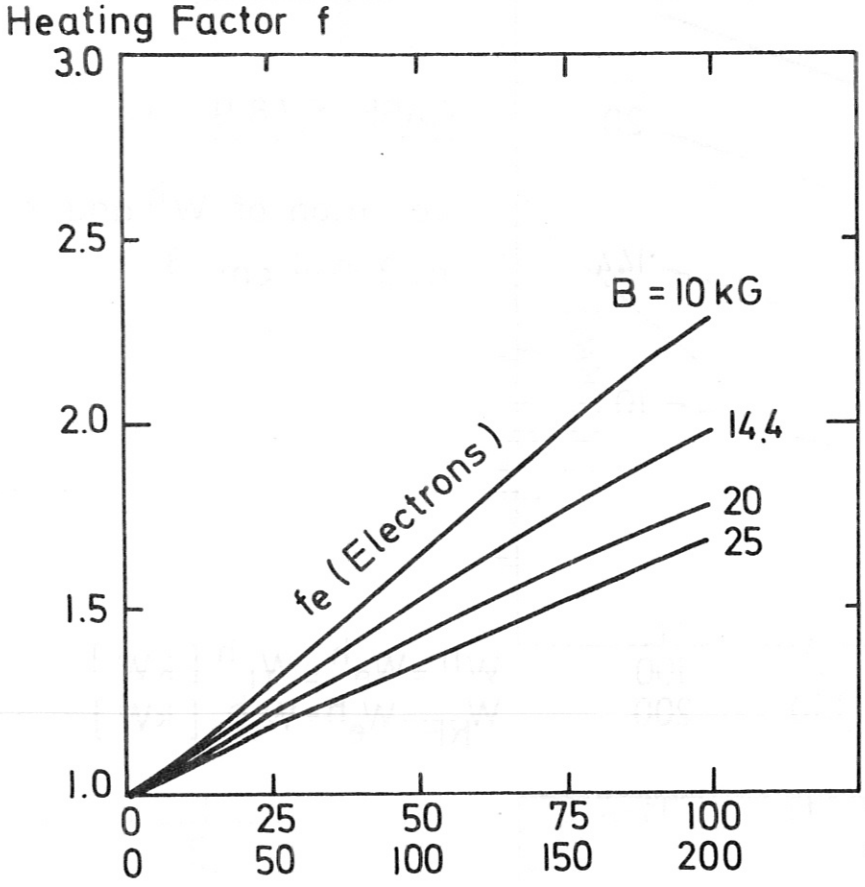

Fig. 32

CASE 6,7,8,9

Heating Factor vs W^h, B

$n = 3 \cdot 10^{13}\ cm^{-3}$

$W^h = W_e{}^h = W_i{}^h$ [kW]

$W_{RF} = W_e{}^h + W_i{}^h$ [kW]

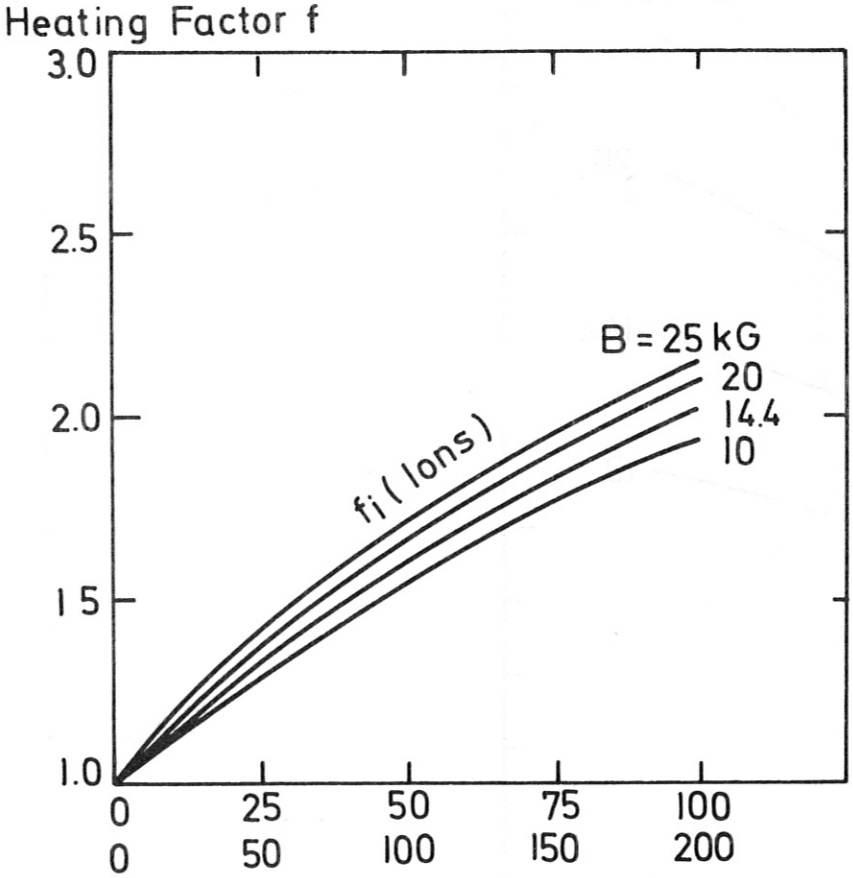

$W^h = W_e{}^h = W_i{}^h$ [kW]

$W_{RF} = W_e{}^h + W_i{}^h$ [kW]

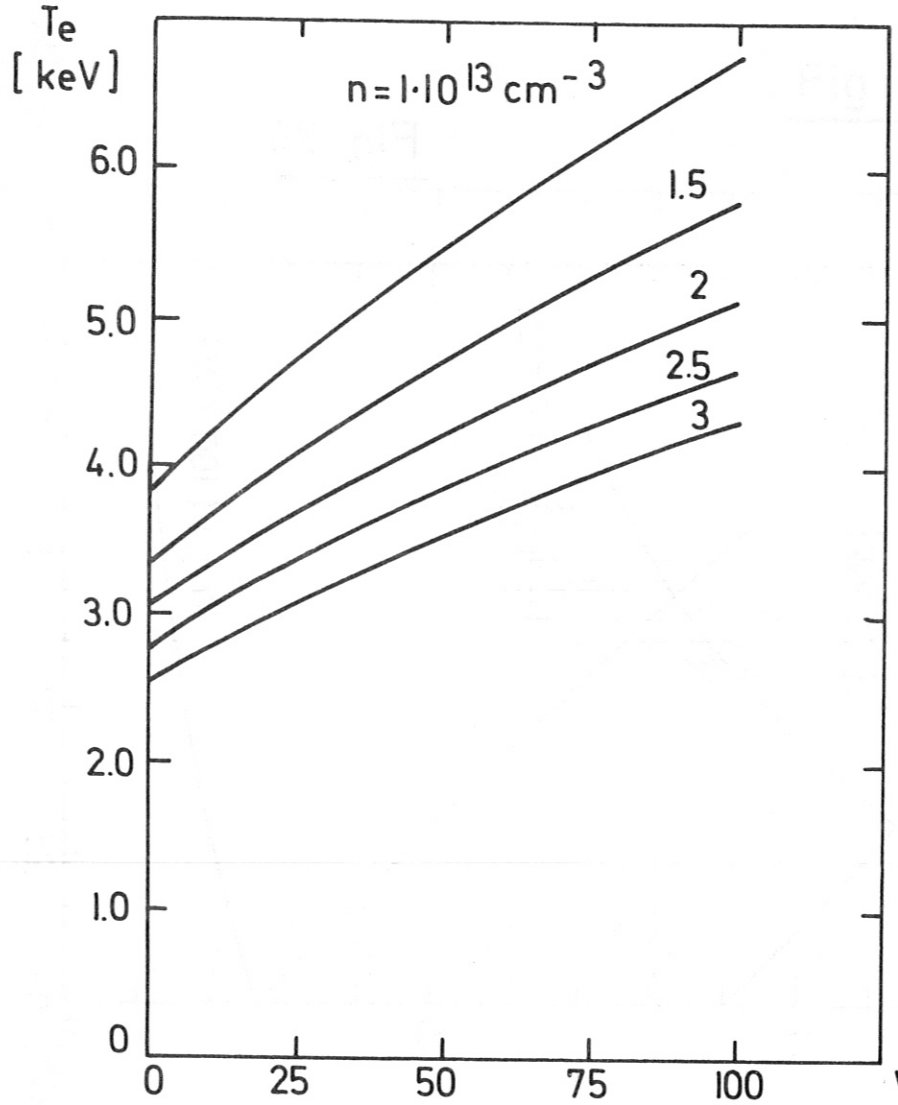

Fig. 33

CASE 9

Variation of W^h and n
B = 25 kG

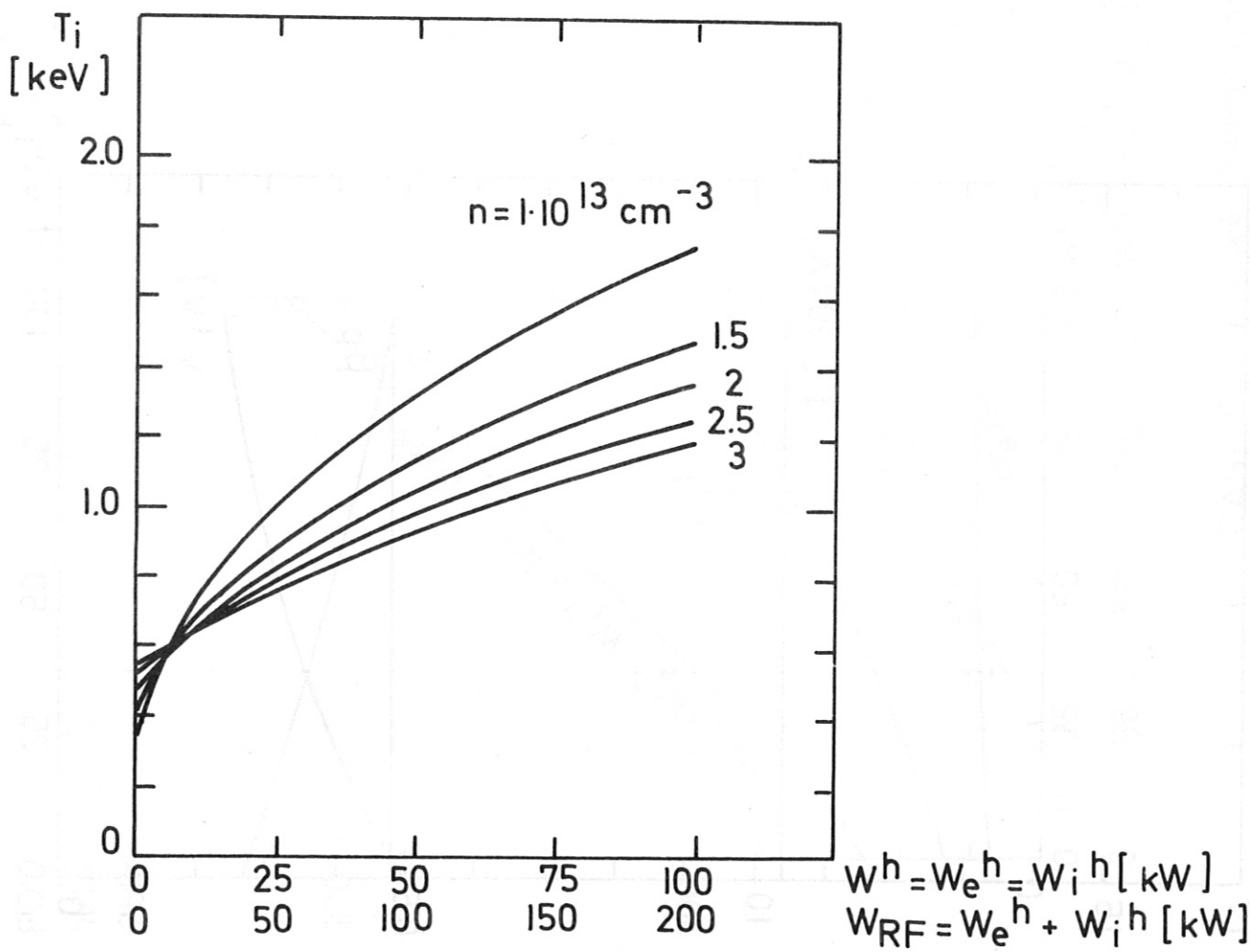

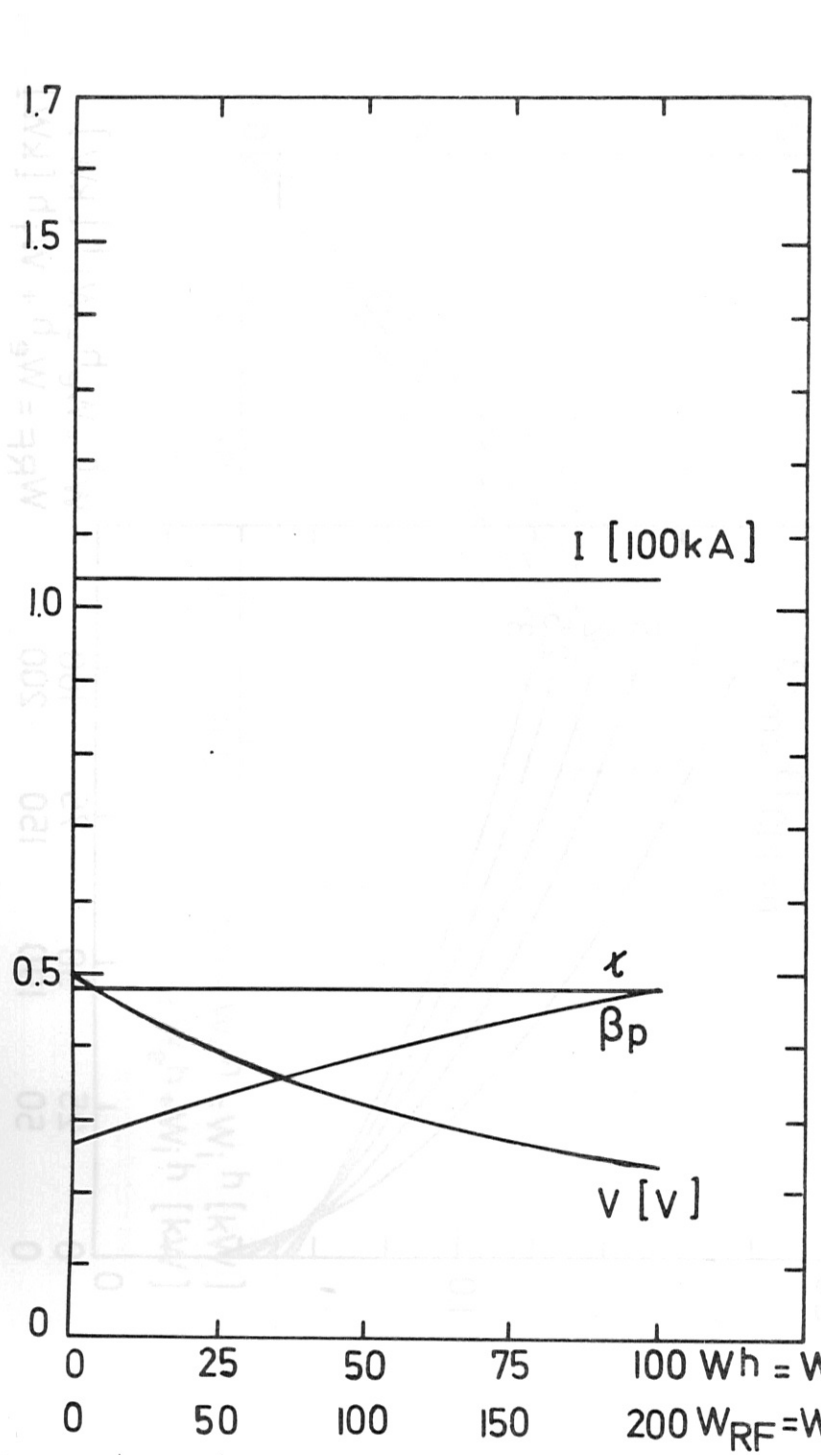

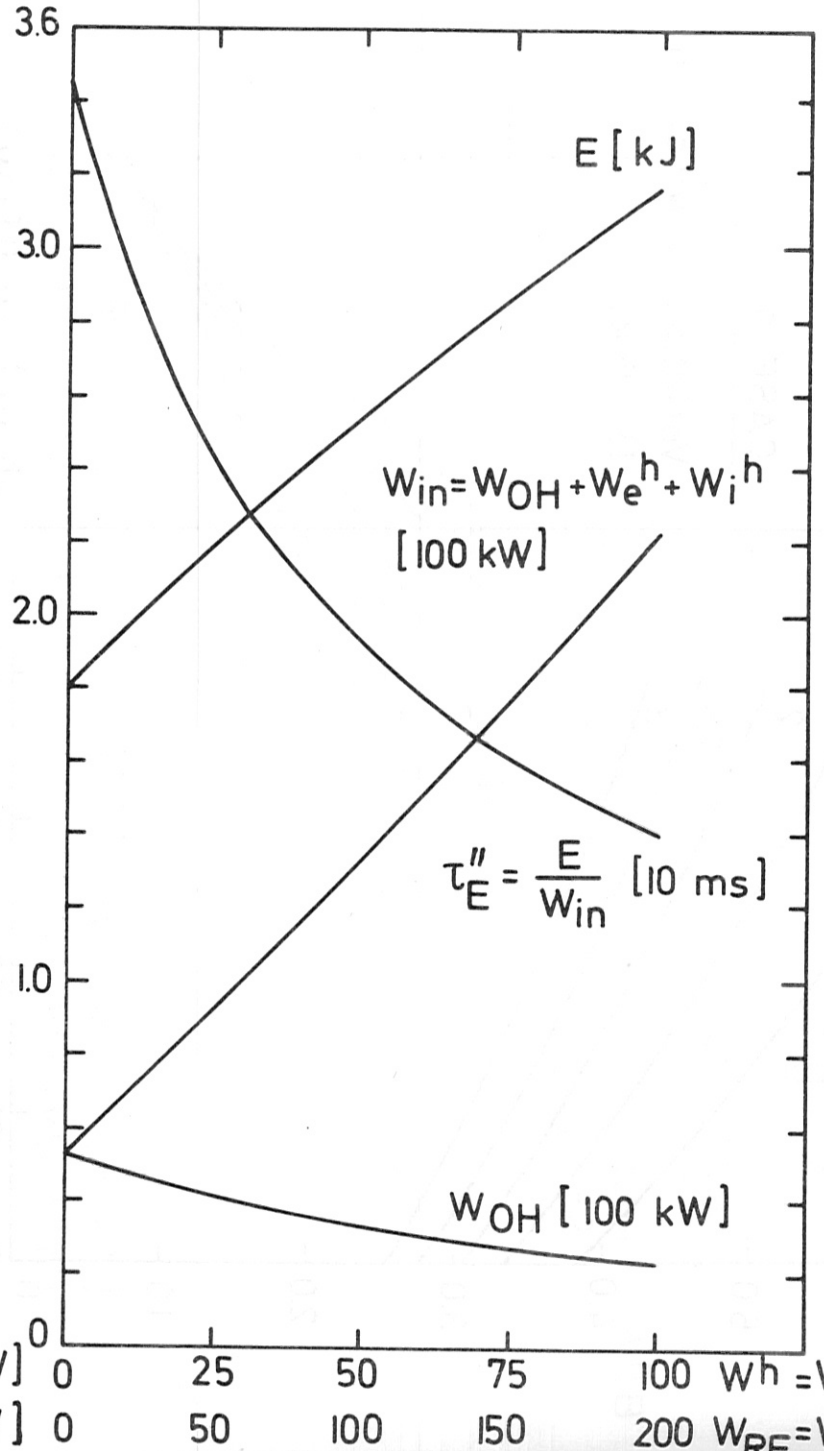

CASE 9

$n = 3 \cdot 10^{13}\ cm^{-3}$

B = 25 kG

Fig. 34

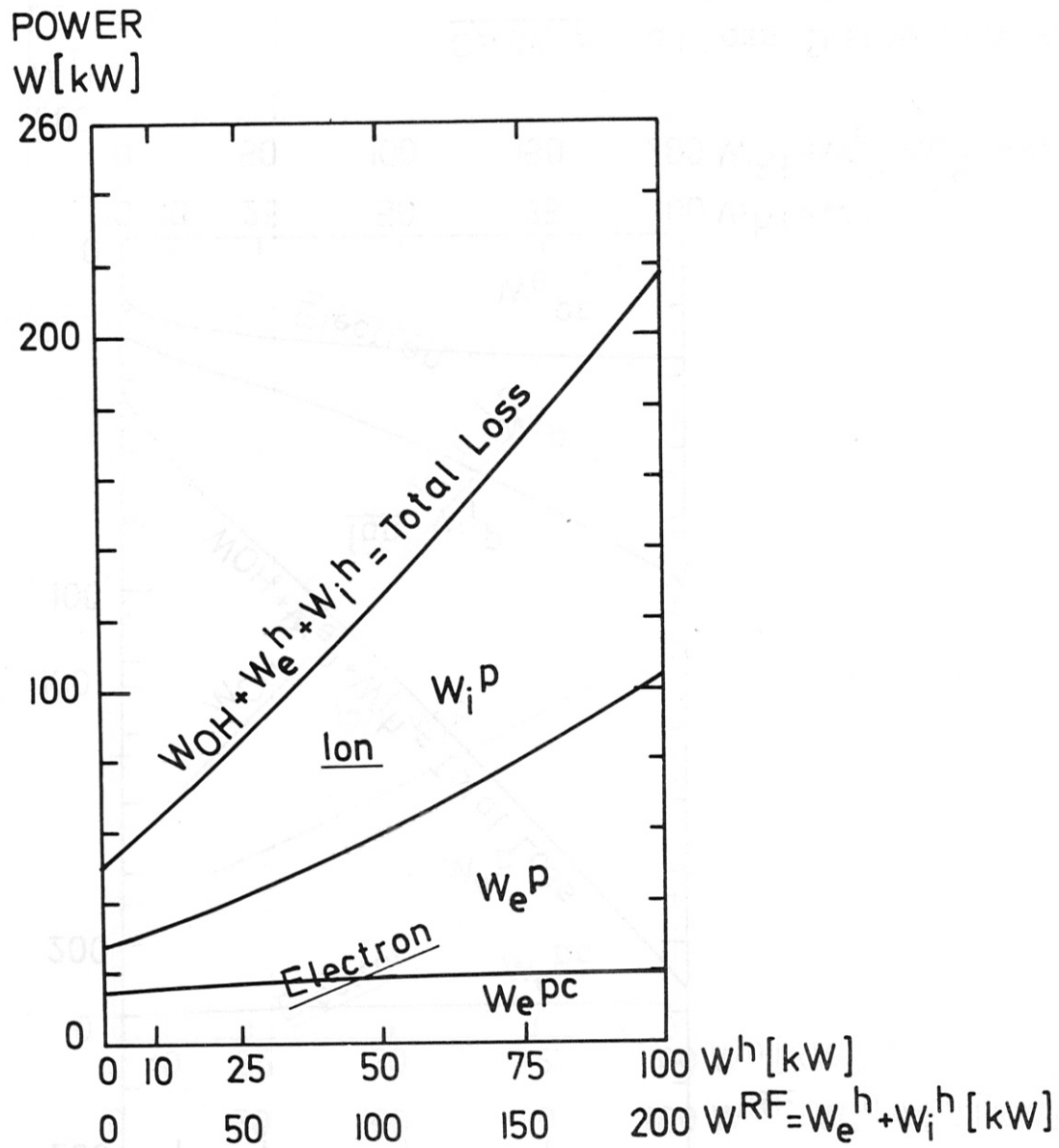

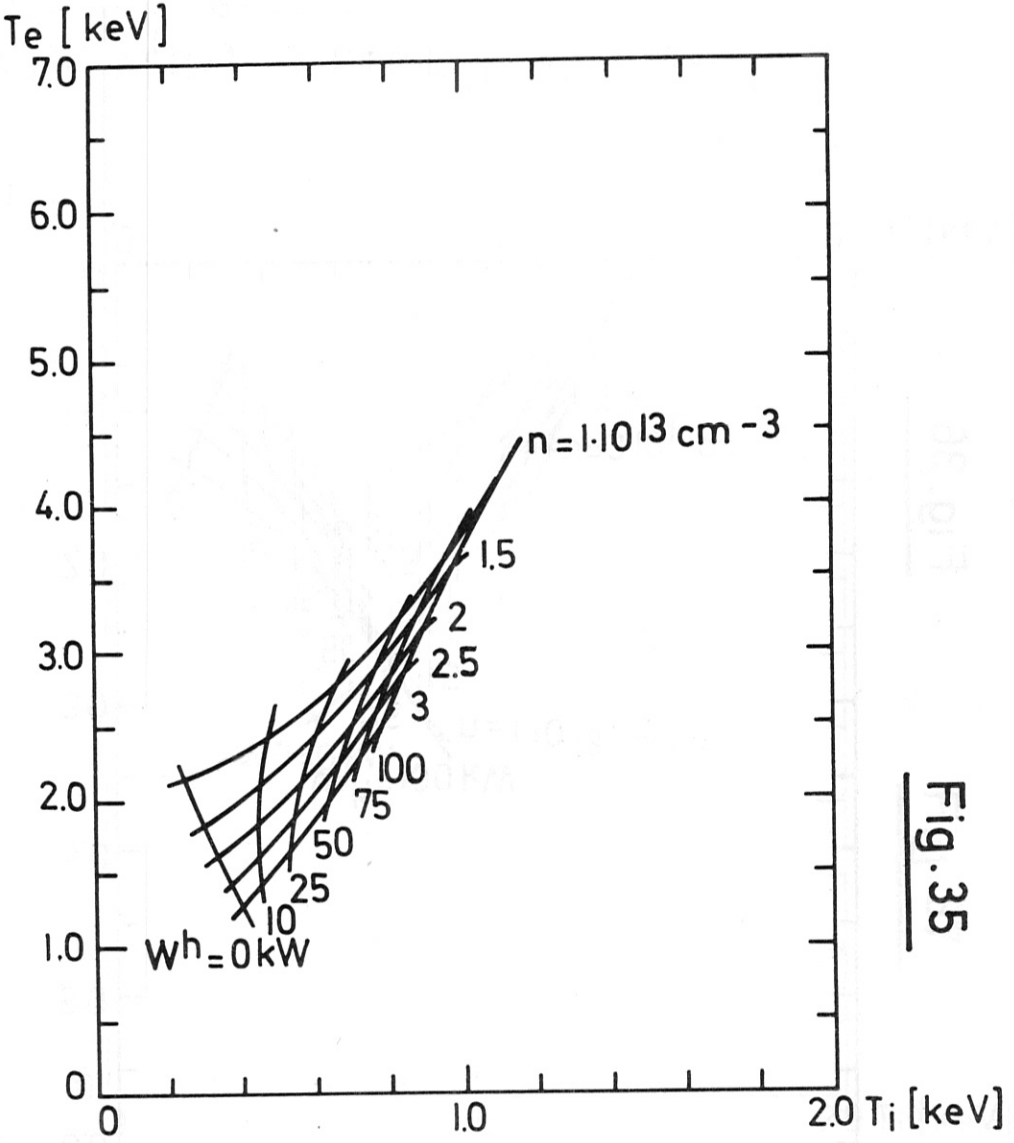

Fig. 35

CASE 6 a) Loss Distribution WITH Heating $n=3\cdot10^{13}$ cm^{-3}, B = 14.4 kG

b) Te vs Ti for various n, W^h_i; B = 14.4 kG

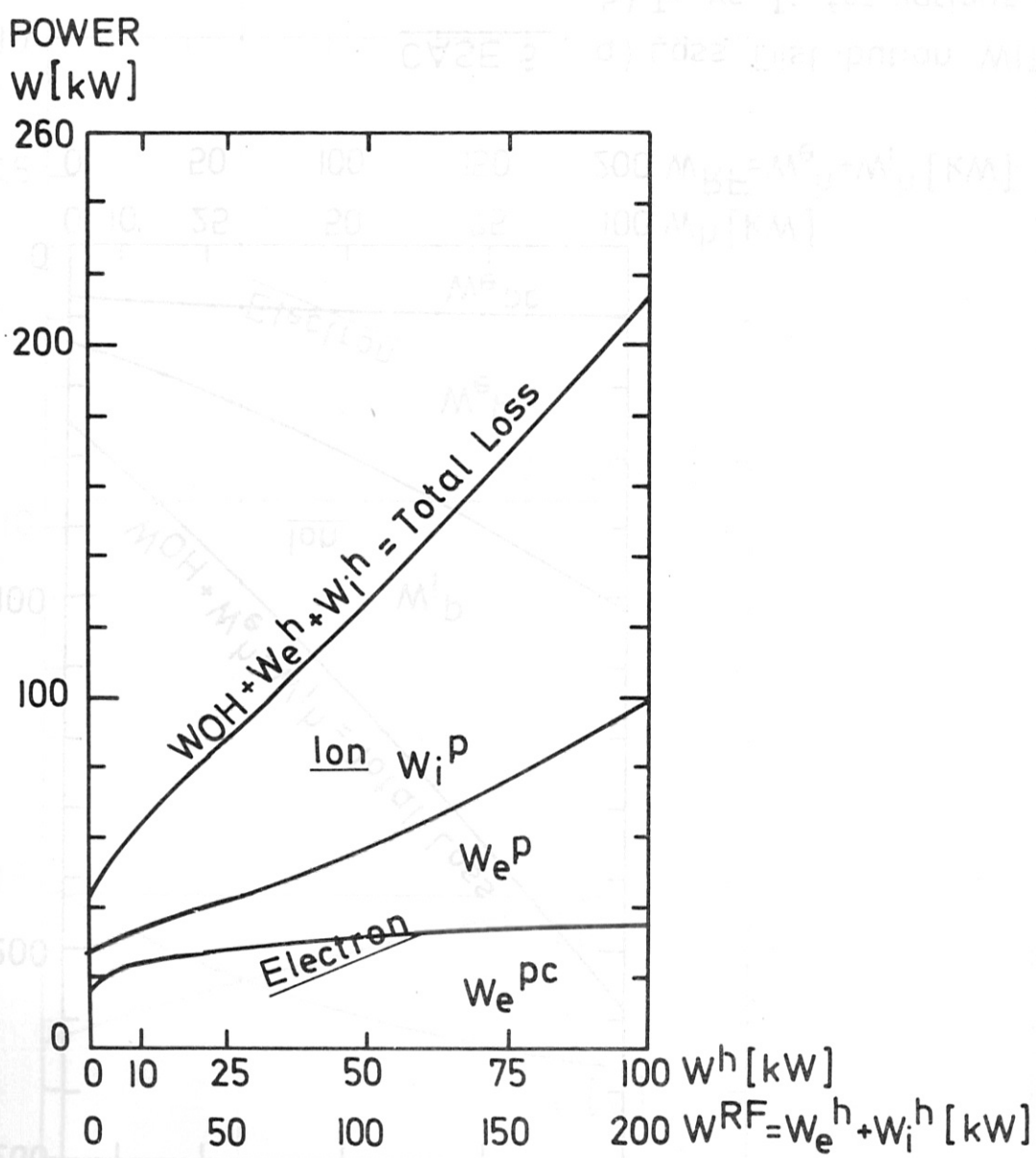

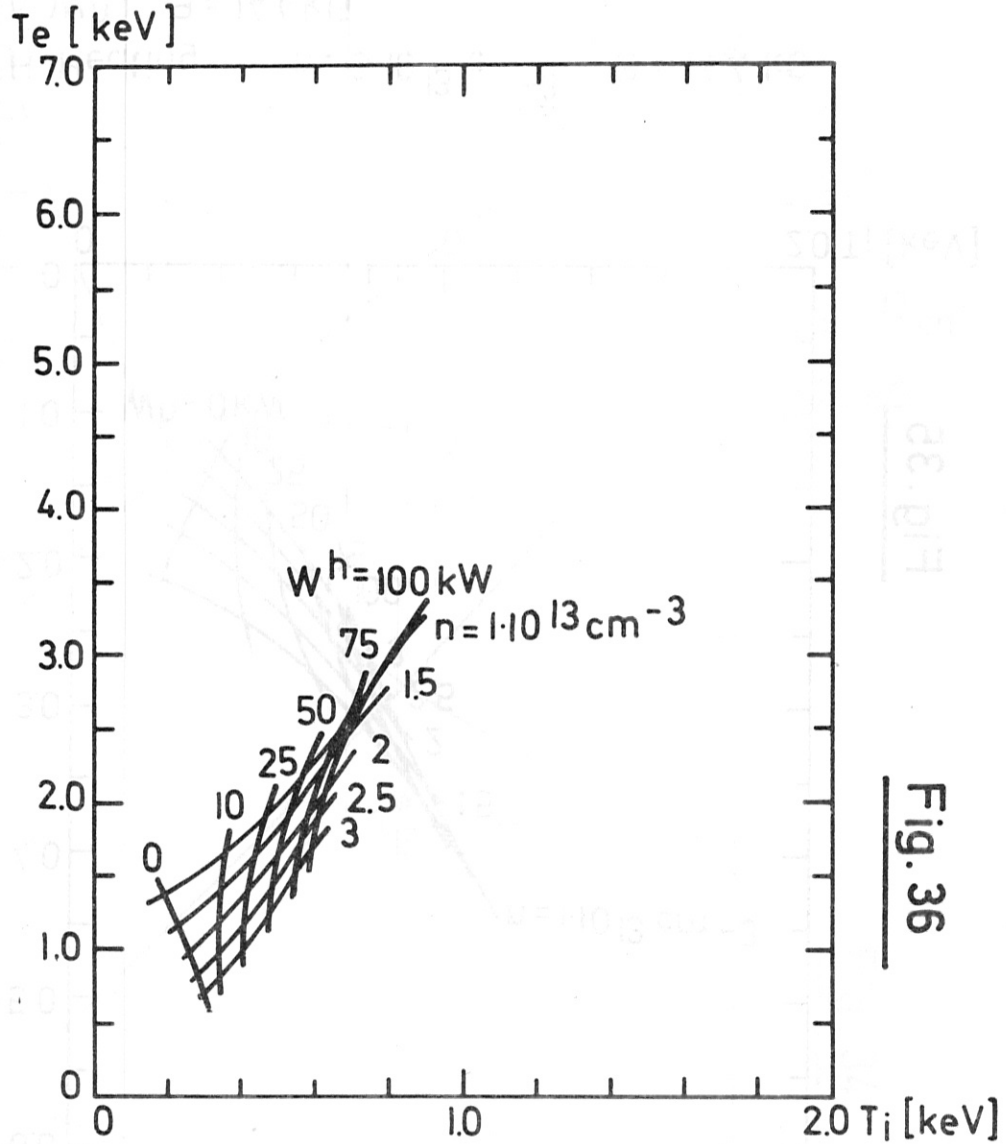

Fig. 36

CASE 7 a) Loss Distribution WITH Heating $n = 3 \cdot 10^{13}\ cm^{-3}$, $B = 10$ kG

b) T_e vs T_i for various n, W^h_i; $B = 10$ kG

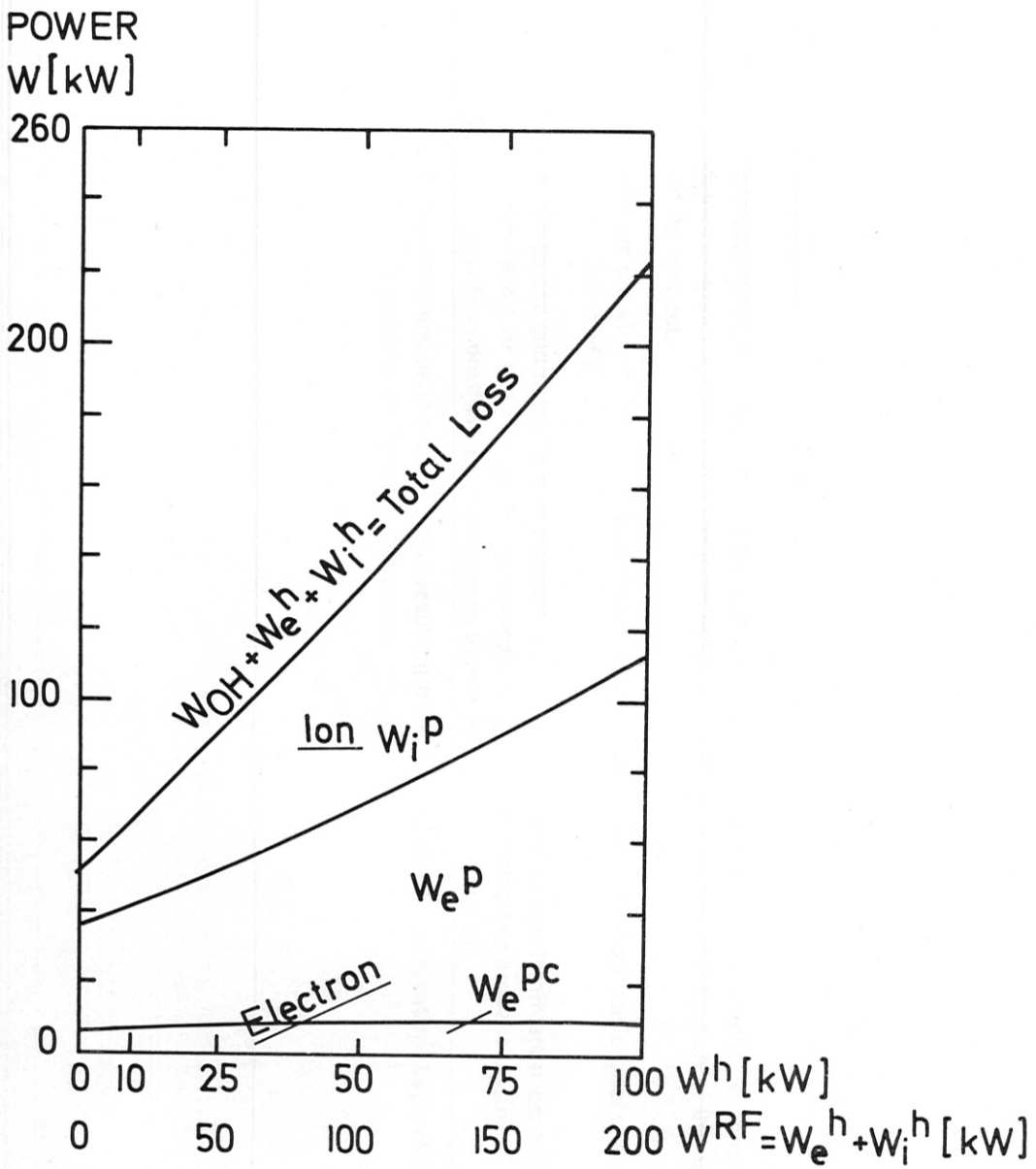

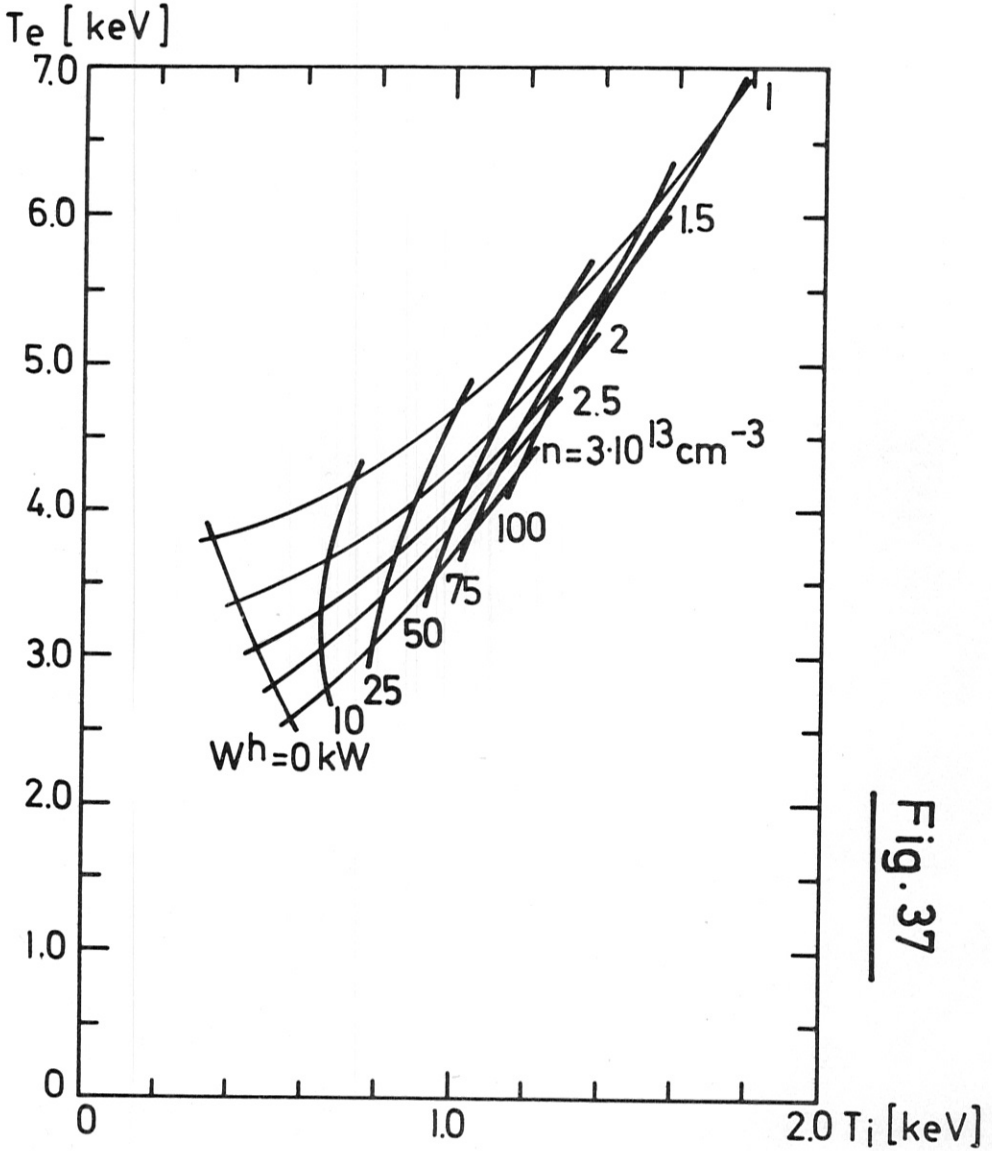

Fig. 37

CASE 9 a) Loss Distribution WITH Heating $n = 3\cdot10^{13}\ cm^{-3}$, B = 25 kG

b) Te vs Ti for various n, W^h_i; B = 25 kG